

Dissertation

zur Erlangung des Doktorgrades der Fakultät für Chemie und Pharmazie
der Ludwig-Maximilians-Universität München

THE STRUCTURE OF SPOVT

A REGULATOR OF SPORULATION IN *BACILLUS SUBTILIS*

Iris Asen

aus
Vilshofen

2008

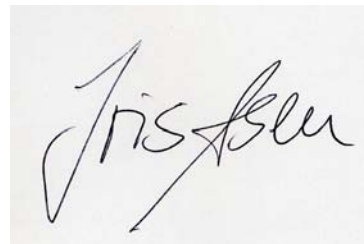
Erklärung

Diese Dissertation wurde im Sinne von § 13 Abs. 3 der Promotionsordnung vom 29. Januar 1998 von Herrn Prof. Dieter Oesterhelt betreut.

Ehrenwörtliche Versicherung

Diese Dissertation wurde selbständig, ohne unerlaubte Hilfe erarbeitet.

München, am 15.05.2008

A handwritten signature in black ink, reading 'Iris Asen'. The signature is written in a cursive style with a large initial 'I' and a long horizontal stroke extending to the right.

Iris Asen

Dissertation eingereicht am 15.05.2008

1. Gutachter Prof. Dieter Oesterhelt

2. Gutachter Prof. Karl-Peter Hopfner

Mündliche Prüfung am 31.07.2008

*Für den gläubigen Menschen steht Gott am Anfang,
für den Wissenschaftler am Ende aller seiner Überlegungen.*

Max Planck

TABLE OF CONTENTS

1. SUMMARY/ZUSAMMENFASSUNG	5
2. INTRODUCTION.....	7
2.1 Cellular Differentiation – Basics and Features	7
2.2 Sporulation in <i>Bacteria</i>	8
2.3 Endospores	9
2.4 Endospore Formation in <i>Bacillus subtilis</i>.....	10
2.4.1 σ - and Transcription Factors	12
2.4.2 σ^E -dependent Transcription Factor SpoVT.....	15
2.5 Scope of Work.....	19
3. RESULTS.....	20
3.1 Overexpression and Purification of <i>B. subtilis</i> SpoVT	20
3.1.1 SpoVT Full-length.....	20
3.1.2 C-terminal Domain of SpoVT	21
3.2 Biochemical Analysis of <i>B. subtilis</i> SpoVT.....	21
3.2.1 Secondary Structure and Thermal Stability	21
3.2.2 Oligomeric Form	24
3.2.2.1 Covalent Linkage	24
3.2.2.2 Native State.....	25
3.2.3 Immunological Detection of Native SpoVT.....	26
3.2.3.1 Generation of Polyclonal Rabbit Anti-SpoVT Antibodies.....	26
3.2.3.2 Purification of Polyclonal Anti-SpoVT Antibodies.....	27
3.2.3.3 Synchronisation of <i>B. subtilis</i> Cells and Induction of Sporulation	28
3.2.3.4 Immuno Blotting	29
3.3 3D-Crystallisation and Structural Analysis of <i>B. subtilis</i> SpoVT.....	31
3.3.1 X-ray Crystallography.....	31
3.3.2 Phasing and Density Fitting	34
3.3.3 Model Building and Structural Refinement	35
3.4 Structure of <i>B. subtilis</i> SpoVT	37
3.4.1 Crystal Packing	37
3.4.2 Overall Fold of Tetrameric Complex.....	38
3.4.3 Asymmetric Tetramer.....	40
3.4.4 Two Different Monomers	42
3.4.5 Multimerisation Modules	43
3.4.5.1 N-terminal Domain.....	43
3.4.5.2 C-terminal Domain	45
3.4.6 Novel Domain Architecture	47
3.4.6.1 Swapped-hairpin β -barrel.....	47
3.4.6.2 GAF Domain	49
3.4.7 New Dimerisation Mode of GAF Domains	51
3.5 DNA- and Ligand Binding Studies of <i>B. subtilis</i> SpoVT.....	53
3.5.1 Biochemical Approach	53
3.5.1.1 Limited Proteolysis with Trypsin and α -Chymotrypsin	53
3.5.1.2 Gel Filtration Chromatography.....	54
3.5.2 Biophysical Approach	55
3.5.2.1 Co-crystallisation and Soaking	55
3.5.2.2 Isothermal Titration Calorimetry (ITC).....	56

4. DISCUSSION	57
4.1 Tetrameric State of <i>B. subtilis</i> SpoVT	57
4.1.1 Biochemical Aspects.....	57
4.1.2 Structural Aspects	59
4.2 DNA-binding Domain (DBD) of <i>B. subtilis</i> SpoVT	62
4.3 Signal Sensing Domain (SSD) of <i>B. subtilis</i> SpoVT	65
4.4 Dimerisation Mode of GAF Domains in <i>B. subtilis</i> SpoVT	68
4.5 Model for SpoVT Mediated Regulation	70
5. MATERIALS	72
5.1 Chemicals and Reagents	72
5.2 Kits and Materials	73
5.3 Media, Buffers, and Solutions.....	74
5.3.1 Growth Media.....	74
5.3.1.1 LB Medium	74
5.3.1.2 TB Medium	74
5.3.1.3 DSM Medium	75
5.3.1.4 LB Agar Plates.....	75
5.3.2 Buffers	76
5.3.3 Solutions.....	77
5.4 Strains, Plasmids, and Oligonucleotides	78
5.4.1 Strains	78
5.4.2 Vector.....	78
5.4.3 Oligonucleotides	79
5.5 Instruments and Devices.....	80
5.6 Computational Software.....	82
6. METHODS	83
6.1 Molecular Biology and Microbiology.....	83
6.1.1 Molecular Biological Methods	83
6.1.1.1 Amplification of SpoVT Operon DNA Sequence by Polymerase Chain Reaction (PCR)	83
6.1.1.2 Isolation and Purification of Vector DNA from <i>E. coli</i>	84
6.1.1.3 Determination of DNA Concentration	84
6.1.1.4 DNA Sequencing.....	84
6.1.2 Microbiological Methods.....	85
6.1.2.1 Transformation of Chemically Competent <i>E. coli</i> Cells.....	85
6.1.2.2 Long-term Stock Cultures	85
6.1.2.3 Cultivation of <i>E. coli</i> and <i>B. subtilis</i>	86
6.1.2.4 Synchronisation of <i>B. subtilis</i> Cells.....	86
6.1.2.5 Induction of Endospore Formation in <i>B. subtilis</i>	86
6.1.2.6 Determination of Cell Density.....	87
6.1.2.7 Growth Curve of Bacteria in Liquid Cultures	87
6.1.2.8 Staining of Endospores.....	87
6.2 Protein Chemistry	88
6.2.1 Heterologous Overexpression of Proteins in <i>E. coli</i>	88
6.2.2 Purification of His-tagged Proteins from <i>E. coli</i> under Native Conditions ..	88
6.2.3 Generation of Polyclonal Rabbit Antibodies	89
6.2.4 Purification of Polyclonal Antibodies	90
6.2.5 Fast Cell Lysis for Determination of Protein Content.....	90
6.2.6 SDS-Polyacrylamide Gel Electrophoresis	91
6.2.7 Native Polyacrylamide Gel Electrophoresis	92
6.2.8 Electro Blotting	92

6.2.9 Immuno (Western) Blotting.....	93
6.2.10 Dialysis	93
6.2.11 Ultrafiltration	94
6.2.12 Determination of Protein Concentration.....	94
6.2.12.1 UV Absorption.....	94
6.2.12.2 BCA Protein Essay	95
6.2.13 Chemical Crosslinking	95
6.3 Biochemistry.....	96
6.3.1 Chromatography	96
6.3.1.1 Affinity Chromatography	96
6.3.1.2 Gel Filtration Chromatography.....	96
6.3.2 High Performance Liquid Chromatography/Mass Spectrometry (HPLC/MS)	97
6.3.3 Matrix Assisted Laser Desorption Ionisation/Time of Flight/Mass Spectrometry (MALDI/TOF/MS).....	97
6.3.4 N-terminal Amino Acid Sequencing	98
6.3.5 Limited Proteolysis.....	98
6.3.6 Preparation of <i>B. subtilis</i> Spores	98
6.4 Molecular Biophysics	99
6.4.1 X-ray Crystallography.....	99
6.4.1.1 Protein Crystallisation, Soaking, Co-crystallisation, and Seeding.....	99
6.4.1.2 Crystal Mounting and Data Collection	100
6.4.1.3 Data Processing and Phasing	101
6.4.1.4 Model Building and Refinement.....	101
6.4.2 Circular Dichroism (CD) Spectroscopy.....	102
6.4.3 Isothermal Titration Calorimetry (ITC)	102
7. ABBREVIATIONS.....	103
8. REFERENCES	105
9. APPENDIX	110
10. ACKNOWLEDGEMENT - DANKSAGUNG	112
11. CURRICULUM VITAE	114

1. SUMMARY/ZUSAMMENFASSUNG

Adaptation to environmental changes is essential for the survival or at least for the continuity of the genetic material of every organism. Some cells adjust to alternating conditions on the basis of cellular differentiation. Gram-positive organisms, such as *Bacillus subtilis*, adapt to unfavourable conditions by protecting their genome in robust endospores. Sporulation is a complex and tightly balanced cell differentiation programme which controls highly specific temporal and spatial gene expression. In *B. subtilis*, endospore formation is orchestrated by five developmental alternative sigma factors and further modulated by several auxiliary transcription factors. One of these, SpoVT, regulates forespore-specific σ^G -dependent genes and plays a key role in the final stages of spore formation.

This work introduces the crystal structure of *B. subtilis* SpoVT comprising a novel domain architecture in transcription factors. The structures of the full-length SpoVT protein and, separately, of its isolated C-terminal domain were determined at 2.6 Å and 1.5 Å, respectively. SpoVT is a tetramer in which the N-terminal domains dimerise to build swapped-hairpin β -barrels and the dimers further assemble through helical interactions between their C-terminal domains. A tetrameric oligomer of SpoVT is supported by biochemical results.

By structure and sequence comparisons between swapped-hairpin β -barrels, a predicted close relationship to the transition state regulator AbrB is confirmed. Structural analysis of the C-terminal domain proves a bioinformatically predicted GAF fold and shows a further homology to the protein CodY. The described helical interaction between the C-terminal domains presents a new mode of dimer formation in GAF domains.

The SpoVT tetramer is characterised by an overall asymmetry due to an anti-parallel assembly of two conformationally differing monomers. Structural investigations show a certain degree of flexibility between the domains in the asymmetric tetramer.

Based on those structural data, it is hypothesised that SpoVT is a GAF domain regulated transcription factor whose DNA-binding activity is controlled by sensing a yet unknown small molecule.

Für jeden Organismus ist es essentiell sich an die sich ständig verändernden Umweltbedingungen anzupassen, um sein Überleben oder zumindest den Fortbestand seines genetischen Materials zu sichern. Manche Zellen gleichen sich durch Spezialisierung an, wobei sie den Prozeß der Zelldifferenzierung durchlaufen. Gram-positive Organismen wie *Bacillus subtilis* schützen ihr Genom vor ungünstigen Umweltbedingungen in robusten Endosporen. Der Sporulationsprozess ist ein komplexes und streng reguliertes Zelldifferenzierungsprogramm, welches die zeitlich und räumlich hoch spezifische Genexpression kontrolliert. Die Endosporenbildung in *B. subtilis* wird von fünf alternativen Sigmafaktoren koordiniert und von mehreren unterstützenden Transkriptionsfaktoren weiter moduliert. Als einer von diesen, reguliert SpoVT vorsporentypische σ^G -abhängige Gene und hat eine Schlüsselfunktion in den finalen Stadien der Sporenentwicklung.

Diese Arbeit beschreibt die Kristallstruktur von *B. subtilis* SpoVT und zugleich eine neuartige Bauweise von Transkriptionsfaktoren. Die Struktur des volllängen SpoVT Proteins wurde bei 2.6 Å bestimmt und die der isolierten C-terminalen Domäne gesondert bei 1.5 Å. SpoVT ist ein Tetramer, in welchem die N-terminalen Domänen dimerisieren, um ein „swapped hairpin β -barrel“ zu formen und die Dimere durch helikale Interaktionen zwischen ihren C-terminalen Domänen weiter assemblieren. Der tetramere Oligomerisierungszustand von SpoVT wird auch von biochemischen Daten untermauert. Anhand von Struktur- und Sequenzvergleichen zwischen „swapped hairpin β -barrels“, wird die vorhergesagte enge Verwandtschaft zu dem Übergangsregulator AbrB bestätigt. Die Strukturanalyse der C-terminalen Domäne weist einen durch bioinformatische Methoden vorhergesagten GAF-Faltungstyp nach und es wird eine gewisse Homologie zu dem Protein CodY gezeigt. Die Art der Interaktion zwischen Helix-Bündel zweier SpoVT GAF-Domänen beschreibt einen neuen Modus der Dimer-Formation innerhalb der Gruppe der GAF-Domänen.

Das SpoVT Tetramer ist charakterisiert durch eine Asymmetrie, die auf einer antiparallelen Anordnung von zwei konformell zu unterscheidenden Monomeren basiert. Strukturuntersuchungen legen einen gewissen Grad an Flexibilität zwischen den Domänen innerhalb des asymmetrischen Tetramers dar.

Aufgrund dieser strukturellen Daten wurde die Hypothese erstellt, dass SpoVT ein von GAF-Domänen regulierter Transkriptionsfaktor ist, dessen DNA-Bindeaktivität durch Detektieren eines bisher unbekannten kleinen Moleküls gesteuert wird.

2. INTRODUCTION

2.1 Cellular Differentiation – Basics and Features

Organisms are complex living systems whose viability is based on the interplay of their functional components. They are in a permanent close relationship to the environment and, consequently, a sophisticated strategy to adapt to continuously changing conditions is of prime importance in evolution. Adaptation in long-term respects proceeds in species and genera over many generations called phyletic adaptation. Individual adaptation in turn, occurs in single individuals as a relatively rapid progress. Such processes always come along with a great effort in reorganisation and restructuring the working system focussing on the continuity of the genetic material. Changing the actual constitution is based on a highly controlled action of specific genes and proteins and can generate a new type of cell presenting completely new functions. This complex developmental procedure is termed cellular differentiation. Cellular differentiation describes the transition by which an unspecialised cell becomes a specialised cell (Fig. 1). Under such a transition, a cell may alter dramatically; size, shape, polarity, metabolic activity, sensitivity to signals, and gene expression profiles can change during differentiation. For single cell organisms, this probably means that they convert into a different life-form.

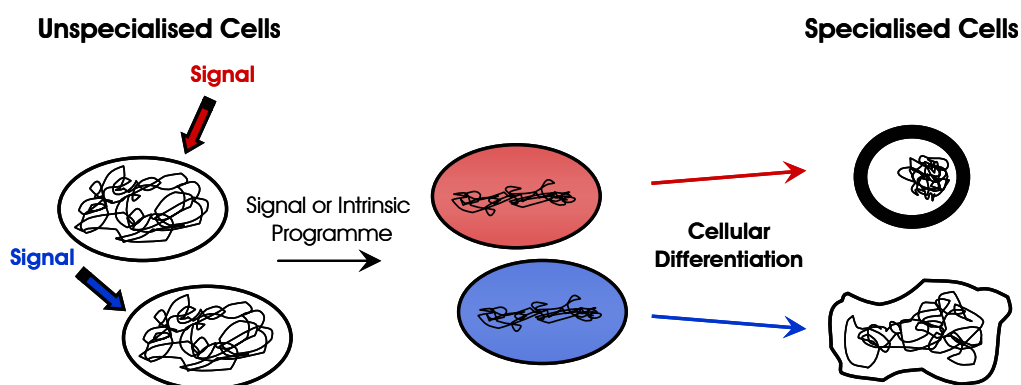


Figure 1. Schematic Illustration of the General Basic Task of Cellular Differentiation. Specific incoming signals (left) turn on specific cellular programmes (middle) and lead to corresponding modifications of the cell (right).

Cells affected by an environmental stimulus start a tightly balanced signal or intrinsic programme (Fig. 1) which leads to a modified gene expression profile. Cellular differentiation is primarily characterised by a differing gene activity in cells. During the differentiation progress, specific genes are up-regulated while other genes are down-regulated. Genes instruct how and when to build the proteins that allow the cell to create new structures and functions. Thereby, the proteins in one cell differ from those in another cell. The coordination of well timed activation and inactivation of genes is intricately regulated and to date, little understood. Studies on cell differentiation processes in lower life-forms might provide an insight into this complex interaction network.

2.2 Sporulation in *Bacteria*

Sporulation is a process in lower life-forms (fungi, moss, ferns, algae, and protozoans) which leads to a distinct developmental stage, featuring a high stress resistance with the intention of reproduction or survival.

The spore formation procedure in *Bacteria* describes a relatively simple form of cell differentiation. Some bacteria, e.g. the genera of *Methylosinus* or *Methylocystis* develop exospores (Whittenbury et al., 1970). This type of spore is aimed to reproduce and arises from pullulation. Spores of *Actinobacteria* are generated in characteristic filaments (Cavalier-Smith, 1987) and function in reproduction, also. *Myxobacteria* form spores within their fruiting bodies (Dworkin and Kaiser, 1993). The myxospores are coated by a thick cell wall and represent resistant dormant bodies. Comparable strategies are pursued by cyst formation in *Azotobacter* (Wyss et al., 1961).

For survival, a group of bacteria generates single endospores internally which are not able to reproduce and by far present the most resistant type of spores. Endospore formation as survival strategy occurs in the families *Bacillaceae*, *Clostridiaceae*, *Peptococcaceae*, *Heliobacteriaceae*, *Oscillospiraceae*, and *Thermoactinomycetaceae*. All families are placed within the classes *Bacilli* and *Clostridia* which are included in the phylum *Firmicutes*. Together with *Actinobacteria*, both phyla gather Gram-positive bacteria which feature a significant thick cell wall (peptidoglycan; covalently

linked N-acetylmuramic acid and N-acetylglucosamine) instead of an outer membrane.

Consistently, endospore-forming organisms are Gram-positive bacteria.

2.3 Endospores

Endospore formation is a process at which a vegetative cell is converted into a non-growing, non-reproductive, and highly resistant structure (Bender and Marquis, 1985; Piggot and Hilbert, 2004; Slepecky and Leadbetter, 1994). Endospores are resistant to desiccation (including vacuum), temperature, ultraviolet and gamma radiation, starvation, most disinfectants, or oxidising agents.

The typical architecture of an endospore is: cytoplasm with DNA and ribosomes, plasma membrane, cell wall, and capsule. Endospores are dehydrated (10-30% of water content of vegetative cells), metabolically inactive cells with an unusually high content of calcium dipicolinate (~ 10% of its dry weight) which is assumed to stabilise the densely packed DNA.

Several resistant dormant forms of endospores are known: centrally (Fig. 2a and Fig. 2b with distention of the mother cell), terminally (Fig. 2c and Fig. 2d and 2e with distention of the mother cell), and laterally arranged (Fig. 2f with distention of the mother cell).

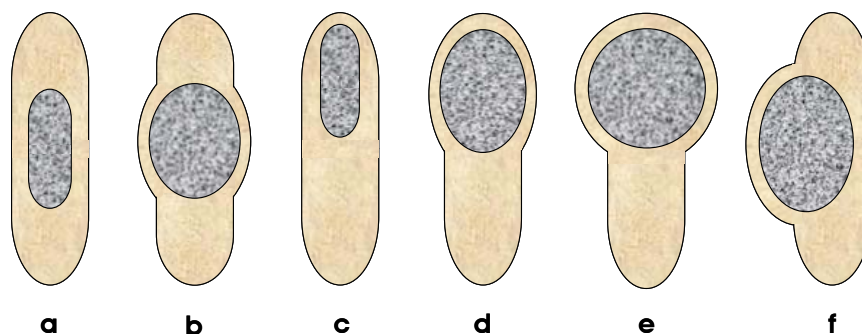


Figure 2. Intracellular Location of Endospores. (a) central (*B. megaterium*), (b) central, mother cell fusiform swollen (*B. polymyxa*), (c) terminal (*B. thuringiensis*), (d) terminal, mother cell swollen (*B. macerans*), (e) terminal, mother cell drumstick-shaped swollen (*B. sphaericus*), and (f) lateral, mother cell fusiform swollen (*B. laterosporus*) (modified from Fuchs and Schlegel, 2006)).

Formation of endospores proceeds as a multistage differentiation programme induced upon nutrient starvation and stress exposure (Sonenshein et al., 1993). Cultures of Gram-positive bacteria develop endospores during the vegetative growth cycle at the transition to stationary phase, for instance. Thereby, lack of food is the initiating signal to start the sporulation process.

Regulation of cell differentiation is mediated by extra- and intra-cellular signals. The two-component system (phosphorelay) senses the primary environmental stimuli and is further implicated in signal transduction and cellular response (Hoch, 1993). Following stages of morphogenesis, which generate the mother and the daughter cell (the spore) are governed mainly by alternative sigma factors. Alternative σ -factors only become active while the cell is exposed to extraordinary circumstances. As part of the RNA polymerase (RNAP), σ -factors recognise specific promoters and initiate transcription of required genes.

2.4 Endospore Formation in *Bacillus subtilis*

Bacillus subtilis is a Gram-positive organism which exhibits the ability to adapt to unfavourable conditions by protecting its genome in robust endospores by sporulation (Errington, 2003; Sonenshein et al., 1993). Endospore formation in *B. subtilis* is a complex seven-step cell differentiation process (Fig. 3) (Errington, 2003). After replication of the DNA, in stage I, septum formation begins near each of the poles of the vegetative cell, denoted as the predivisional cell. The DNA condenses while the septum at one side of the predivisional cell stops its further development. Two different cells are generated by asymmetrical division of the vegetative cell: the mother cell and the prespore (stage II). In stage III, the prespore is engulfed by the mother cell. The small compartment is then surrounded by a double membrane. From this stage on, the prespore is termed forespore. In the mother cell the DNA decomposes while in the forespore chamber it becomes dense during association with small acid-soluble spore proteins (SASP) for protection. At this time, the forespore dehydrates and calcium dipicolinate is incorporated. Stage IV is designated by the formation of the cortex which consists of a

modified form of peptidoglycan and is synthesised between the membranes which separate the cells. A second protective layer, the coat, composed of approximately 50 different proteins, is arranged around the forespore in stage V. Maturation and eventually release of the spore by lysis of the mother cell (stage VI and VII) completes the sporulation cycle (Fig. 3) (Errington, 2003; Wang et al., 2006).

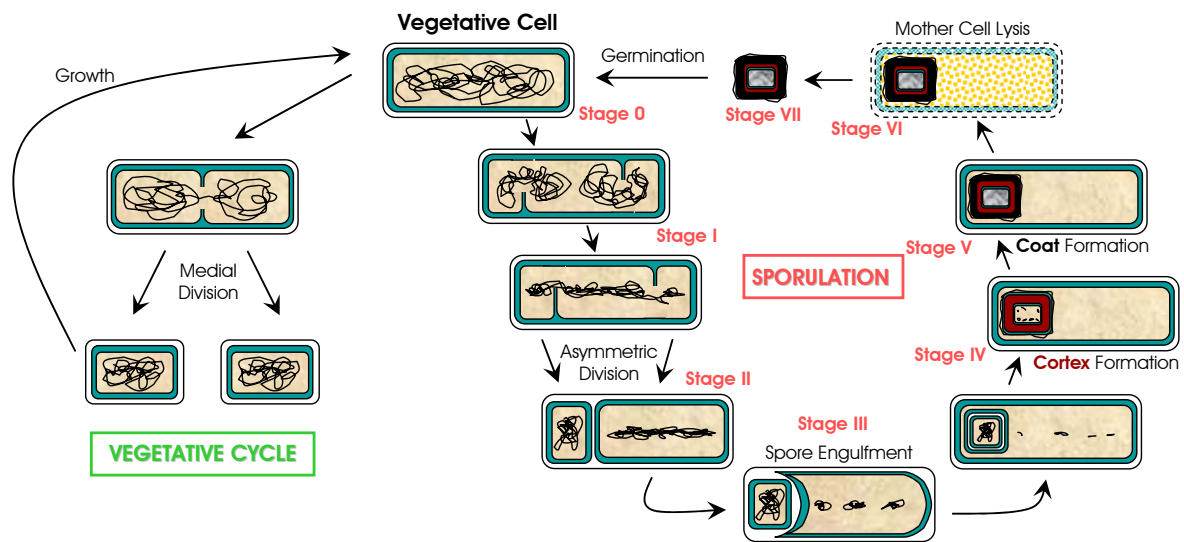


Figure 3. Stages in Endospore Formation and Vegetative Cell Cycle of *B. subtilis*. Simplified schematic representation of vegetative reproduction of a *B. subtilis* cell (left, green) compared to its sporulation cycle during endospore formation (right, red) (created on the basis of Brock et al., 1994).

This alternate life-form can remain dormant for many years. The appearance of beneficial conditions converts the endospore back into a vegetative cell by germination and growth which then is capable of entering the vegetative life cycle (Fig. 3).

2.4.1 σ - and Transcription Factors

The cell differentiation process leading to endospore formation in *B. subtilis* is controlled by the action of five alternative sigma factors which regulate gene transcription in a temporal and cell-type specific manner (Errington, 2003; Wang et al., 2006). In *B. subtilis*, there are at least 17 different alternative σ -factors known which are dedicated to different promoter specificities and trigger changes in the pattern of gene expression (Kunst et al., 1997).

At an early stage of sporulation, in the predivisional cell σ^H is required which directly activates transcription of certain sporulation genes, e.g. the master regulator for entry into sporulation Spo0A (Britton et al., 2002). In the prespore, the sigma factor σ^F becomes active, immediately followed by the activation of σ^E in the mother cell. The concerted action of σ^F and σ^E between the mother and the prespore cell line is implicated in the correct asymmetric division progress during differentiation in *B. subtilis* (Errington, 2003; Wang et al., 2006). 262 genes are switched on under σ^E control, 48 genes are regulated by the prespore-specific σ^F -factor (Wang et al., 2006). In turn, another σ -factor in the prespore is released: σ^G , which governs the engulfment event and influences expression of 95 regulatory and structural genes. σ^K is the final mother cell-specific sigma factor and decisive in the late stage of spore development by turning on ~ 75 genes. Throughout the action of the inter-connected programmes between the two different cell compartments, the expression level of 504 genes is affected (Wang et al., 2006).

Further modulation of gene expression within each of these regulons is achieved by additional specific transcriptional regulators. Specific transcription factors are necessary to mediate RNAP's gene transcription specificity by recruiting the attached σ -factors. In contrast, general transcription factors show a wide variety of activity in regulating gene expression.

For the sporulation-specific transcription factors SpoIIID, GerE, RsfA, and SpoVT, a direct dependence on σ^E , σ^K , σ^F , and σ^G , respectively, was determined (Steil et al., 2005; Wang et al., 2006) (Fig. 4).

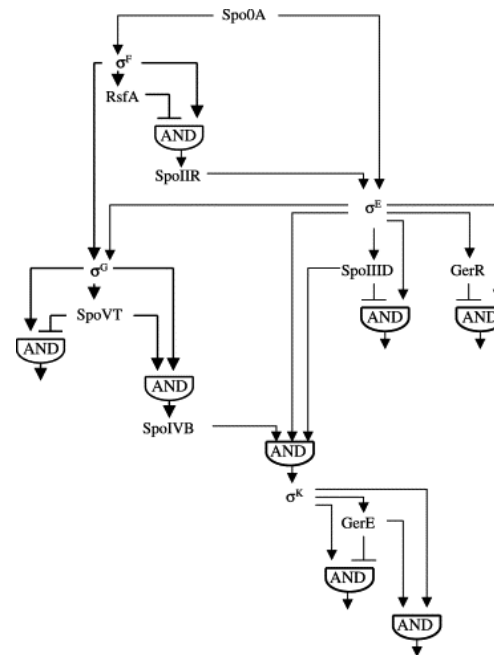


Figure 4. Interplay of σ - and Transcription Factors during Sporulation in *B. subtilis*. Regulatory circuits for the predivisional cell, the forespore, and the mother cell governing sporulation (Wang et al., 2006). AND gates are indicated.

Transcription factors play an important role during the differentiation process since they are the ultimate targets of signal-transduction pathways. Finally, the specific transcription factors regulate endospore formation by binding to a specific DNA site (or set of sites) and thus control the expression of genes (Stragier and Losick, 1996).

Transcription factors can act as inducers or repressors and as activators. Repressors bind to DNA and block transcription of a gene, whereas inducers enable gene transcription by dissociation from DNA. Activating transcription factors enhance the affinity of RNAP to DNA by binding to the activator site which is close to the promoter. In case of far distance between activator site and promoter, association of the transcription factor to DNA enforces DNA looping and thereby allows RNAP to form correct contacts with the promoter region.

For the regulation of the transcription factors itself, there are two levels which can be influenced: the synthesis and the activity of the transcription factor. The rate of synthesis controls the available concentration of the transcription factor. Chemical (post-translational) modification, ligand binding, dimerisation, interactions with co-factors, etc. govern the activity of the transcription factor and affect its DNA-binding affinity.

Activity regulated transcription factors often show a typical assembly composed of a DNA binding domain (DBD), a ligand binding domain or a signal sensing domain (SSD), and occasionally a trans-activation domain (TAD); the latter for binding to other proteins. Transcription factors of *B. subtilis* are at least two-domain proteins offering a DBD (mostly N-terminal) and a multimerisation domain/SSD (often C-terminal) as a result of diverse duplication events (Moreno-Campuzano et al., 2006).

DBDs mostly bind to palindromic or tandem repeats of DNA called transcription factor binding site or response element. In the majority of cases, transcription factors are dimeric, mostly homodimeric, predestined to bind to two consecutive major grooves of the DNA-binding site which usually spans a region of ~ 20 base pairs (bp). In bacteria, the most common DBD structure motif is the so-called winged helix-turn-helix (HTH) motif (Fig. 5a, (Zhao et al., 2002)). Others, like the Zinc-finger (ZnF), helix-loop-helix (HLH), RNA-binding-like domains, and β -sheet anti-parallel DBD (Fig. 5b, (Newman et al., 1998)) are present in a significantly minor proportion (Pabo and Sauer, 1992; Pérez-Rueda and Collado-Vides, 2000; Pérez-Rueda et al., 2004).

DNA-binding via α -helices is based on shape and size most suitable for docking into the major groove of B-DNA (Pabo and Sauer, 1992). Usually, the recognition helix of the HTH structure adapts to the major groove of DNA while the second helix supports the positioning of the first helix and stabilises the interaction (Fig. 5a).

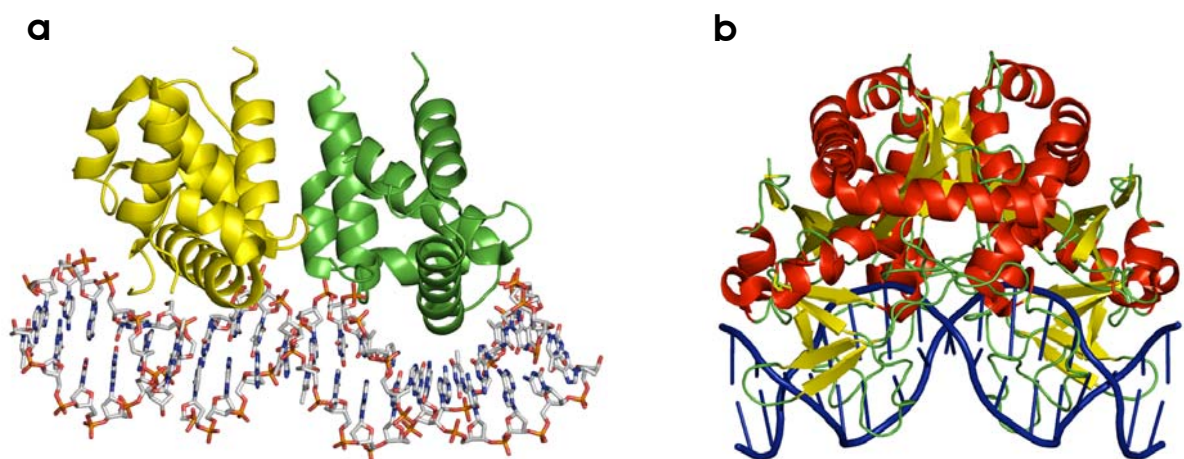


Figure 5. DNA-Binding Structure Motifs. Crystal structure of dimeric (a) effector domain of *B. subtilis* Spo0A presenting a winged HTH DBD (PDB 1LQ1) coloured by monomers and (b) type II restriction endonuclease *BglI* of *B. globigii* showing a β -sheet anti-parallel DBD (PDB 1DMU) coloured according to secondary structure elements, each in complex with its target DNA (left in element colour coded sticks, right cartoon presentation in blue).

In *B. subtilis*, 47% of the whole transcription factor repertoire contains a winged HTH DBD. The transcription factors of *B. subtilis* are classified into 51 different families (based on HMM search and PFAM) presenting a broad variety in the number of family members (Moreno-Campuzano et al., 2006). 19 families include only one member and are presumably important in specific cellular processes. These are for sporulation and related procedures e.g. two families which specify each one of the global regulators AbrB and CodY (Moreno-Campuzano et al., 2006).

2.4.2 σ^G -dependent Transcription Factor SpoVT

Recently, the σ^G -dependent transcription factor SpoVT was grouped into the newly defined class of AbrB-like transcription factors (Coles et al., 2005). Members of the large superfamily are characterised by their DBD which folds into an anti-parallel β -barrel. A precise understanding of the interaction mode between this new structural DBD motif and DNA is missing because of the lack of structural data.

B. subtilis SpoVT coordinates gene expression in the small forespore chamber, which is destined to become the mature dormant spore. SpoVT not only acts as a transcriptional activator, but also as a repressor, whereupon the expression level of 47 genes is affected (Wang et al., 2006). Most of these are of unknown function but also include a spore cortex-lytic enzyme (*sleB*), a sporulation specific SASP (*csgA*), and germination response receptors which are repressed by SpoVT (Igarashi and Setlow, 2006; Wang et al., 2006). Genes coding for e.g. flavohemoglobin (*hmp*), a spore cortex protein (*coxA*), and SASPs are activated by SpoVT (Wang et al., 2006). In addition, for the expression of the SpoVT regulator itself, auto-regulation by binding to its own promoter region in association with σ^G is noted (Dong et al., 2004) (Fig. 6).

at t t t t g t t a c t c t c t g g **TGTATAT** t a c a t t t g a t g t g a c g **GATACTAAT** t t c **aa** g c g a g g c g g a a g g t a c a t a a a
 g t a a c t g c t t t a g g t c t t t c c c a c a t g t a t a t a c c a t c a a a t g **aaagagagg** c a c c a g a g a t g a a a g c a a c c g g t
M K A T G

Figure 6. Promoter Region of *B. subtilis* spoVT. -35 and -10 regions of *spoVT* promoter are highlighted in bold and red capital letters, ribosome binding site is shown in bold green. Start point of transcription is in bold orange and orientation is shown by an arrow. Blue letters indicate start of SpoVT protein coding sequence. Corresponding amino acids are in bold blue capital letters (modified from Bagyan et al., 1996).

B. subtilis *spoVT* mutants have a poorly assembled spore coat (Fig. 7) and are germination defective (Bagyan et al., 1996; Le Breton et al., 2006). SpoVT thus plays an indispensable role in the late stage (stage V) of spore formation and, hence, assures survival of the genetic information.

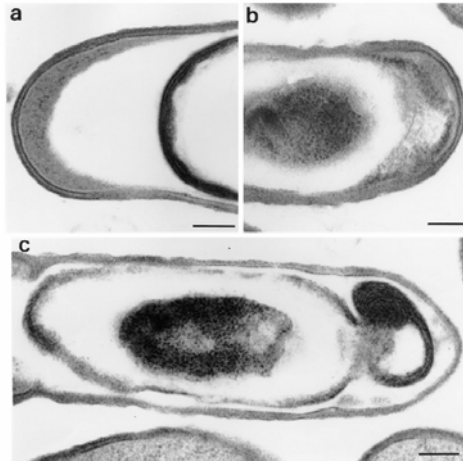


Figure 7. SpoVT Mutant Sporangium. EM micrograph of mature (a) wild type and (b, c) mutant spores in *B. subtilis* cells. Outer coat layer of wild type spores appears in black while absent in mutant spores. In c, misassembled coat material conglomerates at one of the poles (Bagyan et al., 1996).

SpoVT of *B. subtilis* is a protein of 178 amino acids (Fig. 8a), with a molecular weight of 19.7 kDa. SpoVT contains two domains: an N-terminal DBD (residues 1-48) and a C-terminal domain which is much larger (residues 56-178), unique, and obviously important for the structure and function of SpoVT (Dong et al., 2004). The domains are connected by a linker comprising the amino acids 49-55 (Fig. 8b).

a

```

1                                     75
atgaaagcaaccggtatcgtacgtcgtattgatgacttaggtcgggtcgtgattcctaagaaattcgaagaact
1                                     25
M K A T G I V R R I D D L G R V V I P K E I R R T
76                                     150
ctgagaatcaggggaaggcgatccgcttgagattttttagatcgtgacggagaagtgattttgaaaaagtactct
26                                     50
L R I R E G D P L E I F V D R D G E V I L K K Y S
151                                     225
ccgatcagtgagcttgagacttttgcaaaggagtatgcagacgcgctttacgacagcctcggccattcagtgtg
51                                     75
P I S E L G D F A K E Y A D A L Y D S L G H S V L
226                                     300
atgtgtgatcgtgatgtatatattgccgtgtccggcagctccaaaaaagattacttaaacaagtcaatcagcgaa
76                                     100
I C D R D V Y I A V S G S S K K D Y L N K S I S E
301                                     375
atgctggaaagaacaatggatcagcgcagctccgtgcttgagagtgatgcgaaatcagtacagcttgtgaatgga
101                                    125
M L E R T M D Q R S S V L E S D A K S V Q L V N G
376                                     450
attgatgaggacatgaattcttatactgtaggcccaattgtggcgaacgggtgatccgatagggtgctgtggtgatc
126                                    150
I D E D M N S Y T V G P I V A N G D P I G A V V I
451                                     525
ttttcaaaagatcagacaatggggcgaagtagagcataaagccgttgaaacagcagctggatttttggctcgtcaa
151                                    175
F S K D Q T M G E V E H K A V E T A A G F L A R Q
526                                     537
atggaacagtag
176                                     178
M E Q

```

b

Figure 8. Sequence and Schematic Domain Organisation of *B. subtilis* SpoVT. (a) DNA (small letters) and amino acid (capital letters in bold blue) sequence of *B. subtilis* SpoVT. (b) Schematic illustration of the domain organisation of *B. subtilis* SpoVT. Residues defining the domains are indicated.

The DBD of SpoVT has 68% sequence identity (80% similarity) with the N-terminal region of the transcription regulator AbrB (Dong et al., 2004), a key transition state regulator of *B. subtilis* that acts during the transition from vegetative growth to sporulation (Strauch et al., 2005). SpoVT thus belongs to the superfamily of swapped-hairpin transcription factors which fold into homo-dimeric β -barrels via four pairs of interleaved β -hairpins (Benson et al., 2002).

The C-terminal domain of SpoVT was predicted by sequence comparisons to be a GAF (cGMP-specific and -stimulated phosphodiesterases, *Anabaena* adenylate cyclases and *Escherichia coli* EhIA) domain (Söding et al., 2005). GAF domains are represented in a broad range of signal transduction and sensory pathways (SSDs) and protein regulatory systems in all three domains of life (Ho et al., 2000; Martinez, Beavo et al., 2002; Zoraghi et al., 2004). Proteins containing GAF domains typically bind small molecules to exert regulatory functions and thus, GAF domains belong to the widespread small-molecule-binding domains (SMBD) (Anantharaman, 2001). Adenylyl and guanylyl cyclases i.e. catalyse cyclic nucleotide synthesis and PDEs (phosphodiesterases) hydrolyse cGMP (Aravind and Ponting, 1997) or offer a dual specificity for cAMP and cGMP (Zhang et al., 2004). Others bind signal molecules like *N*-(3-oxo-octanoyl)-L-homoserine lactone as it was observed for TraR (Vannini et al., 2002) or show ligand binding specificity towards GTP and the branched-chain amino acids (BCAA) isoleucine and valine as discovered for the GAF domain of CodY of *B. subtilis* (Handke et al., 2008; Levdikov et al., 2006). Some GAF domains do not bind any ligand and may have purely a structural function through dimerisation (Ho et al., 2000; Martinez, Wu et al., 2002). GAF domains show a compact α/β fold with a core sheet of typically five or six anti-parallel β -strands which is flanked by α -helices on one side and by the ligand binding pocket on the other side. This characteristic GAF domain setup can vary with the number of β -sheets and flanking α -helices throughout all GAF domains.

2.5 Scope of Work

Endospore formation in Gram-positive bacteria is a precisely controlled cell differentiation process. SpoVT is a key regulator in the late forespore development during endospore formation in *Bacillus subtilis*.

The transcription factor SpoVT was predicted to integrate two different types of domains: a swapped-hairpin β -barrel which presents a new structural DBD-motif of transcription factors and a GAF domain. GAF domains mostly are SSDs or act as multimerisation modules but its association to a swapped-hairpin β -barrel is novel. The designated GAF domain of SpoVT is essential for the DNA-binding specificity of the transcription factor but the mode of regulating the activity of SpoVT is not understood.

The goal of this work is to solve the molecular structure of *B. subtilis* SpoVT by X-ray crystallography in order to confirm the predicted architecture of the transcription factor. Furthermore, structural and biochemical investigations should deliver insights into the functionality of SpoVT and give answers to following questions:

- Is the DBD of SpoVT highly similar to AbrB in structure and probably in DNA-binding properties?
- Does SpoVT form an oligomer since AbrB-like transcription factors are known to exert their regulatory functions in a tetrameric state?
- What is the role of the SpoVT GAF domain?

3. RESULTS

3.1 Overexpression and Purification of *B. subtilis* SpoVT

3.1.1 SpoVT Full-length

Protein overexpression of SpoVT full-length (SpoVT_{FL}, residues 1-178, Fig. 9a), was accomplished in *E. coli* as described in 6.1.2.1 and 6.2.1. The His₆-tagged protein was purified by immobilised metal affinity chromatography (IMAC) (see 6.2.2 and 6.3.1.1) (Fig. 9b). Elution fractions containing the SpoVT_{FL} protein of 20.6 kDa molecular weight (Fig. 9b) were pooled and dialysed against MOPS (3-morpholinopropane-1-sulfonic acid) buffer (see 5.3.2 and 6.2.10). Increased purity for 3D-crystallisation trials and rabbit immunisation for antibody production was obtained by gel filtration chromatography (see 6.3.1.2) (Fig. 9c).

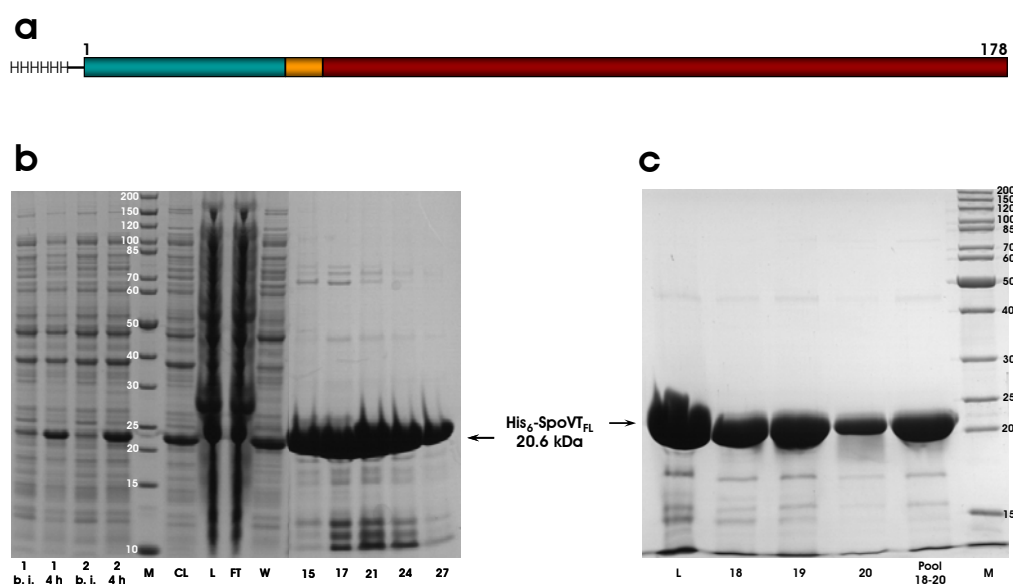


Figure 9. Purification of His₆-tagged SpoVT_{FL}. (a) Schematic illustration of the N-terminally His₆-tagged SpoVT_{FL} with histidines (H) and residues at the N- and C-terminus indicated. (b, c) SDS-PAGE analyses of the (b) initial purification step by IMAC and (c) second purification step by gel filtration chromatography. Shown are samples of *E. coli* cultures 1 and 2 before induction (b. i.) and after 4 h expression (4 h), cell lysate (CL), load (L), flow through (FT), wash (W), elution fractions (15, 17, 21, 24, 27; 18–20), and pooled fractions (Pool 18–20) together with a molecular weight marker (M). M proteins are labelled with corresponding masses in kDa and SpoVT_{FL} protein (20.6 kDa) is specified.

3.1.2 C-terminal Domain of SpoVT

The C-terminal domain of SpoVT (SpoVT_{CT}, residues 56-178, Fig. 10a), was produced and isolated similar as described for SpoVT_{FL} (see 3.1.1) (Fig. 10b).

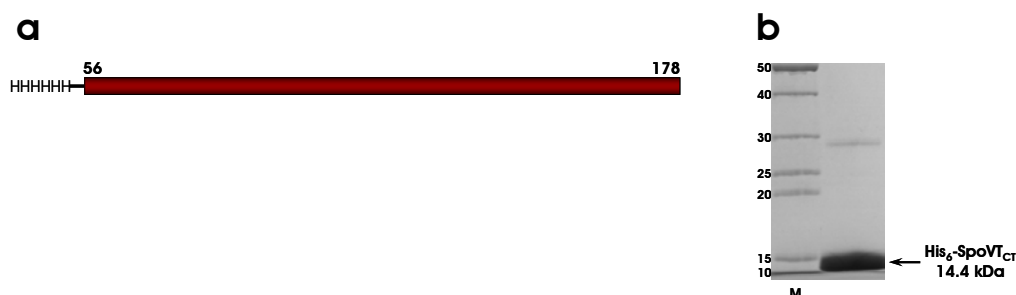


Figure 10. Purified His₆-tagged SpoVT_{CT}. (a) Schematic illustration of the N-terminally His₆-tagged SpoVT_{CT} with histidines (H) and residues at the N- and C-terminus indicated. (b) SDS-PAGE analysis of purified SpoVT_{CT}. Molecular weight marker (M with masses of proteins in kDa) and SpoVT_{CT} protein (14.4 kDa) are specified.

The seleno-methionine (Se-Met) derivate of SpoVT_{CT} for structure solution by X-ray crystallography methods was produced and purified by Dr. Sergej Djuranovic, MPI of Developmental Biology, Tübingen* (Djuranovic, 2007).

3.2 Biochemical Analysis of *B. subtilis* SpoVT

3.2.1 Secondary Structure and Thermal Stability

The SpoVT_{FL} and SpoVT_{CT} proteins overexpressed in *E. coli* were both properly folded, as judged by circular dichroism (CD) spectroscopy (see 6.4.2) (Fig. 11). The shape of the curve obtained from SpoVT_{CT} (Fig. 11, green curve) indicates a protein with a significantly higher content of α -helical structure elements than the SpoVT_{FL} protein (Fig. 11, blue curve).

* Present adress: Howard Hughes Medical Institute, Department of Molecular Biology and Genetics, Johns Hopkins University School of Medicine, Baltimore, Maryland 21205, USA

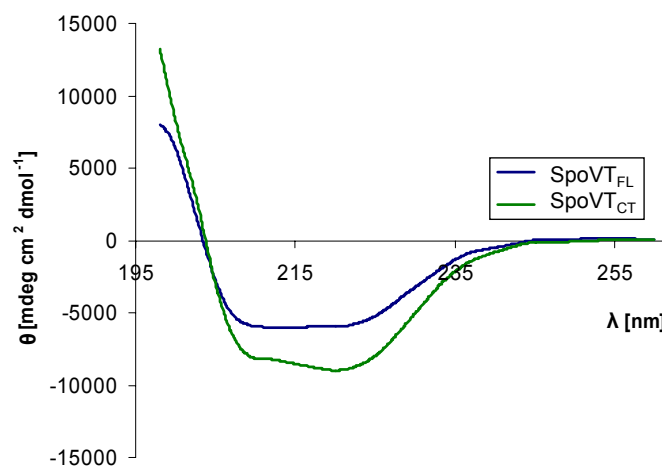


Figure 11. CD Spectroscopy of SpoVT_{FL} and SpoVT_{CT}. CD spectra of SpoVT_{FL} and SpoVT_{CT} protein solutions in blue and green lines, respectively.

Estimations of secondary structure content for SpoVT_{FL} resulted in 17% α -helices and 31% β -sheets and for SpoVT_{CT} in contents of 25% α -helices and 25% β -sheets. The estimations for all secondary structure elements are listed in Table 1.

Secondary Structure	SpoVT _{FL}	SpoVT _{CT}
α -helix	17.2%	24.7%
Anti-parallel β -sheet	24.7%	18.5%
Parallel β -sheet	6.1%	6.2%
β -turn	16.5%	15.1%
Random Coil	33.1%	31.2%
Total Sum	97.6%	95.7%

Table 1. Secondary Structure Contents of SpoVT_{FL} and SpoVT_{CT}. Estimated secondary structure contents of SpoVT_{FL} and SpoVT_{CT} based on CD spectroscopy data (see Fig. 11) within a wavelength range of 200 nm to 260 nm.

The temperature dependent conformational stability of the proteins in solution was studied by thermal denaturing experiments recorded via CD spectroscopy methods (see 6.4.2). Sigmoid melting curves were determined for both proteins, indicating a single-step transition in each case (Fig. 12). The midpoint transition temperature for SpoVT_{FL} was 323 K and 314 K for SpoVT_{CT} (Fig. 12), showing a reduced stability of SpoVT_{CT} against thermal denaturation compared to the full-length protein. Obviously, auxiliary interactions, which are dependent on the presence of the N-terminal domain, stabilise SpoVT_{FL}. The denaturations were not reversible as the proteins precipitated during heating (Fig. 12).

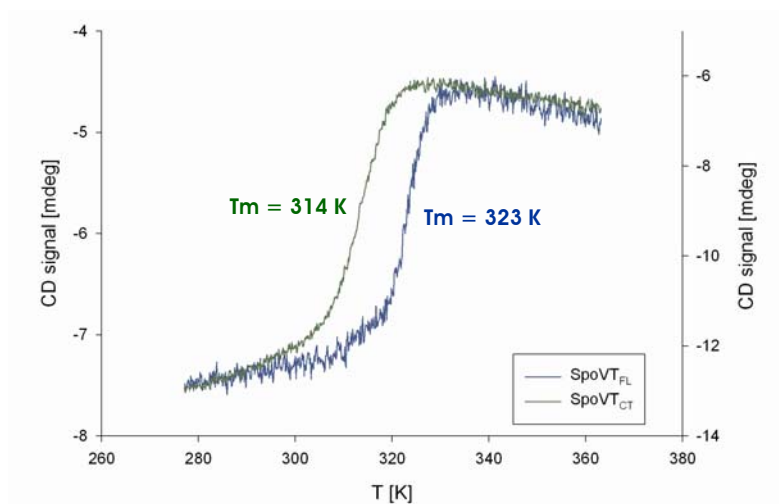


Figure 12. Thermal Denaturing of SpoVT_{FL} and SpoVT_{CT}. Melting curves of SpoVT_{FL} (blue) and SpoVT_{CT} (green) determined by CD spectroscopy. Midpoint transition temperatures (T_m) are indicated in each case.

3.2.2 Oligomeric Form

3.2.2.1 Covalent Linkage

Chemical crosslinking (see 6.2.13) is used to determine oligomeric forms of a protein via SDS-PAGE analysis (see 6.2.6). The crosslink products of the reaction between glutaraldehyde and SpoVT_{FL} or SpoVT_{CT} are shown in Figure 13.

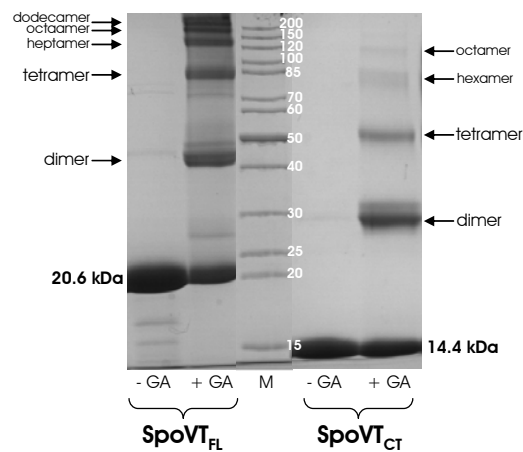


Figure 13. Crosslinking of SpoVT_{FL} and SpoVT_{CT}. SDS-PAGE analysis of chemically crosslinked SpoVT_{FL} (left) and SpoVT_{CT} (right) with 0.025% glutaraldehyde (+GA). Protein samples without glutaraldehyde (-GA) are added in each case with monomeric molecular mass of proteins indicated (kDa). Respective oligomeric states of crosslink products are specified. Proteins of molecular weight marker (M) are highlighted by their mass (kDa).

SpoVT_{FL} showed in crosslinking experiments several oligomeric forms which appeared in approximately similar amounts (Fig. 13). Dimers (~ 40 kDa) and tetramers (~ 80 kDa) were formed in addition to oligomers of high molecular weights which were defined as heptamers (140 kDa), octamers (160 kDa), and dodecamers (220 kDa). In contrast, SpoVT_{CT} mainly associated into dimers (30 kDa) (Fig. 13). Low amounts of tetramers (60 kDa) and very low amounts of hexamers (90 kDa) and octamers (120 kDa) were detected, additionally.

3.2.2.2 Native State

In gel filtration experiments, both proteins eluted as single peaks (Fig. 14) indicating monodisperse protein solutions. Analysis of the peak fractions by SDS-PAGE confirmed the monomeric molecular mass of SpoVT_{FL} (20.6 kDa, Fig. 14) and SpoVT_{CT} (14.4 kDa, Fig. 14). Using a Superdex 75 column (see 6.3.1.2), SpoVT_{FL} eluted at a retention time of 28 min corresponding to a tetrameric protein complex of ~ 80 kDa (Fig. 14). SpoVT_{CT} elution occurred at a retention time of 37 min representing a dimeric protein domain of ~ 30 kDa (Fig. 14).

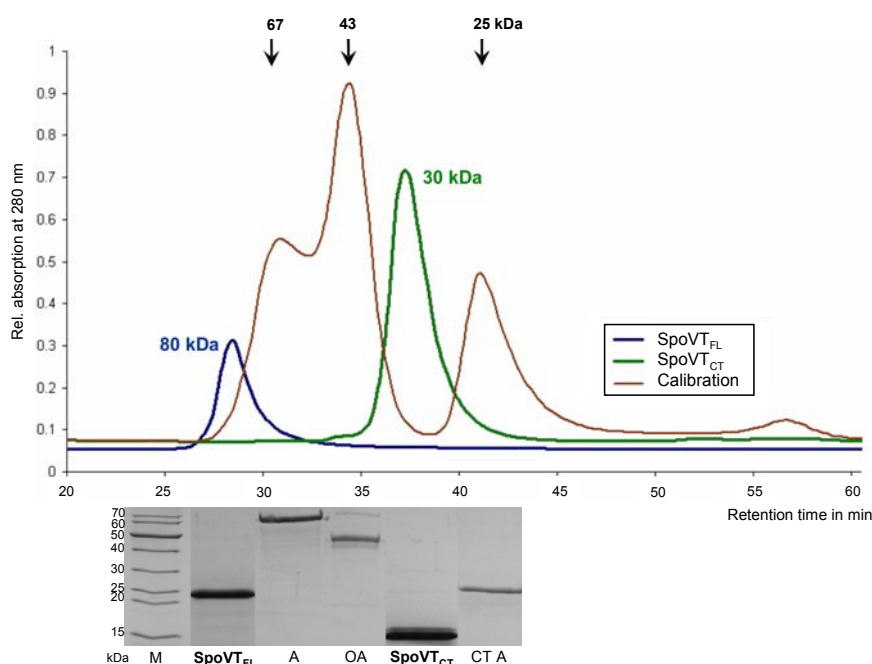


Figure 14. Gel Filtration Chromatography of SpoVT_{FL} and SpoVT_{CT}. Gel filtration chromatogram of SpoVT_{FL} and SpoVT_{CT} using a Superdex 75 column with elution profiles in blue and green, respectively. Column calibration, depicted as a red curve, was performed with albumine (A, 67 kDa), ovalbumine (OA, 43 kDa), and chymotrypsinogen A (CT A, 25 kDa). SDS-PAGE analysis of peak fractions is illustrated by the gel below. Proteins of molecular weight marker (M) are specified.

3.2.3 Immunological Detection of Native SpoVT

3.2.3.1 Generation of Polyclonal Rabbit Anti-SpoVT Antibodies

Polyclonal anti-SpoVT antibodies were generated by rabbit immunisation using two-step purified His₆-tagged SpoVT_{FL} (see 6.2.2 and 6.3.1.2) overexpressed in *E. coli* at a concentration of 2.31 mg*ml⁻¹ in 1x PBS buffer (see 5.3.2). Antibody production was boosted by three consecutive rabbit immunisations (see 6.2.3). Finally, ~ 35 ml of rabbit blood were obtained which left ~ 20 ml blood serum containing the polyclonal anti-SpoVT antibodies. A 1:5000 dilution of the blood serum detected by far < 20 ng of the antigen in an initial immuno (western) blotting experiment (see 6.2.9), judging a sufficient sensitivity of the anti-SpoVT antibodies against the antigen (Fig. 15).

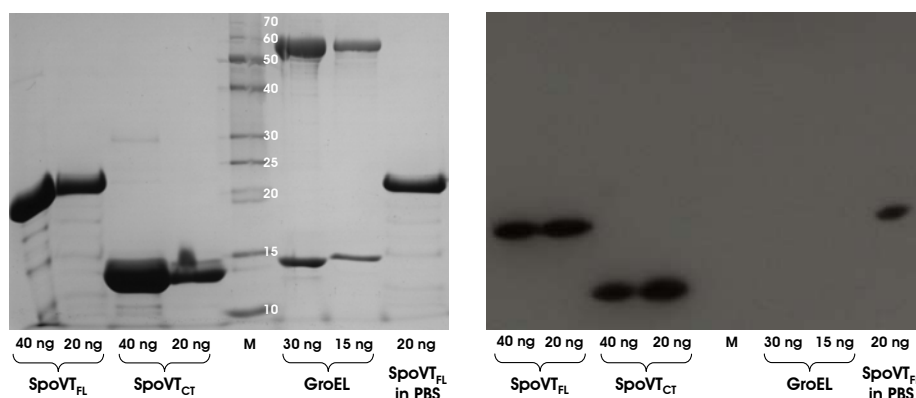


Figure 15. Sensitivity of Polyclonal Rabbit Anti-SpoVT Antibodies. SDS-PAGE analysis (left) and developed X-ray film of equivalent immuno blot (right) of an initial test of rabbit blood serum (1:5000 dilution) containing polyclonal anti-SpoVT antibodies. Applied proteins (His₆-tagged SpoVT_{FL}, 20.6 kDa; His₆-tagged SpoVT_{CT}, 14.4 kDa; and GroEL, 57.2 kDa) in different amounts (40, 30, 20, and 15 ng) and molecular weight marker (M, kDa) are specified.

3.2.3.2 Purification of Polyclonal Anti-SpoVT Antibodies

The polyclonal anti-SpoVT antibodies were purified from rabbit blood serum by affinity chromatography (see 6.2.4) (Fig. 16). The antigen was coupled to an affinity medium as bait which specifically immobilises the antibodies from the serum. Elution of the antigen-antibody complex was performed by a pH-shift.

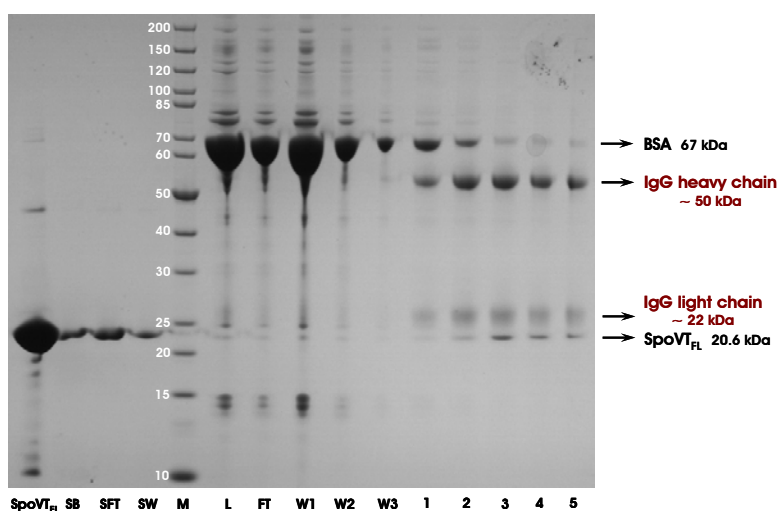


Figure 16. Purification of Anti-SpoVT Antibodies. SDS-PAGE analysis of purification of anti-SpoVT antibodies via affinity chromatography showing samples of the antigen (SpoVT_{FL}), SpoVT_{FL} coupled to affinity beads (SB), flow through (SFT) and wash (SW) of coupling procedure, blood serum (load, L), serum flow through (FT), washing steps (W1-W3), and elution fractions (1-5). Molecular weight marker (M) and proteins of the eluates are specified and labelled with respective masses in kDa.

Eluates 2-5 (Fig. 16) were pooled and extensively dialysed against 1x PBS buffer (see 6.2.10). During the dialysis procedure, proteins precipitated and efforts in solubilisation and refolding the denatured protein agglomerates were not successful. Changing of dialysis conditions regarding temperature and application of glycerol for protein protection did not improve the stability of the proteins. Purification of 1 ml rabbit blood serum yielded ~ 1.1 mg anti-SpoVT antibodies.

3.2.3.3 Synchronisation of *B. subtilis* Cells and Induction of Sporulation

For detection of homologously expressed native SpoVT, *B. subtilis* cells were synchronised and sporulation was induced by exhaustion in DSM medium as written in 6.1.2.3 – 6.1.2.5. Growth curve determination of *B. subtilis* cells in liquid culture is described in 6.1.2.7 (Fig. 17).

The developmental expression profile of SpoVT in *B. subtilis* was determined by Bagyan et al. (Bagyan et al., 1996). According to this, SpoVT expression starts 2.5 h ($t = 150$, blue figure, Fig. 17) after initiation of sporulation ($t = 0$, blue figure, Fig. 17) and increases continuously within the following 3.5 h. 2.5 h after entering the stationary phase ($T_{2.5}$, green arrow, Fig. 17), SpoVT attains its highest expression level (Bagyan et al., 1996).

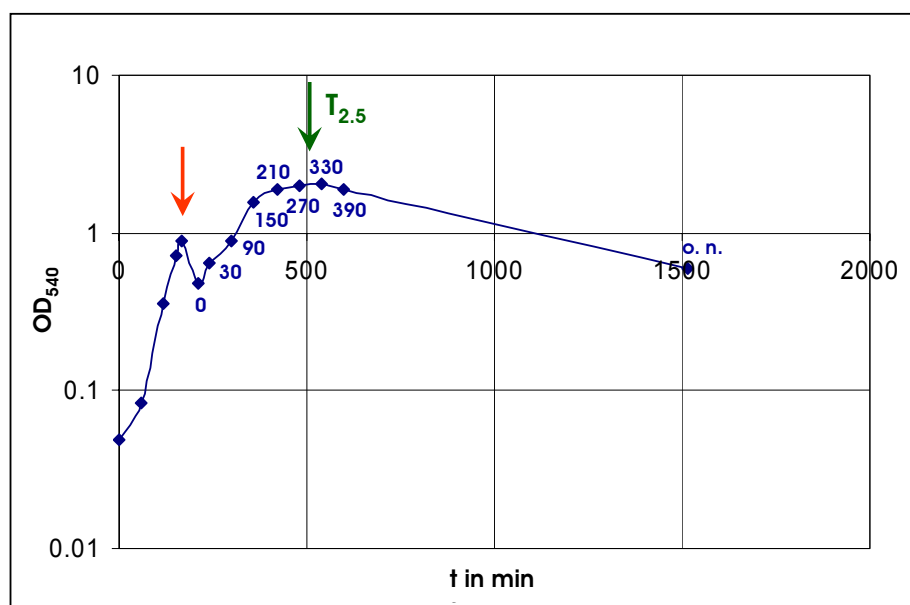


Figure 17. Growth Curve of Synchronised Sporulating *B. subtilis* Cell Culture. Growth curve of synchronised *B. subtilis* cell culture with arrow in orange indicating harvest of cells from LB medium. Figures in blue count for cultivation in DSM medium. Green arrow points at term of presumed highest SpoVT expression level ($T_{2.5}$).

Endospore formation was verified by light microscopy (LM) inspection of cells after spore staining (see 6.1.2.8) in comparison to *B. subtilis* cells which were not incited to sporulate (LB medium) (see 6.1.2.3) (Fig. 18).

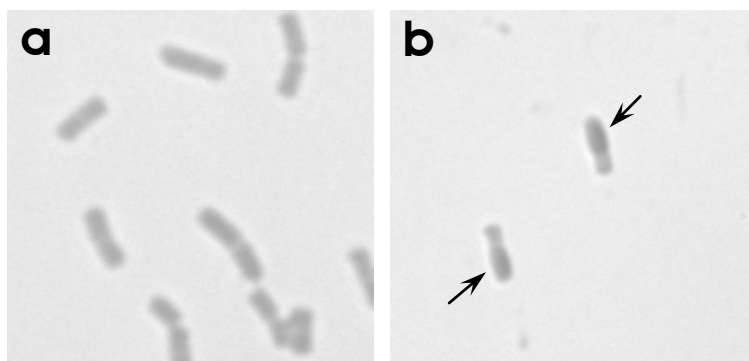


Figure 18. Black-and-white Shots of LM-micrographs of *B. subtilis* Cells. (a) Vegetative life-form of *B. subtilis*. (b) Terminal endospores in *B. subtilis* cells and distention of mother cells are indicated with arrows. Stained spores appear as dark cell compartments.

3.2.3.4 Immuno Blotting

Samples of sporulating *B. subtilis* cells, taken from liquid culture at different stages of development (see Fig. 17, blue figures), were treated as described in 6.3.6. Solutions containing solubilised spore proteins were analysed by immuno (western) blotting using polyclonal rabbit anti-SpoVT antibodies (see 3.2.3.2) as the primary antibody. As the secondary antibody, goat anti-rabbit IgG linked to horseradish peroxidase was applied (see 6.2.8 and 6.2.9). Figure 19 shows an image of an X-ray film which was exposed to the chemoluminescent agent treated membrane of such an immuno blotting experiment.

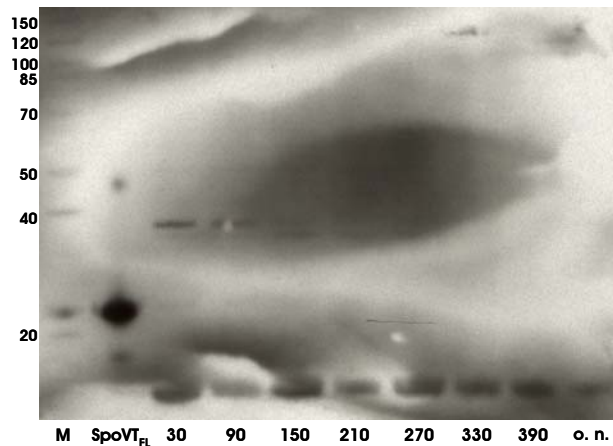


Figure 19. Western Blot Analysis of Spore Extracts. Developed X-ray film of western blot experiment analysing spore extracts drawn from *B. subtilis* cell culture at denoted time points (30 – 390 min and over night (o. n.)) as described in Figure 17 using specific anti-SpoVT antibodies. Purified SpoVT_{FL} (~ 100 ng) is added as positive control. Proteins of molecular weight marker (M) are specified (kDa).

Detection of SpoVT in *B. subtilis* spore extracts using anti-SpoVT antibodies failed (Fig. 19). A protein of low molecular weight (below 10 kDa) was recognised by the anti-SpoVT antibodies in each sample applied to western blot experiments (30 min - o. n., Fig. 19). In samples taken from the sporulating culture till its entry into the stationary phase ($t = 150$, see Fig. 17), a protein of about 38 kDa and during the stationary phase ($t = 150 - 270$), a protein of a slightly lower molecular mass was recorded by the anti-SpoVT antibodies (Fig. 19). It is assumed that this might be due to unspecific interactions. Variations in the experimental setup concerning the amount of applied spore proteins and/or anti-SpoVT antibodies had no influence.

3.3 3D-Crystallisation and Structural Analysis of *B. subtilis* SpoVT

3.3.1 X-ray Crystallography

3D-crystallisation experiments were carried out by Dr. Sergej Djuranovic, MPI of Developmental Biology, Tübingen* as described in 6.4.1.1. The protein solutions of SpoVT_{FL}, SpoVT_{CT}, and the Se-Met derivate of SpoVT_{CT} have been adjusted to final concentrations of 10 and 20 mg*ml⁻¹ (see 6.2.11).

The SpoVT_{FL} crystals were of a robust cubic morphology (Fig. 20a) grown with addition of 1 M NaCl, 100 mM cacodylate pH 6.5, 30% (v/v) PEG (polyethyleneglycol) 600, and 10% (v/v) glycerol (Emerald BioSystems, Cryo screen II, condition 6). Crystals of SpoVT_{CT} can be described as clusters of thin and tapered plates (Fig. 20b) and emerged in 200 mM NaCl, 100 mM HEPES (4-(2-hydroxyethyl)-1-piperazineethanesulfonic acid) pH 7.5, and 25% (w/v) PEG 3350 (Hampton Research, Index screen, condition 72) while its Se-Met derivate produced fragile tubular crystals in 200 mM MgCl₂, 100 mM HEPES pH 7.5, and 25% (w/v) PEG 3350 (Hampton Research, Index screen, condition 84). The initial crystallisation condition of the Se-Met protein was optimised by application of additives (Hampton Research, Additive screen, see 6.4.1.1). Fast-growing Se-Met SpoVT_{CT} crystals appeared in clusters of tubes, needles, and/or plates of variable size (Fig. 20c). After an incubation period of 3.5 months, in conditions including 3% (w/v) dextran sulfate Se-Met SpoVT_{CT} crystals of a different morphology re-emerged. These slow-growing SpoVT_{CT} Se-Met crystals formed single crystals of a hexagonal cigar-like shape in different dimensions (Fig. 20d).

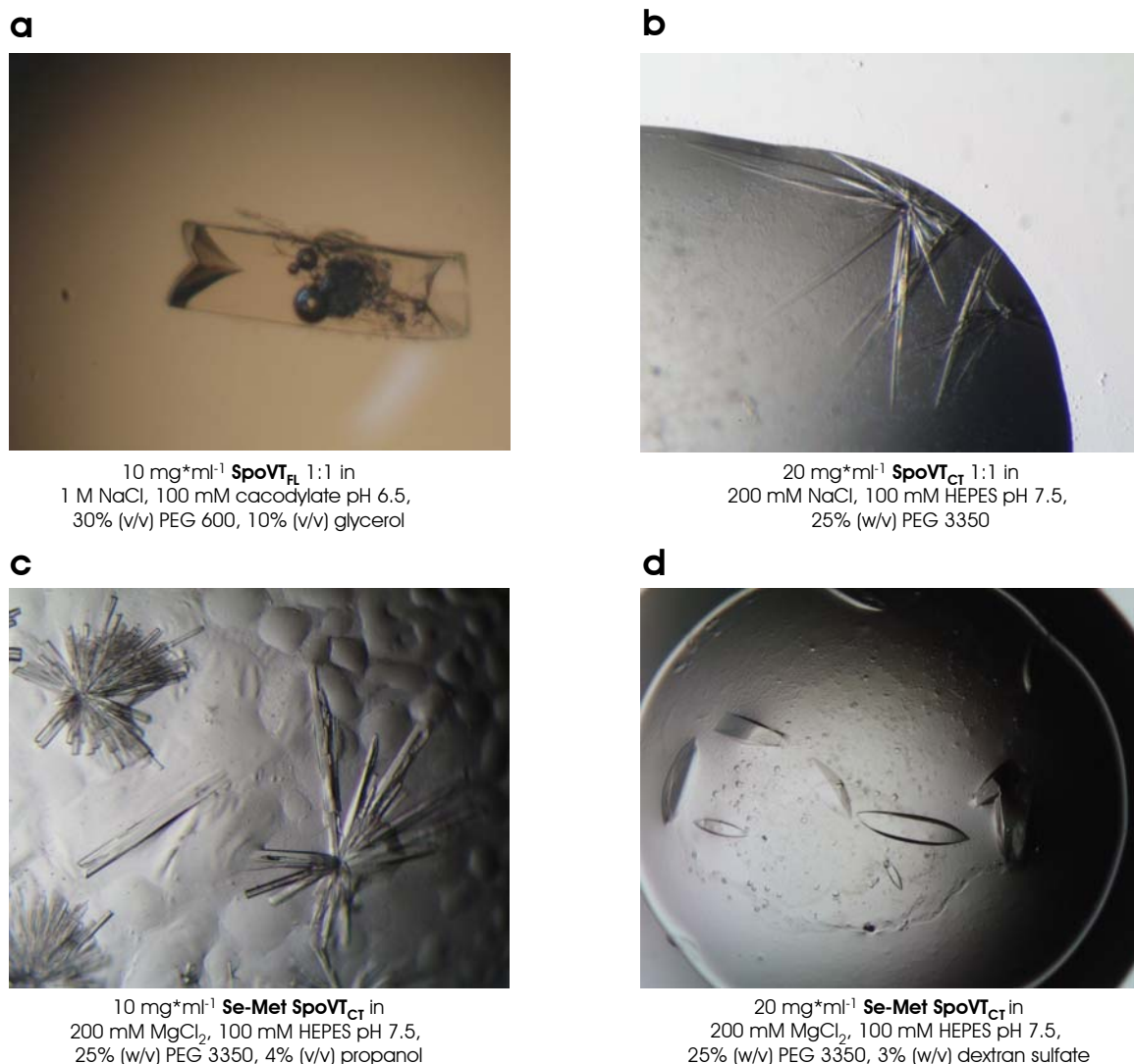


Figure 20. Protein Crystals of SpoVT. Light microscope images of protein crystals of (a) SpoVT_{FL}, 0.5 x 0.15 x 0.15 mm, (b) SpoVT_{CT}, 0.5-0.1 x 0.07-0.03 x 0.02-0.01 mm, (c) Se-Met SpoVT_{CT} fast-growing, 0.2 x 0.03 x 0.03 mm, and (d) SeMet SpoVT_{CT} slow-growing, 0.4-0.1 x 0.1-0.03 x 0.1-0.03 mm. Crystallisation conditons and protein concentrations are added in each case.

Single protein crystals were mounted in cryo loops (see 6.4.1.2), frozen, and exposed to X-ray radiation at the SLS beamline X10SA PXII at the PSI in Villigen, Switzerland. X-ray diffraction images were recorded on a mar225 CCD detector (Fig. 21). Data for SpoVT_{FL} were aquired at a wavelength of 0.978 Å, for SpoVT_{CT} and its Se-Met derivate at 0.979 Å (see 6.4.1.2).

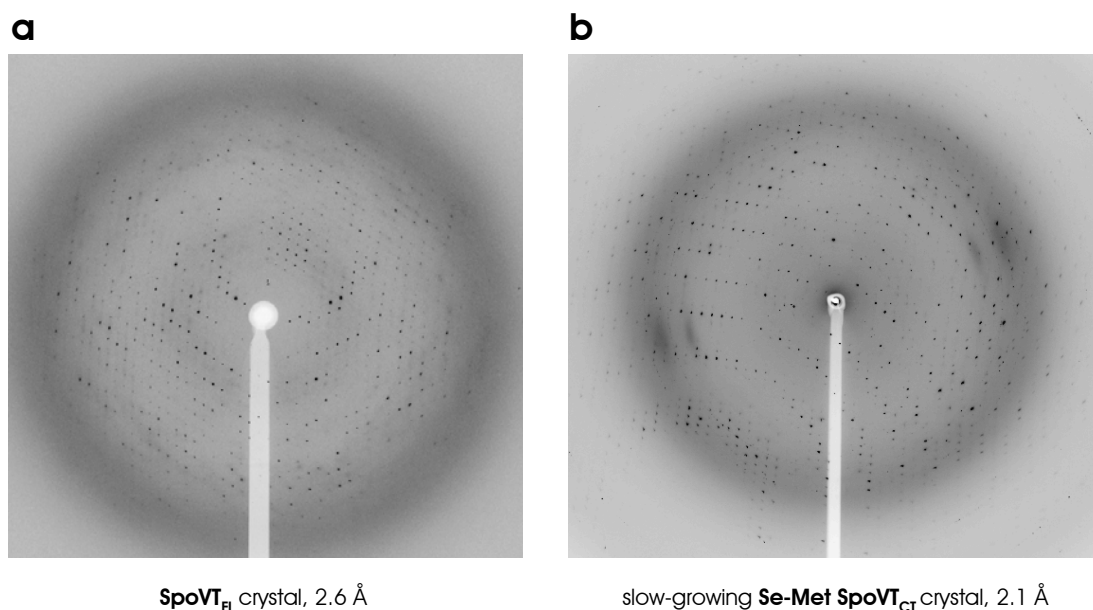


Figure 21. Diffraction Images of SpoVT Crystals. Diffraction images of protein crystals of (a) SpoVT_{FL} and (b) slow-growing Se-Met SpoVT_{CT} with respective resolutions.

The native crystals diffracted to resolutions of 2.6 Å for SpoVT_{FL} (Fig. 21a) and 1.5 Å for SpoVT_{CT} (data not shown). The fast-growing SpoVT_{CT} Se-Met crystals diffracted poorly to only 3.5 Å with a diffraction pattern showing multiple lattices caused by the cluster formation of the crystals (data not shown). For the slow-growing crystals of the Se-Met derivate, a resolution of 2.1 Å was obtained (Fig. 21b) and a highly redundant SAD (single anomalous dispersion) dataset at the selenium absorption edge was collected (see 6.4.1.2).

SpoVT crystals occurred in the tetragonal crystal form and space group $P4_32_12$. The unit cell of the Se-Met derivate of SpoVT_{CT} showed dimensions of $a = b = 64.6$ and $c = 78.6$ Å, $\alpha = \beta = \gamma = 90^\circ$. R_{merge} and $\langle I/\sigma(I) \rangle$ were defined to 8.5 and 14.3 for resolution range 20.0-2.06 Å, respectively. Native SpoVT_{CT} crystallised in a slightly smaller unit cell with dimensions of $a = b = 63.9$ and $c = 77.3$ Å. For resolution range 20.0-1.50 Å, an R_{merge} of 6.3 and $\langle I/\sigma(I) \rangle$ of 14.8 was determined. The unit cell of SpoVT_{FL} was considerably bigger and of dimensions $a = b = 94.5$ and $c = 110.8$ Å, $\alpha = \beta = \gamma = 90^\circ$. R_{merge} and $\langle I/\sigma(I) \rangle$ of 10.5 and 13.9, respectively were specified for resolution range 20.0-2.60 Å. Data collection statistics are shown in more detail in Table 2.

<i>Data Collection</i>	<i>Se-Met SpoVT_{CT}</i>	<i>Native SpoVT_{CT}</i>	<i>Native SpoVT_{FL}</i>
Residues	56-178	56-178	1-178
Wavelength (Å)	0.979	0.979	0.978
Resolution Range (Å)	20.00 - 2.06	20.00 - 1.50	20.00-2.60
(outer shell)	(2.19 - 2.06)	(1.71 - 1.50)	(2.80 - 2.60)
Crystal form	tetragonal	tetragonal	tetragonal
Space group	P4 ₃ 2 ₁ 2	P4 ₃ 2 ₁ 2	P4 ₃ 2 ₁ 2
Cell dimensions (Å)	$a = b = 64.6, c = 78.6$	$a = b = 63.9, c = 77.3$	$a = b = 94.5, c = 110.8$
Unique reflections	19148 (2866)	25488 (3818)	18815 (2783)
Observed reflections	220814 (31146)	182057 (28670)	177074 (20904)
Redundancy	11.5 (10.9)	7.1 (7.5)	9.4 (7.5)
Completeness (%)	97.8 (91.3)	99.0 (100)	99.4 (90.4)
R_{merge} (%)	8.5 (26.9)	6.3 (25.4)	10.5 (46.2)
$I/\sigma(I)$	14.3 (4.7)	14.8 (4.5)	13.9 (3.0)

Table 2. X-ray Data Collection Statistics. Collected X-ray data of protein crystals of SpoVT_{CT} Se-Met derivate, native SpoVT_{CT}, and native SpoVT_{FL}.

3.3.2 Phasing and Density Fitting

X-ray data analysis of Se-Met SpoVT_{CT} determined six selenium sites which were located using Patterson methods (Patterson, 1934). The experimental phases were determined at 2.1 Å (see 6.4.1.3) (Terwilliger, 2000; Terwilliger and Berendzen, 1999). The calculated Matthews coefficient of 2.9 and a solvent content of 58.1% (Matthews, 1968) suggested that the asymmetric unit of SpoVT_{CT} is consisting of one molecule.

The structure of SpoVT_{FL} was solved by molecular replacement (see 6.4.1.3) using the refined model of SpoVT_{CT} as search model (Vagin and Teplyakov, 1997). Attempts to complete the SpoVT_{FL} structure by molecular replacement using one chain of the NMR-structure of the N-terminal part of the homologous AbrB protein (PDB entry 1YFB) failed. Solvent flattening techniques were applied to improve the quality of the phases and an electron density was achieved by reducing the model bias via prime-and-switch phasing (RESOLVE, (Terwilliger, 2003)). The SpoVT_{FL} structure was completed by density fitting the N-terminal part of AbrB, AbrB_{NT} (PDB entry 1YFB), into the improved and averaged map (see 6.4.1.4). Two SpoVT_{FL} monomers were found in the asymmetric unit and a Matthews coefficient of 3.2 and solvent content of 61.1% was determined (Matthews, 1968).

3.3.3 Model Building and Structural Refinement

With the data of the Se-Met derivate of SpoVT_{CT}, RESOLVE (Terwilliger, 2003) built a partial model of SpoVT_{CT} automatically (Fig. 22). Missing parts of the protein were built manually by placing appropriate amino acids into the electron density map. The model was refined by iterative cycles of manual model rebuilding (Emsley and Cowtan, 2004) and refinement (Murshudov et al., 1997) (see 6.4.1.4) and later refined against the native data set of SpoVT_{CT} at 1.5 Å. The improved quality of the electron density gained by the refinement processes is illustrated in Figure 22. 138 solvent waters were added automatically (Perrakis et al., 2001) and the refined model of SpoVT_{CT} showed an $R_{\text{cryst}}/R_{\text{free}}$ ratio of 19.7%/22.6% and a good stereochemistry (see Table 3). The SpoVT_{CT} model consisted of 120 consecutive amino acids. The N-terminal His₆-tag and the following amino acid as well as the last two residues of the protein domain were missing due to a low quality of the electron density at the N- and C-terminus of the structure.

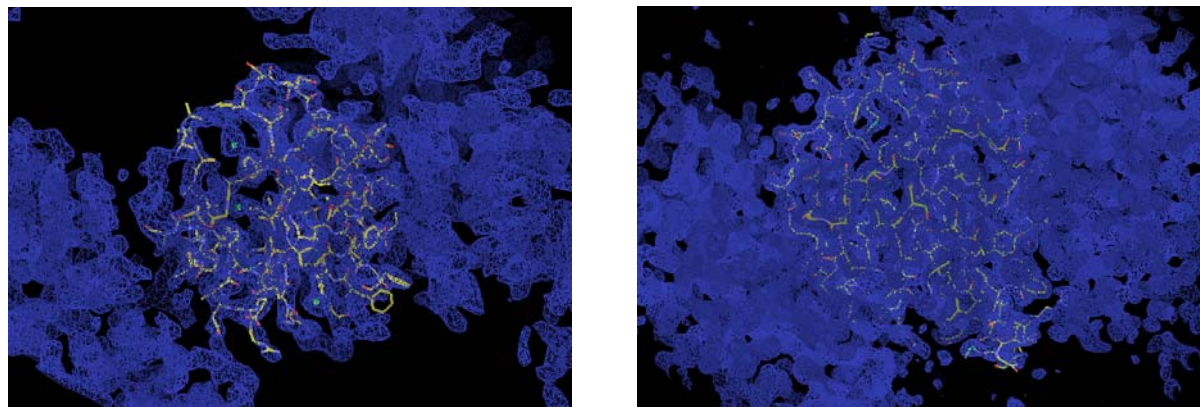


Figure 22. Electron Density of SpoVT_{CT} Data. Initial (left) and improved (right) electron density of SpoVT_{CT} data including initial fragmentary and completed SpoVT_{CT} model, respectively. Electron density map is shown in blue at 1.5 σ and chain of SpoVT_{CT} model is coloured by atoms.

The initial SpoVT_{FL} model was constituted from two protein domains; SpoVT_{CT}, which was solved as described above, and AbrB_{NT}, deposited at the PDB under accession number 1YFB. Residues different between the N-terminus of SpoVT (SpoVT_{NT}, amino acids 1-48) and AbrB_{NT} were exchanged and missing domain connecting residues were placed

manually. The model was refined by several cycles of manual model rebuilding and automatically structural refinement with twin lattice symmetry (TLS) and NCS restraints. For TLS refinement, the two different domains of SpoVT_{FL} were defined as two separate rigid bodies (amino acids 2-51 and 56-177). The TLS parameters were refined for each molecule of the asymmetric unit. NCS restraints were placed between these two monomers. NCS-related atoms were defined as two regions spanning the amino acids 10-49 and 57-175, leaving the domain connecting linker unrestrained. The current model of SpoVT_{FL} consists of four chains with residues 2–176 for chain A and C (N-terminal His₆-tag, initial methionine, and two amino acids at the C-terminus absent) and residues 4-176 for chain B and D (N-terminal His₆-tag, following three amino acids, and two residues at the C-terminus absent) with proper stereochemistry and an $R_{\text{cryst}}/R_{\text{free}}$ ratio of 23.4%/28.6%. 28 water molecules were found. All refinement data statistics are shown in Table 3.

Refinement	Native SpoVT_{CT}	Native SpoVT_{FL}
Residues	56-178	1-178
Resolution range (Å)	20.00-1.50	20.00-2.60
Unique reflections	24816	15100
$R_{\text{cryst}}/R_{\text{free}}$ (%)	19.7/22.6	23.4/28.6
No. of protein atoms	1038	2668
No. of waters	138	28
r.m.s.d. of bond length (Å)	0.01	0.02
r.m.s.d. of bond angles (°)	1.3	2.2
Average <i>B</i> factor (Å ²)	55.7	64.8
Ramachandran plot statistics, residues		
in most favoured regions (%)	92.3	84.2
in add. allowed regions (%)	5.8	13.5
in gen. allowed regions (%)	1.0	1.6
in disallowed regions (%)	1.0	0.6

Table 3. X-ray Data Refinement Statistics. Refinement of X-ray data of SpoVT_{CT} and SpoVT_{FL}.

3.4 Structure of *B. subtilis* SpoVT

3.4.1 Crystal Packing

SpoVT proteins crystallised in a primitive tetragonal Bravais lattice (Pt) with space group $P4_32_12$. The space group defines a 4-fold axis with two perpendicular diagonal 2-fold axes (point group 422). The 2-fold screw axis (2_1) defines a rotation of 180° and $\frac{1}{2}$ translation (Fig. 23a1 and b1) and the 4-fold screw axis (4_3) describes a rotation of 90° and translation of $\frac{3}{4}$ of the unit cell (Fig. 23a2 and b2).

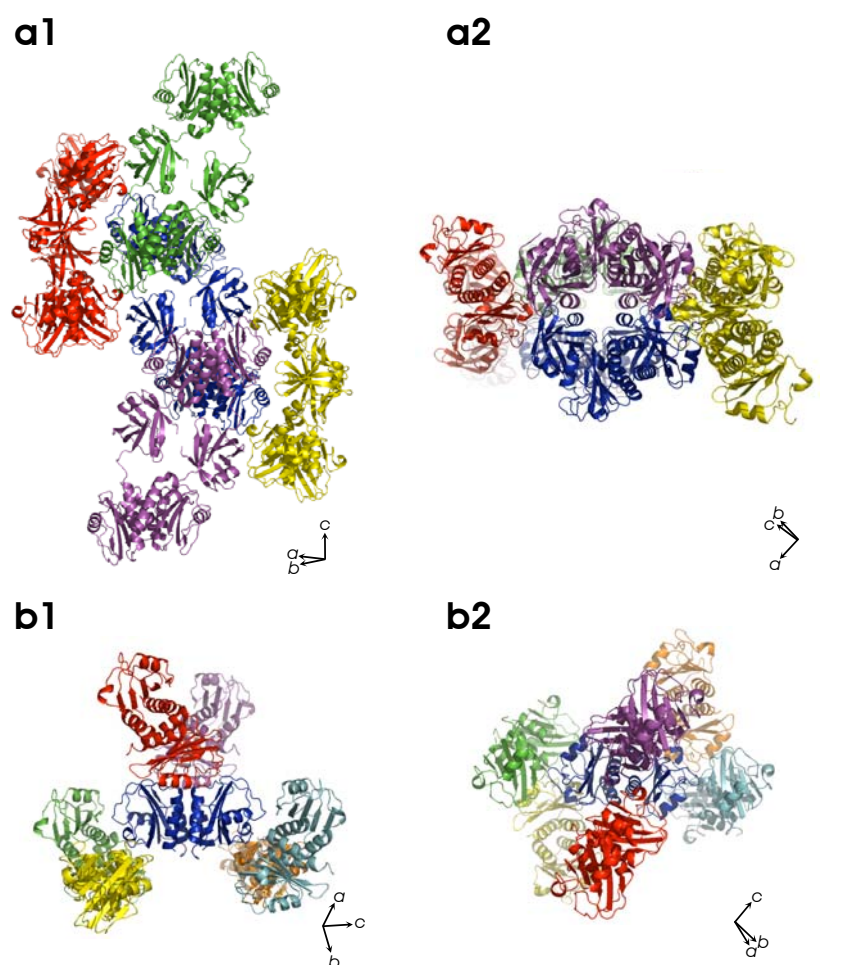


Figure 23. Crystal Packing of SpoVT Crystals. Crystal packing of (a) SpoVT_{FL} and (b) SpoVT_{CT} in space group $P4_32_12$ with homotetramers and homodimers in different colours, respectively. (a1) and (b1) show view along the 2-fold screw axis and (a2) and (b2) along the 4-fold screw axis.

3.4.2 Overall Fold of Tetrameric Complex

The structure of SpoVT_{FL} determined by X-ray crystallography revealed that native SpoVT_{FL} forms a complex of four monomers (chain A, B, C, and D, Fig. 24a). The SpoVT_{FL} tetramer is an elongated protein complex with dimensions of approximately 10 x 5 x 5 nm (Fig. 24) and of a convex shape (Fig. 24b). The tetrameric complex forms a spiral with an overall twist of about 50° which can be observed in the stereogram of the SpoVT_{FL} model in Figure 25.

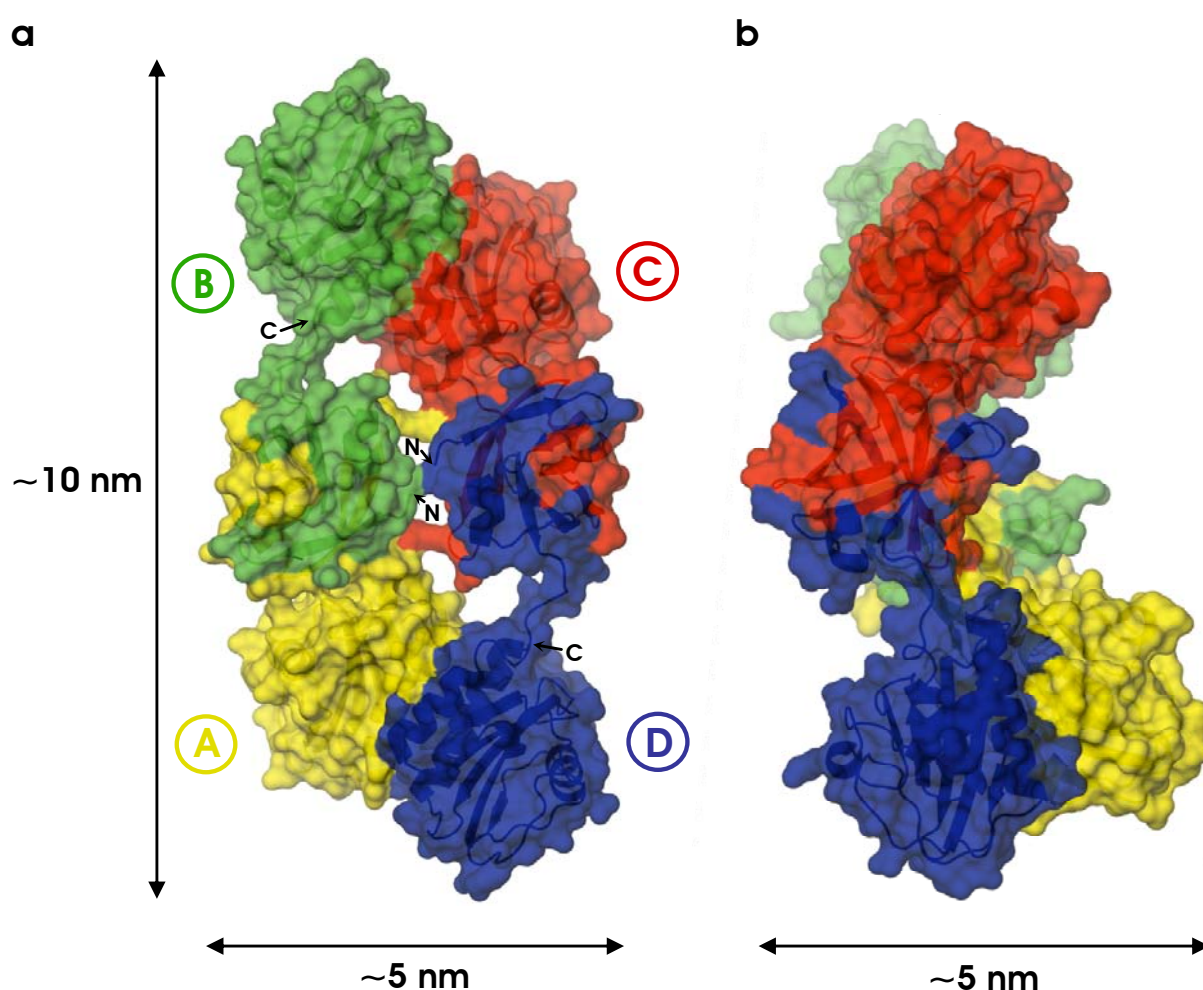


Figure 24. Overall Fold of SpoVT_{FL} Tetramer. Transparent surface representation with underlying C_α traces showing secondary structure elements of the SpoVT_{FL} tetramer. Tetramers are coloured by monomers (chain A in yellow, B in green, C in red, and D in blue). (a) Topview with monomers, dimensions, and N- and C-termini of monomers B and D indicated. (b) Presentation similar to (a) with focus onto the convex shape.

The SpoVT_{FL} complex is a dimer of dimers. Monomers associate pairwise via their SpoVT_{NT} domains and the dimers further assemble through their SpoVT_{CT} domains which extend in opposite directions (Fig. 24 and Fig. 25). Thereby, the SpoVT_{NT} domains form a core-like structure which is surrounded by the SpoVT_{CT} domains. The SpoVT_{FL} tetramer shows an overall asymmetry based on an anti-parallel arrangement of asymmetric dimers (Fig. 24 and Fig. 25). Thus, in the tetramer, monomer A is the symmetry equivalent to monomer C and monomer B to monomer D (Fig. 24a).

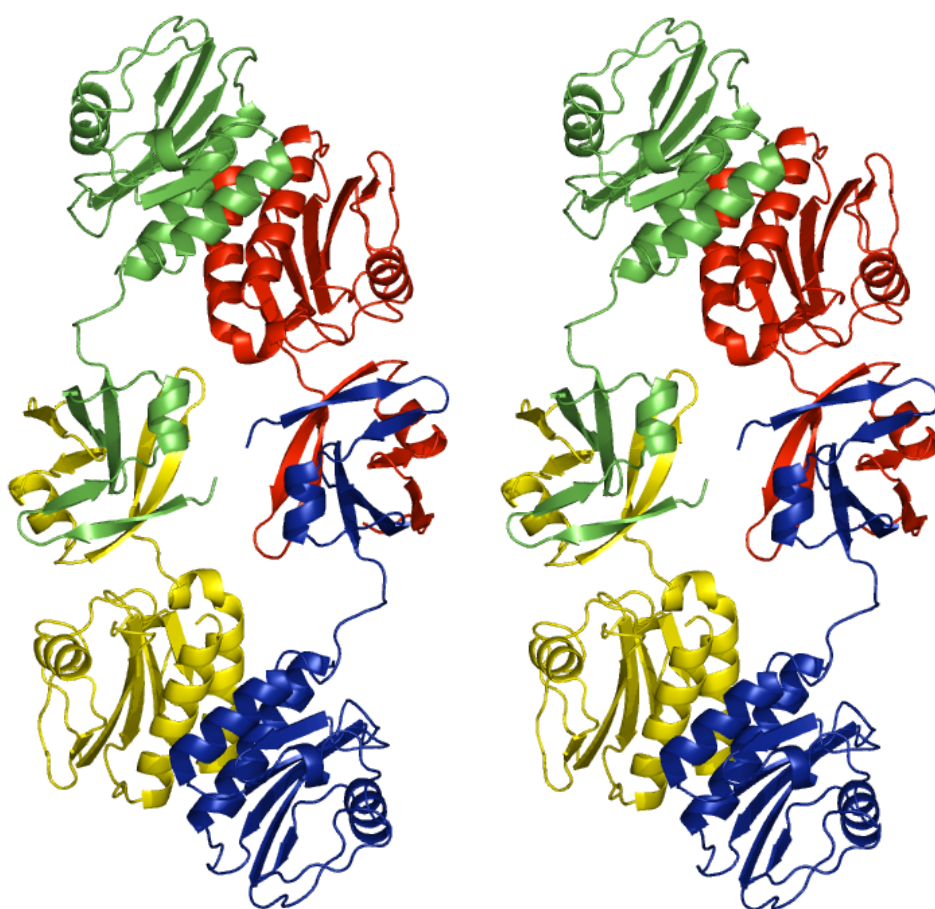


Figure 25. Stereo Presentation of SpoVT_{FL} Tetramer. Cartoon illustration of the tetrameric SpoVT_{FL} with colour code as shown in Figure 24.

3.4.3 Asymmetric Tetramer

The asymmetric SpoVT_{FL} dimers are curved with a bend of $\sim 80^\circ$ and the central SpoVT_{NT} domains shifted by about 6 Å (Fig. 26a). The asymmetry of the dimer is based on different conformations of the monomers (Fig. 26a). In the crystal structure of SpoVT_{FL}, a monomer with an elongated overall fold showing an expanded domain connecting linker, termed *E*, and a more compact monomer with a conjoined and structured inter-connecting linker, termed *S*, is obvious (Fig. 26a).

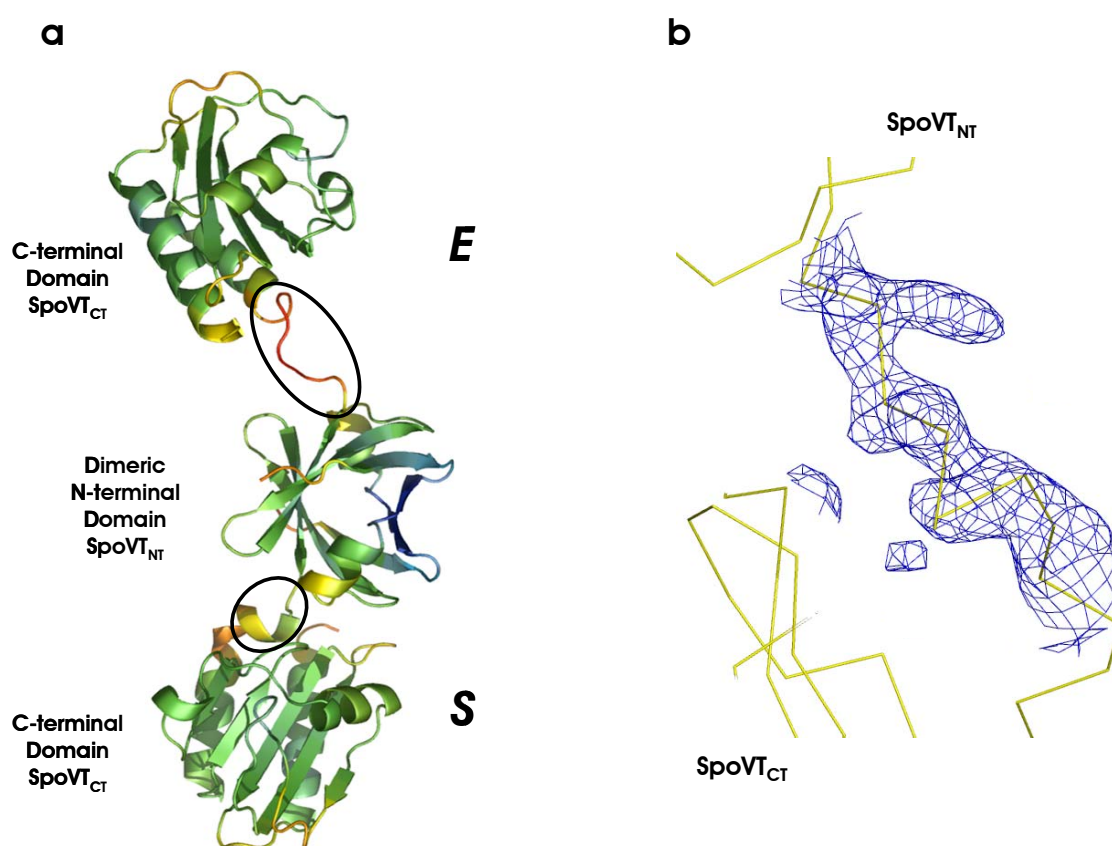


Figure 26. Asymmetry of SpoVT_{FL} and Structured *S* Linker. (a) Cartoon presentation of SpoVT_{FL} dimer in colours according to calculated B-factors from high (red) to low (blue) values. Domains are indicated and connecting linkers are marked by ellipses. Monomers are termed according to the conformation of the linker; *E* (elongated) and *S* (structured). (b) Electron density of the *S* linker peptide. *S* monomer is depicted in yellow in a ribbon presentation with domains denoted. Electron density map is shown in blue at 1.2 σ .

The residues composing the linker in *E* have high B-factors and a poor quality of the electron density in the central linker region together indicate a substantial flexibility (Fig. 26a). The linker in *S* is more well-defined (Fig. 26b) and contributes to the

stabilisation of the SpoVT_{FL} tetramer. Two pairs of salt bridges (Arg40 and Glu54) are formed between the opposing S monomers A and C (Fig. 27a). These constrain the flexibility of the linker and lead to the formation of an α -helical turn in this region (Fig. 26). The resulting rotation of SpoVT_{NT} relative to SpoVT_{CT} arranges the two domains that they interact via two salt bridges between residues Arg29 and Asp80, and Arg27 and Glu103, respectively (data not shown).

Residues stabilising the S conformation are highly conserved among the SpoVT orthologs taken for the alignment in Figure 27b, except for the amino acid Arg40 regarding SpoVT from *Caldicellulosiruptor saccharolyticus*.

These intra- and intermolecular salt bridges within the SpoVT_{FL} tetramer are supposed to support the unusual asymmetry of the entire protein complex.

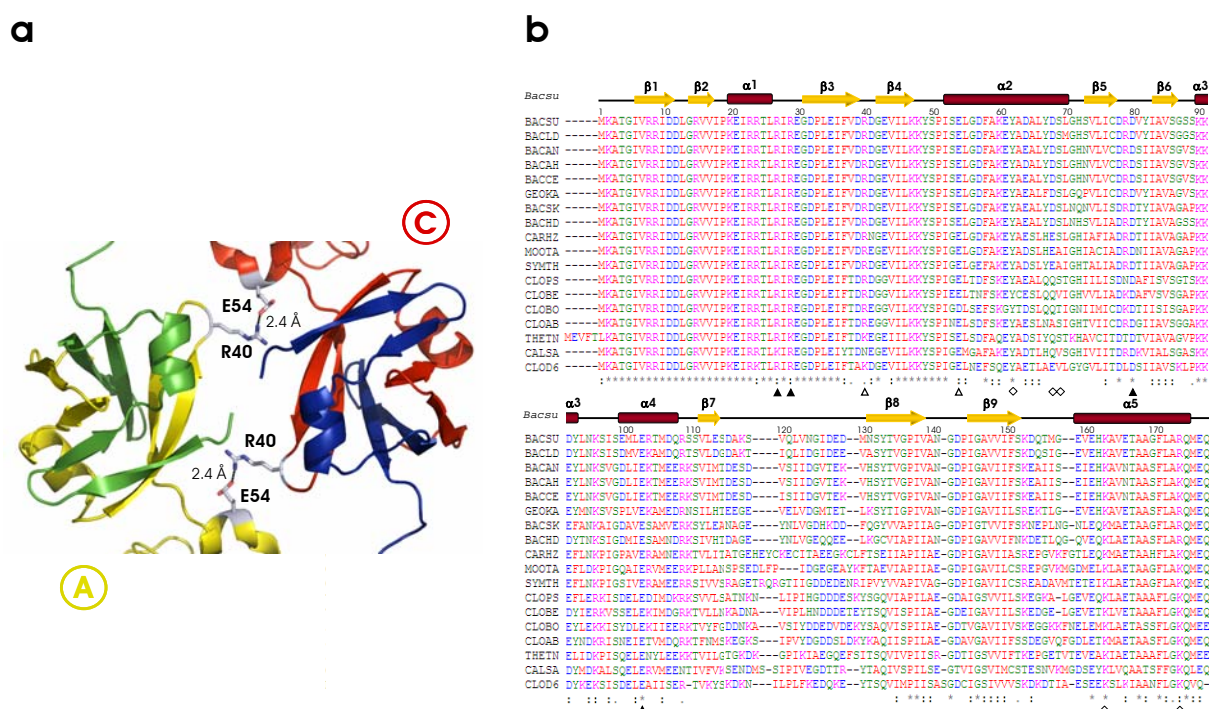


Figure 27. Stabilisation of the Asymmetry of SpoVT_{FL} and Sequence Alignment. (a) Zoom-in depiction to the intermolecular interaction of S. Amino acids are presented as sticks with element colour code and labels. Interacting monomers are specified with colour code as shown in Figure 25. (b) Alignment of SpoVT orthologs: BACSU, *B. subtilis*; BACLD, *B. licheniformis*; BACAN, *B. anthracis*; BACAH, *B. thuringiensis*; BACCE, *B. cereus*; GEOKA, *G. kaustophilus*; BACSK, *B. clausii*; BACHD, *B. halodurans*; CARHZ, *C. hydrogenoformans*; MOOTA, *M. thermoacetica*; SYMTH, *S. thermophilum*; CLOPS, *C. perfringens*; CLOBE, *C. beijerinckii*; CLOBO, *C. botulinum*; CLOAB, *C. acetobutylicum*; THETN, *T. tengcongensis*; CALSA, *C. saccharolyticus*; CLOD6, *C. difficile*. Secondary structure elements of *B. subtilis* SpoVT (Bacsu) are indicated above with β -sheets as yellow arrows and α -helices as red tubes. Triangles mark amino acids involved in stabilisation of the asymmetry; blank (Δ) for intermolecular and filled (\blacktriangle) for intramolecular interactions in S. Squares (\diamond) point at amino acids which form contacts between SpoVT_{CT} in the SpoVT_{FL} tetramer. Colour-coding is based on ClustaW (Higgins et al., 1994); (*) invariant, (:) strongly conserved, and (.) semi-conserved amino acids.

3.4.4 Two Different Monomers

The two different monomers in the structure of the SpoVT_{FL} tetramer are of substantial conformational variability. The SpoVT_{FL} monomers are composed of a structured SpoVT_{NT} domain which encompasses the amino acids 1-48 and a compact SpoVT_{CT} domain which is built by the residues 56-178. SpoVT_{NT} folds as two pairs of β -hairpins ($\beta 1$, $\beta 2$ and $\beta 3$, $\beta 4$) with an interjacent α -helix ($\alpha 1$) as displayed in Figure 28. The globular SpoVT_{CT} consists of four α -helices ($\alpha 2$ - $\alpha 5$) and an anti-parallel five-stranded β -sheet ($\beta 5$ - $\beta 9$) (Fig. 28b). The amino acids 49-55 form the domain-connecting linker which represents the most flexible part of the protein (see Fig. 26a).

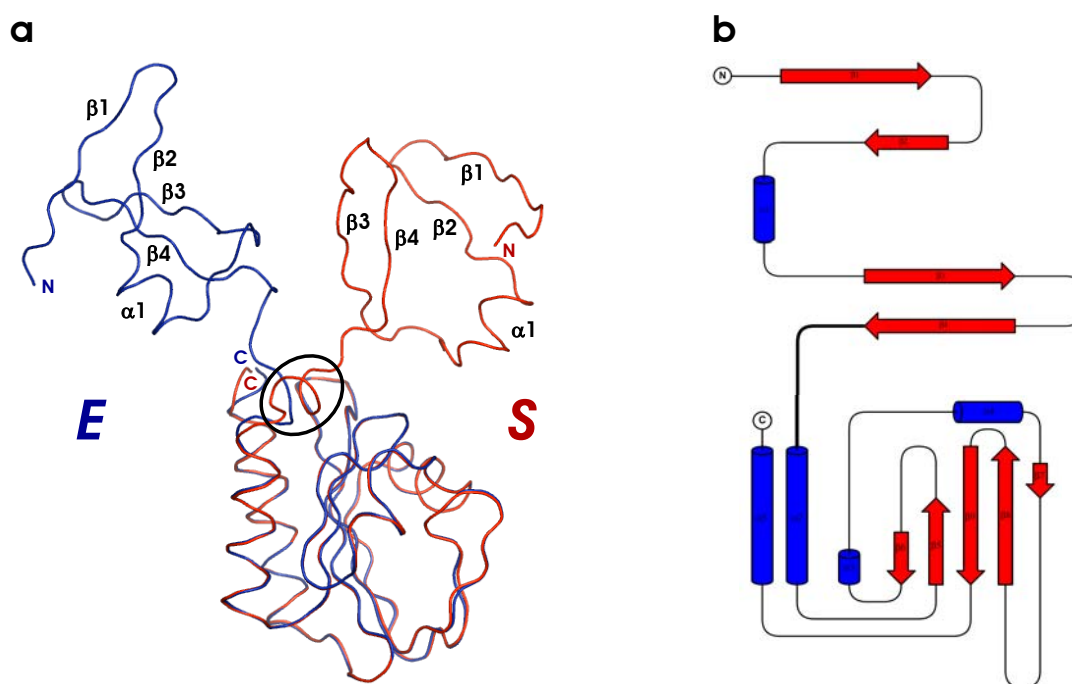


Figure 28. SpoVT_{FL} Monomers. (a) Ribbon representation of superposed monomers of SpoVT_{FL}; E (blue) and S (red). N- and C-termini and secondary structure elements of SpoVT_{NT} are labelled in each monomer. α -helix of the linker in S is marked by an ellipse. (b) Topology diagram (Bond, 2003) of SpoVT_{FL} with β -sheets as arrows (red) and α -helices as barrels (blue). N- and C-terminus and secondary structure elements are indicated. Domain connecting linker is pointed out as a bold line.

A superposition of the differing monomers E and S demonstrates the extent of the rotation of SpoVT_{NT} relative to SpoVT_{CT} which is enabled by the flexibility of the domain connecting linker (Fig. 28a). This rotation of SpoVT_{NT} is responsible for the overall twist of

$\sim 50^\circ$ observed in the tetrameric complex, stabilised by salt bridges which lock the SpoVT_{FL} tetramer in the asymmetric conformation (see 3.4.3). In *S*, interaction of the domains generates an interaction area of 200 \AA^2 (Krissinel and Henrick, 2007) which leads to a more compact overall fold compared to *E*. The elongated monomer *E* adopts a hook-shaped structure grasping with SpoVT_{NT} the SpoVT_{NT} domain of *S*, as clearly visible in the surface illustration of the tetrameric model presented in Figure 24a (monomers B and D). The SpoVT_{CT} domains of the varying monomers are, in contrast to their positional variability, almost similar which is reflected by a root mean square deviation (r.m.s.d.) of 0.4 \AA (122 superimposed C_α atoms) (Claude et al., 2004). The largest structural variations exist for the loop which locks the putative ligand binding pocket (data not shown).

3.4.5 Multimerisation Modules

Two dimerisation modules organise the quaternary structure of SpoVT_{FL}: SpoVT_{NT} domains of two monomers form a tight connection and act in a central close alliance; their globular SpoVT_{CT} domains are stretched out in opposite directions and couple two dimers in an anti-parallel manner via helical interactions.

3.4.5.1 N-terminal Domain

The interleaving of the four β -hairpin elements of two SpoVT_{NT} domains results in a homodimeric eight-stranded anti-parallel β -barrel. The barrel is capped on both ends by two opposite and symmetry related helices $\alpha 1$ and $\alpha 1'$ (Fig. 29a). The central $\beta\alpha\beta$ -element and the characteristically exposed $\beta 1$ - $\beta 2/\beta 1'$ - $\beta 2'$ loops (Fig. 29) assign this type of fold into the group of swapped-hairpin β -barrels (Coles et al., 2005). The name of this fold derives from the characteristic topology as depicted in Figure 29b.

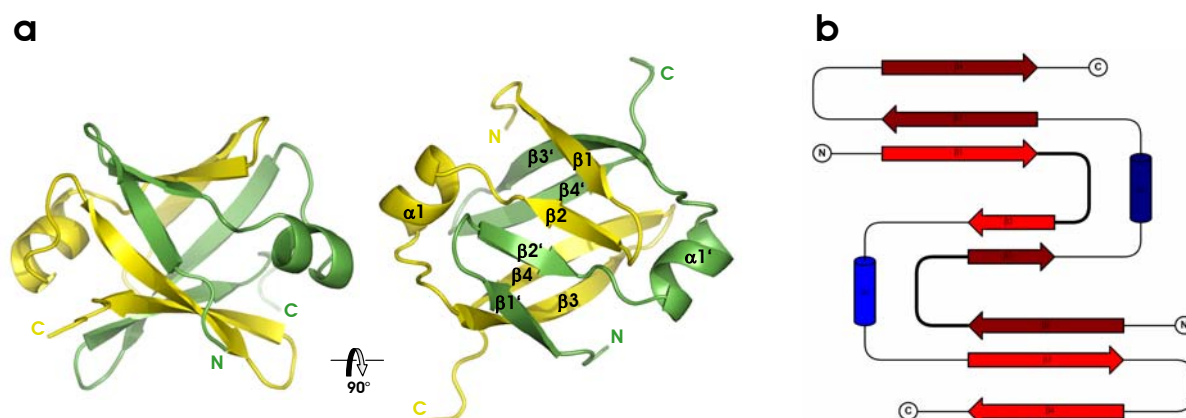


Figure 29. Dimer of SpoVT_{NT}. N- and C-termini and secondary structure elements of dimeric SpoVT_{NT} are indicated. (a) Overall structure of dimeric SpoVT_{NT} in a cartoon representation in side (left) and top (right) view. Monomers are colour-coded. (b) Topology diagram (Bond, 2003) of dimeric SpoVT_{NT} with β -sheets as arrows (red) and α -helices as barrels (blue). Monomers are in different colour intensities and characteristic $\beta 1$ - $\beta 2/\beta 1'$ - $\beta 2'$ loops are highlighted as bold lines.

The extensive dimerisation interface of 1690 Å² is stabilised by a large network of hydrogen bonds (Krissinel and Henrick, 2007) mediated by residues which are highly conserved throughout SpoVT orthologs (see Fig. 27b and Table 4).

No.	Chain, Residue, Atom	Distance (Å)	Chain, Residue, Atom
1	A, Ile36, N	2.8	B, Ile6, O
2	A, Leu34, N	2.6	B, Arg8, O
3	A, Gly31, N	2.8	B, Ile10, O
4	A, Ile18, N	3.1	B, Gly14, O
5	A, Val16, N	3.1	B, Val16, O
6	A, Ile10, N	3.5	B, Asp32, O
7	A, Arg8, N	3.0	B, Leu34, O
8	A, Thr4, OG1	2.6	B, Ile36, O
9	A, Leu46, N	3.0	B, Val44, O
10	A, Val44, N	2.8	B, Leu46, O
11	A, Ile6, O	3.0	B, Ile36, N
12	A, Arg8, O	2.6	B, Leu34, N
13	A, Ile10, O	2.6	B, Gly31, N
14	A, Gly14, O	3.3	B, Ile18, N
15	A, Val16, O	3.0	B, Val16, N
16	A, Asp32, O	3.7	B, Ile10, N
17	A, Leu34, O	2.9	B, Arg8, N
18	A, Ile36, O	3.1	B, Thr4, OG1
19	A, Val44, O	2.9	B, Leu46, N
20	A, Leu46, O	2.9	B, Val44, N

Table 4. Details of the SpoVT_{NT} β -barrel Interface. Contacts (No. 1-20) mediating dimerisation of SpoVT_{NT} with corresponding distances (Krissinel and Henrick, 2007). Interactions conserved between β -barrels of SpoVT_{NT} and AbrB_{NT} are coloured in green.

The swapped-hairpin β -barrel of SpoVT is characterised by 24 highly conserved and positively charged amino acids taken for the sequence alignment in Figure 27b. Eight arginines (Arg8, Arg9, Arg15, Arg23, Arg24, Arg27, Arg29, and Arg40) and four lysines (Lys2, Lys20, Lys47, and Lys48) of each monomer contribute to an unusually high charge density of the protein domain. The surface representation in Figure 30 illustrates the charge property of SpoVT_{NT} with a net charge of plus three. Particularly the α 1-helices, which are part of a girdle of positive charges surrounding the protruding β 1- β 2 and β 1'/ β 2' loops, define patches of an extraordinarily high positive charge distribution (Fig. 30). The arginines are exclusively oriented to one face of the domain (Fig. 30), except for Arg40 which was discovered to be important in tetramer stabilisation (see 3.4.3).

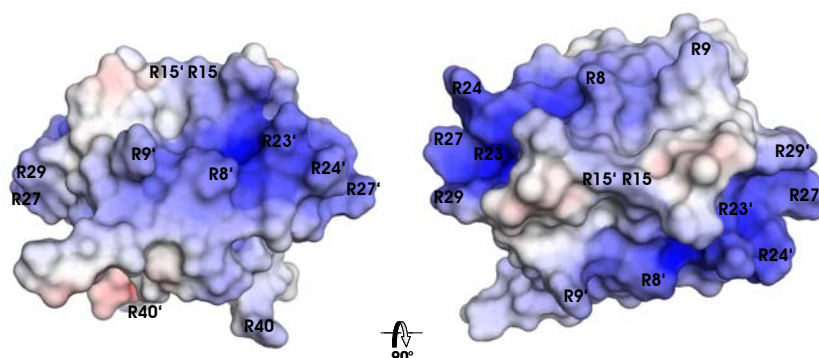


Figure 30. Surface Charge Potential of Dimeric SpoVT_{NT}. SpoVT_{NT} in surface representation illustrating its surface charge potentials. Domain orientations are similar to Figure 29a and arginines are marked. Charge potentials are coloured in blue and red for basicity and acidity, respectively (values coloured from -10 (red) to 10 (blue) kT/e).

3.4.5.2 C-terminal Domain

As observed by X-ray crystallography and gel filtration chromatography, SpoVT_{CT} forms a homodimer which adopts a highly compact overall shape (Fig. 31). The SpoVT_{CT} dimer has a strong net negative charge (Fig. 31a), quite contrary to the positively charged SpoVT_{NT} domain (see Fig. 30). Intensive negatively charged patches are located around the connecting region (Fig. 31a).

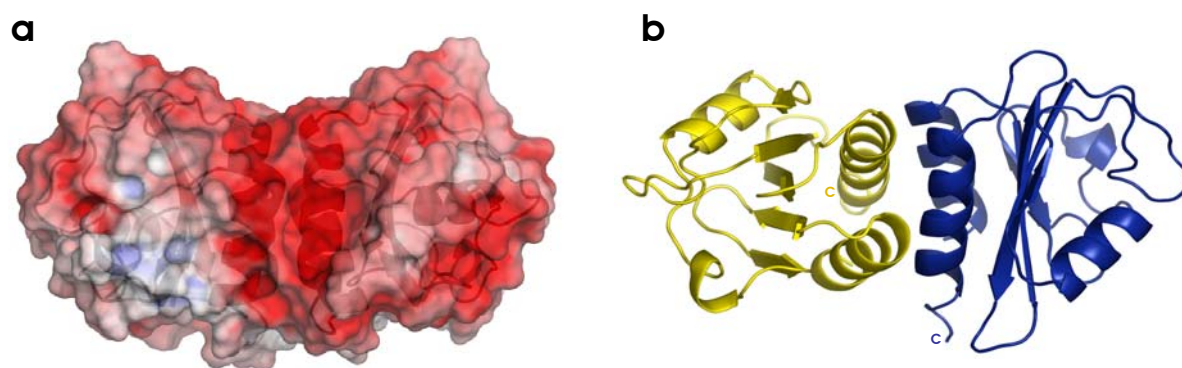


Figure 31. Dimer of SpoVT_{CT}. (a) SpoVT_{CT} dimer in transparent surface representation demonstrating its surface charge potentials. Underlying C_α trace highlights secondary structure elements. Charge potentials are coloured in blue and red for basicity and acidity, respectively (values coloured from -10 (red) to 10 (blue) kT/e). (b) Cartoon representation of the overall fold of dimeric SpoVT_{CT} coloured by monomers. C-termini are indicated.

In the SpoVT_{CT} dimer, the interface is an anti-parallel four-helical coiled coil to which each monomer contributes two helices (Fig. 31b). Thereby, the N-terminal helix of one monomer contacts the C-terminal helix of the second monomer and vice versa. The interaction area of 610 Å² (Krissinel and Henrick, 2007) is quite small which is based on the peculiar twist of the monomers against each other (Fig. 31b and 32a). A pair of Arg174 and Asp68 forms two intermolecular salt bridges between two SpoVT_{CT} monomers and Lys163 and Ser69 support interaction by hydrogen bond formation between the oxygen of the main chain of the lysine and the OH-group of serine and the NH-group of the side chain of lysine and the oxygen of the main chain of serine. Additionally, Tyr62 of each monomer contributes a hydrogen bond between the OH-groups (Fig. 32b). The amino acids Tyr62 and Lys163 are invariant and Arg174 is strongly conserved among the SpoVT orthologs according to the sequence alignment shown in Figure 27b.

The overall fold and the dimerisation mode observed in the structure of SpoVT_{CT} in isolation are essentially identical to that in the full-length protein (compare Fig. 25) (r.m.s.d. between 120 C_α atoms of 0.5 Å, data not shown) (Claude et al., 2004).

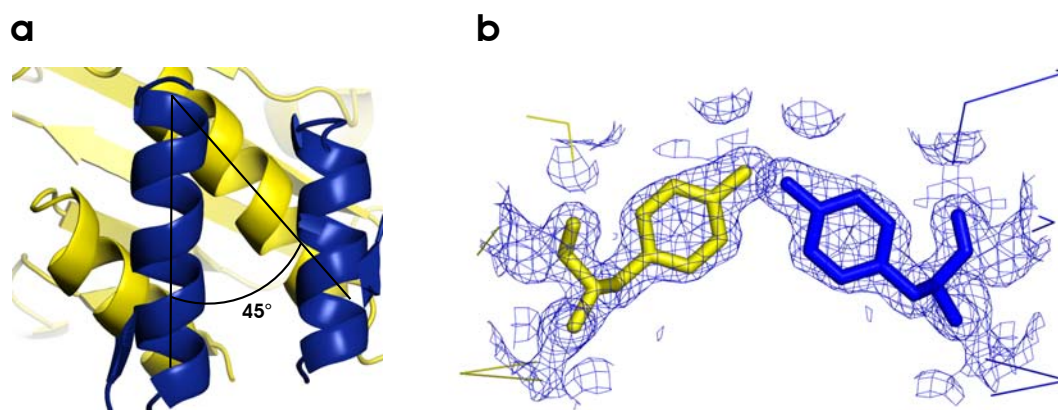


Figure 32. SpoVT_{CT} Dimer Interface. (a) Illustration of the twist (45°) of the SpoVT_{CT} dimer. Monomers are coloured as shown in Figure 31b. (b). Electron density of interacting tyrosines (Tyr62) at the SpoVT_{CT} dimer interface. Residues are presented as sticks and electron density map is depicted in blue at 1.5 σ . Subunits in ribbon presentation are with colour code similar to (a).

3.4.6 Novel Domain Architecture

3.4.6.1 Swapped-hairpin β -barrel

The swapped-hairpin β -barrel classifies SpoVT as a member of the AbrB-like transcription factor superfamily (Coles et al., 2005). SpoVT_{NT} closely resembles the structure of AbrB_{NT} (PDB entry 1YSF) (Fig. 33a) which is the core structure element of the superfamily. The homology between SpoVT_{NT} and AbrB_{NT} is reflected by an r.m.s.d. of 1.0 Å between 48 aligned C $_{\alpha}$ atoms (Claude et al., 2004). A sequence alignment (Higgins et al., 1994) reveals 68% identity and arginines essential for the DNA-binding activity of AbrB_{NT} (Strauch et al., 2005) are conserved between both proteins (Fig. 33b). The arginines which are conserved in sequence and structure (Arg8, Arg15, Arg23, and Arg24) are exposed similarly to one face of the barrel (Fig. 33a) presumably to generate a domain moiety prone to bind selected segments of negatively charged DNA. Non-homologous residues between the closely related domains are present solely in the region around the linker which connects the α -helix to the β 3-sheet. Additionally, the amino acid Arg40 which seems to be important in SpoVT_{FL} is not present in AbrB (Fig. 33).

Structural similarities to other members of the AbrB-like superfamily are noted for Abh (PDB entry 2FY9) which is a paralogue of AbrB in *B. subtilis* (Bobay et al., 2006) and the

E. coli DNA-binding proteins MazE (Loris et al., 2003) and MraZ (PDB entry 1N0G) (Chen et al., 2004). The N-terminal part of MazE (MazE_{NT}) forms an intertwined homodimeric β -barrel (PDB entry 1MVF (Loris et al., 2003)) quite similar to the swapped-hairpin β -barrel of AbrB_{NT} and SpoVT_{NT}. A Z-score of 4.7 (Holm and Sander, 1993) and an r.m.s.d. of 1.1 Å between 41 aligned C $_{\alpha}$ atoms (Claude et al., 2004) was observed by a superposition of SpoVT_{NT} and MazE_{NT}. The arginines of the MazE_{NT} dimer are crucial in specific DNA-binding (Loris et al., 2003) and perfectly positioned for attaching to DNA (see 4.2, Fig. 41).

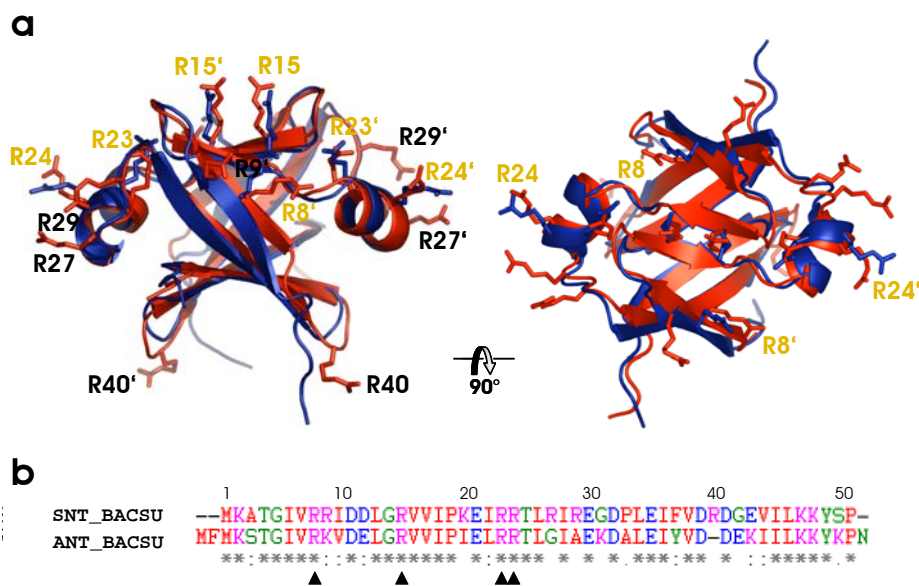


Figure 33. Swapped-hairpin β -barrels of SpoVT_{NT} and AbrB_{NT}. (a) Side (left) and top (right) view of superposed swapped-hairpin β -barrels of SpoVT_{NT} (red) and AbrB_{NT} (PDB entry 1YSF) (blue) with arginines shown as sticks. Arginines of SpoVT_{NT} are labelled with yellow colour indicating conserved arginines according to sequence alignment in (b). (b) Sequence alignment of SpoVT_{NT} of *B. subtilis* (1-51, SNT_BACSU) and AbrB_{NT} of *B. subtilis* (1-53, ANT_BACSU). Filled triangles (▲) assign conserved arginines responsible for AbrB mediated DNA-binding. Colour-coding is based on ClustalW (Higgins et al., 1994); (*) invariant, (:) strongly conserved, and (.) semi-conserved amino acids.

All homologs presented have no particular protein domain at their C-terminus. Except for the monomeric MraZ, simply elongated and unfolded polypeptide chains of 30-40 amino acids are assumed or known to display the C-terminal part. On the contrary, SpoVT_{FL} defines a compact and globular SpoVT_{CT} domain which is unique throughout AbrB-like transcription factors. This represents a novel domain architecture in transcription factors.

3.4.6.2 GAF Domain

SpoVT_{CT} was predicted to belong to the large GAF domain family clade according to sequence and structure comparison methods (Coles et al., 2005).

Structure determination of SpoVT_{CT} confirmed that the domain adopts a GAF fold (Fig. 34). SpoVT_{CT} with a molecular weight of 13.5 kDa (123 amino acids) forms a central five-stranded anti-parallel β -sheet with the strand order $\beta 6$ - $\beta 5$ - $\beta 9$ - $\beta 8$ - $\beta 7$ (Fig. 34) flanked on one side by an anti-parallel two-helix bundle which comprises the N- ($\alpha 2$, residues 1-13) and C-terminus ($\alpha 5$, residues 104-123) of the domain (Fig. 34a). On the other side of the core β -sheet, another pair of helices ($\alpha 3$ and $\alpha 4$), however, much smaller in length, and an extended $\beta 7$ - $\beta 8$ loop (Fig. 34b) co-build the potential ligand binding pocket of the GAF domain (Fig. 34a). The negatively charged protein domain (see Fig. 31a) with a surplus of 10 charges (11 positively and 21 negatively charged residues) shows hydrophobic patches arranged around the helix bundle (in particular $\alpha 5$) and central parts of the β -sheets which are not solvent accessible (data not shown). The presumed ligand binding pocket of SpoVT_{CT} is covered with hydrophobic residues (Leu75, Ile98, Leu102, Val120, Leu122, Val135, Val149, and Phe151) (see 4.3, Fig. 44).

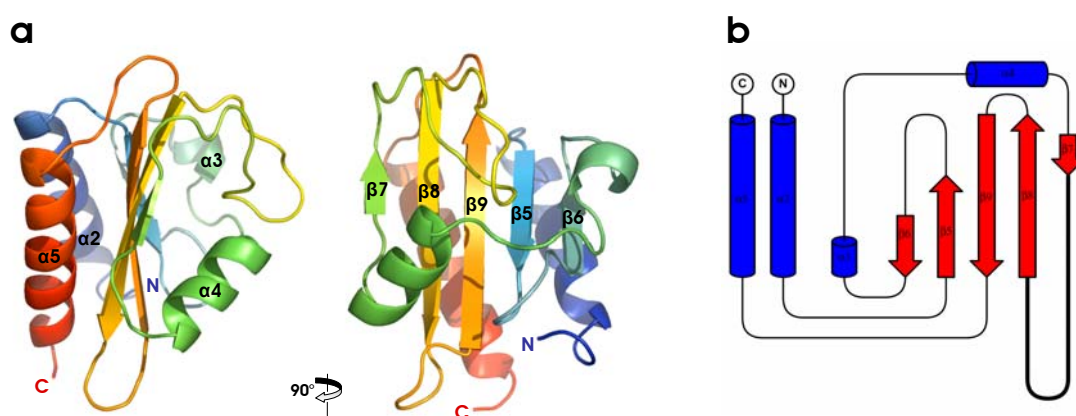


Figure 34. SpoVT_{CT}. N- and C-terminus and secondary structure elements of SpoVT_{CT} are indicated. (a) Overall fold of SpoVT_{CT} in cartoon representation and rainbow colour code with focus at the helices (left) and at the core five-stranded anti-parallel β -sheet (right). (b) Topology diagram (Bond, 2003) of SpoVT_{CT} with β - sheets as arrows (red) and α -helices as barrels (blue). $\beta 7$ - $\beta 8$ loop of potential ligand binding pocket is highlighted as a bold line.

GAF domains are present in diverse transcription factors families and mainly act as SSDs. HHpred analyses (Söding et al., 2005) of SpoVT_{CT} show high similarity to YebR, an *E. coli* protein with unknown function representing a GAF fold (PDB entry 1VHM). A DALI database search (Holm and Sander, 1993) spotlights TM-IcIR (*Thermotoga maritima* isocitrate lyase regulator) (PDB entry 1MKM) (Zhang et al., 2002) with a Z-score of 13.2, and CodY, a global regulator of *B. subtilis* (PDB entry 2B18 and 2HGV) (Levdikov et al., 2006) with a Z-score of 11.0. The C-terminal domain of TM-IcIR (IcIR_{CT}) mostly resembles the structure of profilin (PDB entry 3NUL and 1FIL). The structural similarity to SpoVT_{CT} is represented by an r.m.s.d. of 1.5 Å between 101 aligned C_α atoms (Claude et al., 2004) (see 4.3, Fig. 43). For the N-terminal GAF domain of CodY (CodY_{NT}), an r.m.s.d. of 1.5 Å over 94 superimposed C_α atoms was observed (Fig. 35a and Fig. 43) (Claude et al., 2004).

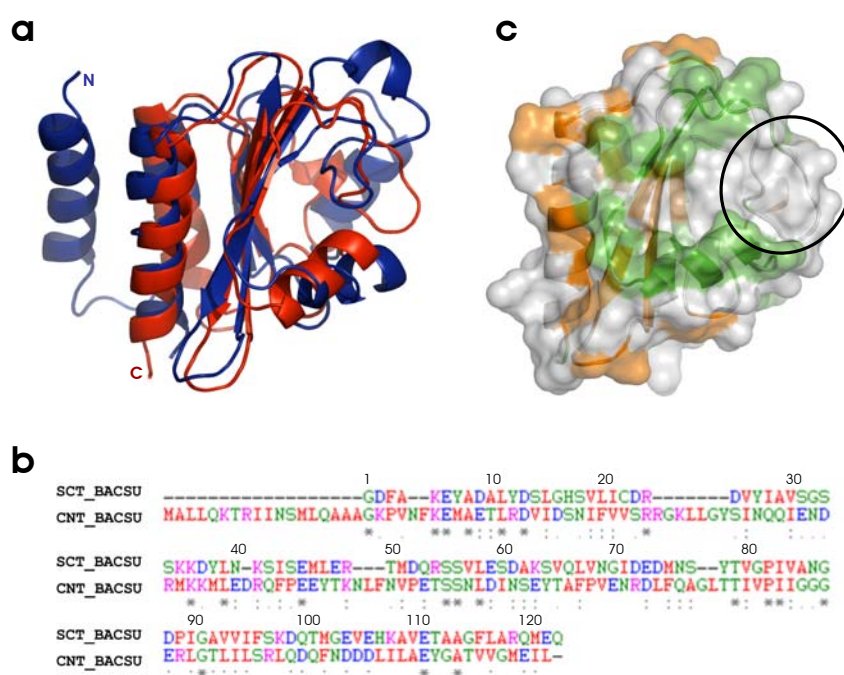


Figure 35. GAF Domains of SpoVT_{CT} and CodY_{NT}. (a) Superposition of SpoVT_{CT} (red, C-terminus labelled) and CodY_{NT} (PDB entry 2B18) (blue, N-terminus labelled). (b) Alignment of sequences of *B. subtilis* SpoVT_{CT} (residues 56(1)-178(123), SCT_BACSU) and *B. subtilis* CodY_{NT} (residues 1-155, CNT_BACSU). Colour-coding is based on ClustalW (Higgins et al., 1994); (*) invariant, (:) strongly conserved, and (.) semi-conserved amino acids. (c) Transparent surface representation of SpoVT_{CT} with an underlying C_α trace showing secondary structure elements. Conserved residues according to the sequence alignment in (b) are highlighted by colour. Residues conserved in sequence and structure (superposition in (a)) are coloured in orange. Loop locking the potential ligand binding pocket is marked with an ellipse.

Despite similarities between SpoVT_{CT} and GAF domains of known structure, there is a certain lack of substantial sequence similarity. In sequence comparisons, SpoVT_{CT} is most similar to the GAF domain of CodY, CodY_{NT} (residues 1-155), (Levdikov et al., 2006) showing 46% similarity (14% identity) (Fig. 35b). CodY_{NT} has a three-helix bundle while SpoVT_{CT} offers a two-helix bundle represented by the absence of 18 amino acids at the N-terminus of SpoVT_{CT} (Fig. 35a and 35b). The result of sequence and structure alignments between these two GAF domains is summarised in the surface presentation of SpoVT_{CT} in Figure 35c. Notably, no conserved residues were found adjacent to the ligand binding pocket, especially in the loop region which presumably locks the pocket (Fig. 35c).

3.4.7 New Dimerisation Mode of GAF Domains

GAF domains are reported to act as multimerisation domains. In SpoVT_{FL}, interaction between the helix bundles of the C-terminal GAF domains mediates tetramer formation of the transcription factor (see 3.4.2).

The related CodY_{NT} dimerises via helical interactions similarly. The CodY_{NT} dimer interface is an anti-parallel six-helical bundle mediated by the anti-parallel three-helical coiled coil of the monomers (see Fig. 35a). Two helices from each monomer form the dimer interface as a parallel four-helical coiled coil (Fig. 36a) generating an interface area of 1050 Å² (Levdikov et al., 2006). For coiled coils, a helical constitution displaying hydrophobic amino acids in positions one and four is characteristic. The helices of CodY_{NT} have a hendecad periodicity (11 residue repeat over 3 helical turns = 3.67 residues per turn, repeat positions *a-k*, hydrophobic core positions *a*, *d*, *e*, and *h*) which causes a minimal right-handed supercoil with helix crossing angles close to 0°. This is quite contrary to the anti-parallel four-helical coiled coil dimer interface of SpoVT_{CT} (Fig. 36a). The helices of SpoVT_{CT} have a pentadecad periodicity; 15 residues repeat over 4 helical turns resulting in 3.75 residues per turn. The repeat positions are *a-o* with the hydrophobic core positions in *a*, *d*, *e*, *h*, and *l* (Fig. 36b). A right-handed supercoil with helix crossing angles between 25° and 45° is formed (see Fig. 36a).

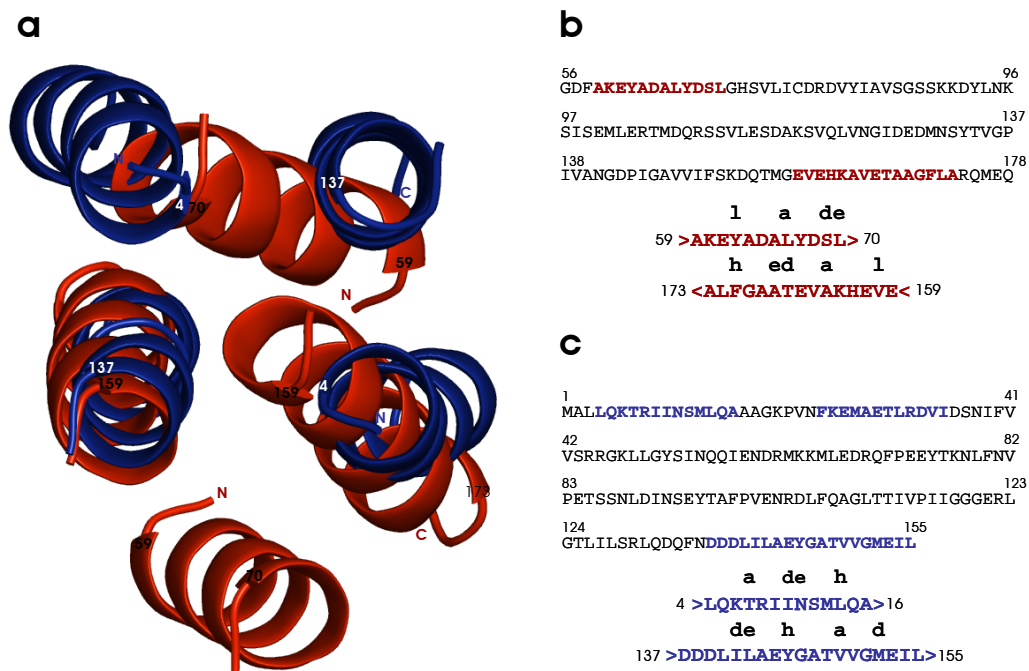


Figure 36. Details of the Coiled Coil Interface of SpoVT_{CT} and CodY_{NT}. (a) Superposition of the four-helical coiled coil dimer interfaces of SpoVT_{CT} (red) and CodY_{NT} (blue). Visible N- and C-termini and first residues of the helices, according to their sequence, are indicated. (b) Amino acid sequence of SpoVT_{CT} (top). Residues shaping helices of the dimer interface are highlighted in bold red. Amino acids of the helices which adopt hydrophobic core positions in the four-helical interface are labelled (a, d, e, h, and l) (bottom). (c) Amino acid sequence of CodY_{NT} (top). Residues shaping helices of the six-helical bundle of the dimer are highlighted in bold blue. Amino acids of the helices which adopt hydrophobic core positions in the four-helical interface are labelled (a, d, e, and h) (bottom).

The cores of the helices in SpoVT_{CT} are not in register, but offset (Fig. 36b) which results in unusual core geometries, including two layers with *complementary x-da* packing: Leu66 (a) - Ala164 (a), Thr167 (d) and Ser69 (d), Leu70 (e) - Ala168 (e) (Fig. 36b). The offset of the cores of the CodY_{NT} helices are shown in Figure 36c (intramolecular coiled coil not shown). The coiled coils of CodY_{NT} are fairly uniform in cross section while the bundle of SpoVT_{CT} is not uniform, being closer to a square at one end and to a rhombus at the other. The vectors connecting the central axes of symmetry-related helices have a length ratio of 16 Å to 15 Å in the first core layer (Tyr62 – Phe171) and of 20 Å to 10 Å in the last (Ser69, Leu70 – Ala164) (Fig. 36a). In CodY_{NT}, the intermolecular coiled coil has an axial ratio of about 14 Å to 17 Å.

The helical packing mode of SpoVT_{CT} dimers described here presents a new mode of dimer formation in GAF domains.

3.5 DNA- and Ligand Binding Studies of *B. subtilis* SpoVT

SpoVT is a GAF domain regulated transcription factor (Dong et al., 2004) suggesting that the DNA-binding activity of the protein is controlled by sensing a small signal molecule. To determine DNA- and ligand binding properties of SpoVT, different approaches to study possible interactions were performed.

3.5.1 Biochemical Approach

3.5.1.1 Limited Proteolysis with Trypsin and α -Chymotrypsin

The apo-form of a protein often shows differences in its conformation compared to the holo-form. An elegant method to determine conformational changes of a protein or a protein domain induced by ligand binding is provided by limited proteolysis. To investigate the ligand binding capacity of SpoVT, limited proteolysis was performed with a subset of presumed ligands and trypsin and α -chymotrypsin (see 6.3.5). Both enzymes are serine endopeptidases; trypsin hydrolyses peptide bonds predominantly at the carboxyl side of the amino acids lysine and arginine, except in case proline follows, and α -chymotrypsin affects the carboxyl side of tyrosine, tryptophan, and phenylalanine. The studies were done with the isolated SpoVT_{CT} domain and SpoVT_{FL}. The set of tested potential binding partners included cGMP, GTP, DPA, isoleucine, and valine. DNA fragments specifying the sequence of the SpoVT promoter region (see 2.4.2 and 6.1.1.1) were added to the reaction batches containing SpoVT_{FL}. Representatively for all performed experiments, Figure 37 shows SDS-PAGE analyses of limited proteolysis experiments done with SpoVT_{FL} incubated with DNA and isoleucine (Fig. 37a) and SpoVT_{CT} incubated with valine (Fig. 37b). The gels present the cleavage patterns of trypsin and α -chymotrypsin exerted on SpoVT_{FL} and SpoVT_{CT}, respectively. No significant differences are visible between samples with and without ligand added.

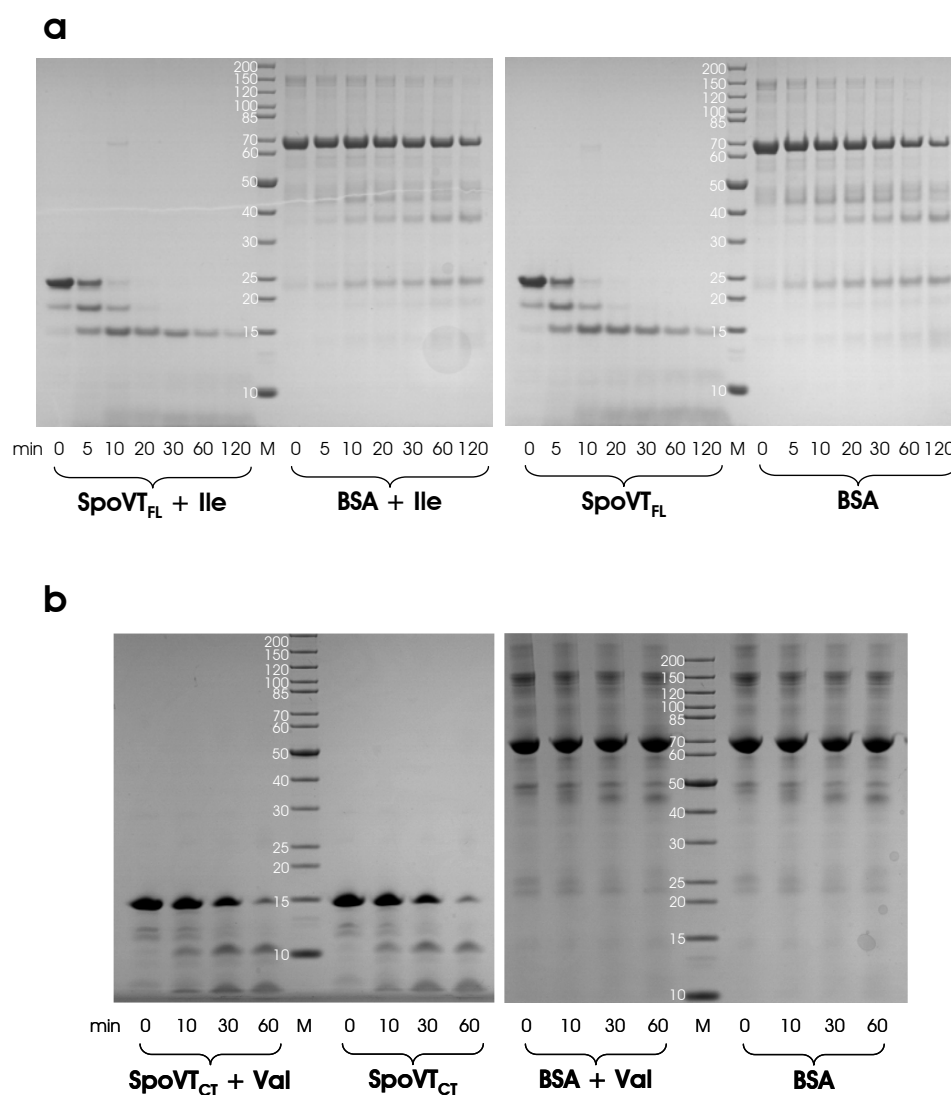


Figure 37. Ligand Binding Studies of SpoVT_{FL} and SpoVT_{CT}. SDS-PAGE analyses of limited proteolysis experiments of (a) SpoVT_{FL} including DNA fragment and isoleucine (Ile) as potential ligand and treated with trypsin and (b) SpoVT_{CT} containing valine (Val) as potential ligand and treated with α -chymotrypsin. As controls, SpoVT proteins without potential ligand and BSA were digested comparatively. Samples taken at different points in time are indicated. Proteins of the molecular weight marker (M) are specified (kDa).

3.5.1.2 Gel Filtration Chromatography

Gel filtration chromatography is another biochemical technique to examine conformational changes of a protein or a protein complex. Protein solutions of SpoVT_{FL} and SpoVT_{CT} were incubated with solutions including diverse small molecules supposed to bind to the GAF domain of SpoVT (see 6.3.1.2). Isoleucine, valine, cGMP, GTP, and

DPA were tested and in the case of SpoVT_{FL}, DNA fragments containing the promoter sequence of SpoVT (see 2.4.2 and 6.1.1.1) were added. Chromatography of the applied solutions resulted in elution profiles which in each case were completely identical to the elution profiles of pure protein solutions of SpoVT_{FL} or SpoVT_{CT} presented in the gel filtration chromatogram in Figure 14 (see 3.2.2.2) (data not shown).

3.5.2 Biophysical Approach

3.5.2.1 Co-crystallisation and Soaking

Existing crystals of the Se-Met derivate of SpoVT_{CT} were soaked with solutions of presumed ligands (cGMP, isoleucine, and DPA) (see 6.4.1.1) and analysed by X-ray crystallography methods (see 6.4.1.2). All tested crystals diffracted poorly and the collected data were not usable for further processing (data not shown). The micro-seeding technique was applied to induce crystal growth of crystal seeds obtained from existing crystals. Emerging crystals were of bad quality, comparably.

Attempts for co-crystallisation were done with protein solutions of SpoVT_{CT} and SpoVT_{FL} (see 6.4.1.1). SpoVT_{CT} co-crystallisation trials were carried out in the presence of either GTP, cGMP, or isoleucine and in the case of SpoVT_{FL}, a DNA fragment presenting the promoter region of SpoVT (see 2.4.2 and 6.1.1.1) was added in each case. SpoVT_{CT} crystals appeared under several conditions, all of small-sized morphology and very bad quality (data not shown). Crystals of SpoVT_{FL} exclusively emerged under known conditions (see 3.3.1) with addition of GTP or isoleucine. Processing of the collected X-ray data and structure determination by molecular replacement (see 6.4.1.3) revealed that none of the tested ligand binds to the GAF domain nor DNA-binding to the β -barrel of SpoVT_{NT} occurred (data not shown).

3.5.2.2 Isothermal Titration Calorimetry (ITC)

Detection of thermal variations which are associated to molecular interaction processes is the basic principle of isothermal titration calorimetry. SpoVT_{FL} and SpoVT_{CT} protein solutions were titrated with solutions containing molecules which possibly offer a specific binding affinity towards the GAF domain of SpoVT (see 6.4.3). GTP, cGMP, isoleucine, and valine were tested for both proteins but not any of the experiments significantly affirmed ligand binding occurrence (data not shown).

Due to the results of ligand binding studies performed with the chemicals cGMP, GTP, isoleucine, valine, and DPA, it is assumed that probably none of the tested molecules is designated to specifically bind to the GAF domain of SpoVT.

4. DISCUSSION

4.1 Tetrameric State of *B. subtilis* SpoVT

4.1.1 Biochemical Aspects

On the basis of the structures of SpoVT_{FL} and SpoVT_{CT}, secondary structure elements of the proteins are summed up to contents of 31% α -helices and 32% β -sheets and 37% α -helices and 25% β -sheets, respectively. The content of β -sheet elements of both proteins is consistent with values from CD measurements (see 3.2.1) (31% in SpoVT_{FL} and 25% in SpoVT_{CT}). The α -helical content was estimated to be >10% less in CD analyses for both proteins (17% in SpoVT_{FL} and 25% in SpoVT_{CT}) compared to the content revealed by the 3D-structures. This divergence probably originates from a misleading identification of α -helices as random coiled structures that at the same time would explain the unusually high content of random coils in the estimations based upon the CD data (33% in SpoVT_{FL} and 31% in SpoVT_{CT}, see Table 1). Generally, estimates with this method typically have an uncertainty of +/- 5%.

Further CD measurements, concerning heat denaturing of SpoVT_{FL} and SpoVT_{CT} (see 3.2.1), provided surprising results with respect to the tetrameric SpoVT_{FL} structure. According to the tetrameric assembly, a two-step transition would be expected at which first the tetramers would separate into dimers. The first midpoint transition temperature of SpoVT_{FL} would be assumed to be higher than for the isolated SpoVT_{CT} dimer, because of the two interaction sites between four SpoVT_{CT} domains in the tetramer. The unfolding of the tightly connected SpoVT_{NT} domains would present the second transition step anticipating a high midpoint transition temperature.

The determined melting curve of SpoVT_{FL} (see Fig. 12) presents a sigmoid shape describing a single-step transition, however. Hence, heat denaturing of the SpoVT_{FL} tetramer is supposedly a progress at which dissociation into dimers and monomers proceeds simultaneously.

In comparison to the dimeric single domain protein SpoVT_{CT}, tetrameric SpoVT_{FL} is stabilised against heat induced unfolding. This implicates less intra- and/or intermolecular interactions of the single domain protein SpoVT_{CT} in contrast to SpoVT_{FL}. The SpoVT_{FL} tetramer shows an extensive interaction area of at least 4600 Å² which is added up by twice the interaction area of SpoVT_{NT} (1690 Å²) and SpoVT_{CT} (610 Å²). The difference between midpoint transition temperatures of both proteins, which was 323 K for SpoVT_{FL} and 314 K for the isolated SpoVT_{CT} domain, was determined to be 9 K (see Fig. 12).

Biochemical analyses referring the quaternary structure of SpoVT_{FL} and SpoVT_{CT} showed that both proteins form oligomers. Gel filtration chromatography experiments clearly demonstrated that SpoVT_{FL} assembles into a tetramer and SpoVT_{CT} into a dimer (see 3.2.2.2, Fig. 14). The results obtained by crosslinking experiments were consistent as the existence of SpoVT_{FL} tetramers and SpoVT_{CT} dimers was proven (see 3.2.2.1, Fig. 13). The appearance of further oligomers is presumably due to unspecific linkage of oligomers by glutaraldehyde. In particular, for SpoVT_{FL}, the formation of diverse high molecular weight oligomers is probably based on the solvent accessible lysines in SpoVT_{NT}. Glutaraldehyde uses preferentially primary amino groups of lysines for conjugation of proteins.

The efforts in detection of homologous expressed native SpoVT in sporulating *B. subtilis* cells via anti-SpoVT antibodies were not fruitful as described in 3.2.3.4 (see Fig. 19). It is assumed, that SpoVT is expressed in such low amounts that detection by western blot techniques was not possible. Even at highest expression level of SpoVT (T_{2.5}, see 3.2.3.3, Fig. 17) (Bagyan et al., 1996), the sensitivity of the anti-SpoVT antibodies was obviously not sufficient to detect SpoVT in the endospores.

4.1.2 Structural Aspects

Several dimeric transcription factors bind palindromic DNA-sequences spanning a region of ~ 20 bps (Baleja et al., 1991; Jordan and Pabo, 1988; Vannini et al., 2002). Thereby, the two DBDs dock into two consecutive major grooves (Fig. 38) at a distance of ~ 34 Å in B-DNA.

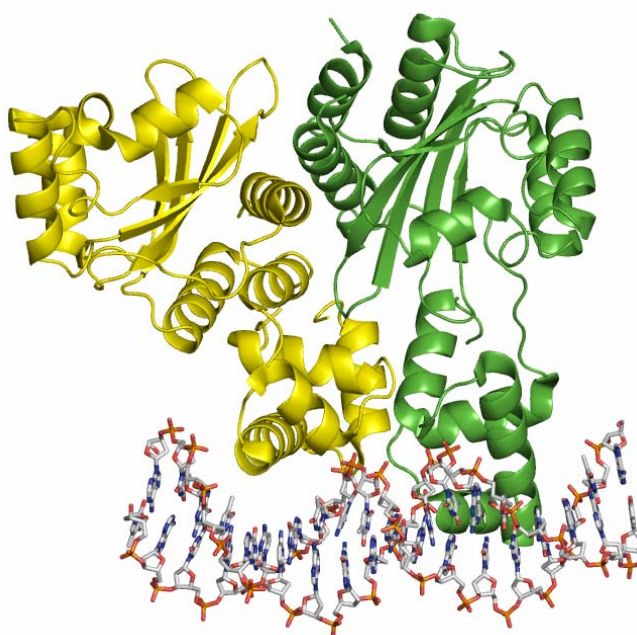


Figure 38. TraR/DNA Complex. Cartoon presentation of the dimeric quorum sensing protein TraR (monomer A in yellow and monomer B in green) bound to its target DNA shown as sticks in element colour code (PDB 1HOM).

Swapped-hairpin β -barrels require tetramerisation for such an interaction, since each DNA-binding domain is itself dimeric, and indeed, AbrB-like transcription factors have been found to need tetramerisation for their biological activity (Bobay et al., 2006; Strauch et al., 2005; Yao and Strauch, 2005).

In the crystal structure presented here, the asymmetric SpoVT_{FL} tetramer exposes two core SpoVT_{NT} DBDs with a distance of ~ 37 Å between two equal points and the potential DNA-binding clefts (the anti-parallel $\beta 2/\beta 2'$ -sheet of SpoVT_{NT}, see 3.4.5.1, Fig. 29a) are twisted significantly against each other (Fig. 39).

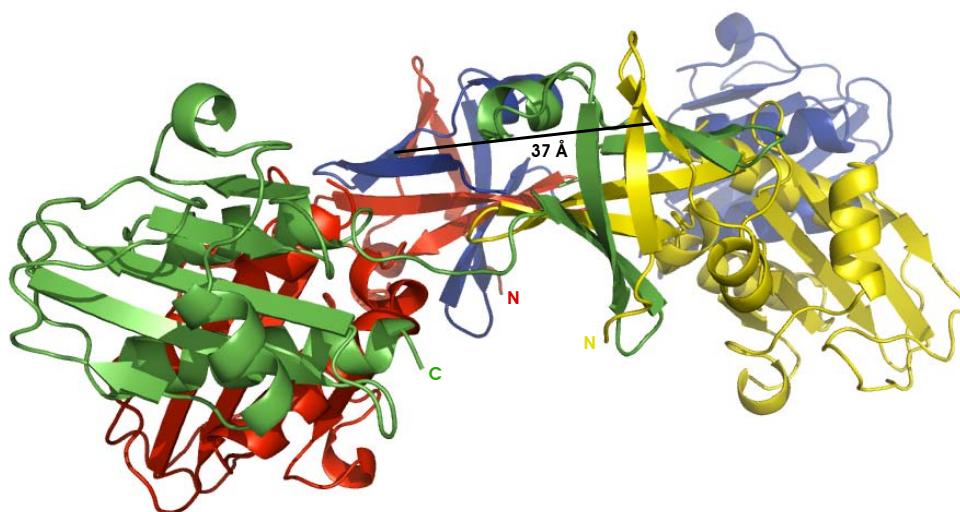


Figure 39. Asymmetric SpoVT_{FL} Tetramer. Cartoon presentation of the asymmetric SpoVT_{FL} tetramer illustrating the distortion of the SpoVT_{NT} DBDs. The distance between Val16 of monomer D (blue) and B (green) of 37 Å is pointed out as a black line. Monomers are coloured as shown in Figure 25 and visible N- and C-termini are labelled.

Binding of DNA often induces its bending as a result of the adaption to the proteins architecture (Baleja et al., 1991; Chen et al., 2001; Ducros et al., 2001; Steitz, 1990; Vannini et al., 2002). In the case of SpoVT_{FL}, the central SpoVT_{NT} DBDs needs to conformationally rearrange to bind to a DNA target of about 20 bps. For docking into two consecutive major grooves of the B-DNA, the SpoVT_{NT} domains have to rotate and reduce their distance by about 3 Å. Flexibility of the SpoVT_{FL} tetramer is ensured by the domain inter-connecting linkers which provide conformational freedom between the domains (see 3.4.3, Fig. 26a). A defined rotation of SpoVT_{NT} could attain a parallel position of the DNA-binding β-barrels in the tetramer which can be reported as a conformational restrain for binding two consecutive major grooves of the DNA target.

Recently, the crystal structures of two transcription factors were solved which show an asymmetry in dimer formation. IclR of *T. maritima* (PDB entry 1MKM) (Zhang et al., 2002) is composed of an N-terminally HTH DBD and a C-terminally profilin-like SSD (in this work termed as IclR_{CT}, see 3.4.6.2) and was found to be distantly related to SpoVT_{CT} (see 3.4.6.2 and 4.3, Fig. 43). TraR of *Agrobacterium tumefaciens*, involved in the quorum sensing system, consists of an N-terminal GAF SSD domain and a C-terminal HTH DBD (PDB entry 1H0M) (Vannini et al., 2002) (see Fig. 38). The SSD in TraR supports the

formation of the dimer (Vannini et al., 2002) (see Fig. 38) and in TM-IcIR, they presumably mediate tetramerisation (Zhang et al., 2002) (Fig. 40).

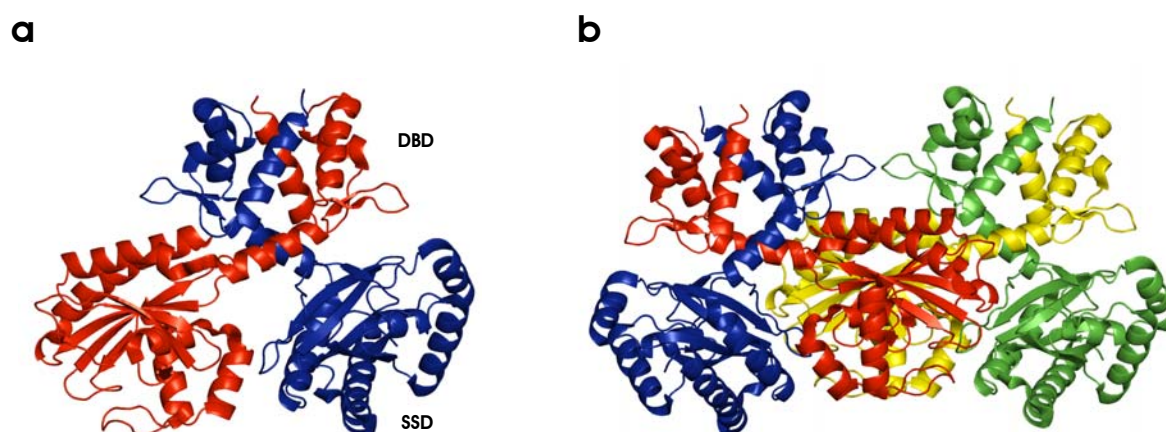


Figure 40. Oligomers of TM-IcIR. Cartoon presentation of the (a) dimeric and (b) tetrameric transcription factor IcIR of *T. maritima* (PDB 1MKM). Monomers are in different colours and in (a), domains are indicated.

The dimer asymmetry in both structures relies on different conformations of the domain connecting linkers and in both cases the asymmetry implies biological relevance. In TraR, an elongated and a compact monomer form the dimer (see Fig. 38) which leads to a defined orientation of the exposed DBDs. Thereby, a precise binding to its recognition site by docking into the two consecutive major grooves of the DNA segment is enabled (Vannini et al., 2002). Based on particular crystal contacts, in TM-IcIR the two asymmetric dimers assemble into a tetrameric complex in conjunction with ligand and DNA-binding processes (Zhang et al., 2002). Their presented TM-IcIR model shows a tetramer which exposes two dimeric DBDs in a parallel orientation perfectly arranged to dock into two consecutive major grooves of B-DNA (Fig. 40b).

For SpoVT_{FL}, it was shown that *in vitro* neither a DNA-binding specificity nor a DNA-binding activity exists (Dong et al., 2004). The authors revealed that SpoVT_{FL} exclusively displays DNA-binding activity when SpoVT_{CT} is missing. Interestingly, an attended loss of binding specificity was noted for the truncated SpoVT_{FL} protein. Based on the determined structure of SpoVT_{FL}, the prevented DNA-binding capacity of SpoVT_{FL} derives from the distortion of the SpoVT_{NT} DBDs in the asymmetric tetramer (see Fig. 39). The unspecific

DNA-binding activity of the truncated SpoVT_{FL} is presumably due to the surface properties of swapped-hairpin β -barrels which are predestined to bind to DNA even as a dimer (see 3.4.5.1, Fig. 30 and 4.2, Fig. 42). The DNA-binding specificity of the transcription factor is facilitated by the tetramerisation which is mediated by the SpoVT_{CT} domains. According to this, the conformation of the asymmetric SpoVT_{FL} tetramer presented here, is supposed to represent an inactive form of SpoVT_{FL}.

The formation of the asymmetric dimers within the tetrameric SpoVT_{FL} complex is likely based on several salt bridges arranged by amino acids which are conserved throughout SpoVT orthologs (see 3.4.3, Fig. 27b). The interaction between and within the S monomers (see 3.4.3) seem to lock the tetramer in its asymmetric arrangement. These contacts have to disrupt in a putative rotational movement process of SpoVT_{NT} leading to the critical parallel orientation essential for DNA-binding. The role of the residues mediating these interactions could be tested by mutagenesis. Investigations on the DNA-binding properties of such mutants would be a challenge, probably providing informative insights into the functionality of SpoVT.

4.2 DNA-binding Domain (DBD) of *B. subtilis* SpoVT

In *B. subtilis*, there are 237 DNA-binding transcription factors which are induced during the life cycle of the cell (Moreno-Campuzano et al., 2006). In the sporulation process, at least five DNA-binding proteins and five RNAP sigma factors are known to govern the tightly controlled cell differentiation scenario (Wang et al., 2006).

The structure of one of these, the σ^G -dependent transcription factor SpoVT presented in this work, is remarkable as it combines structural features of two other regulators of *B. subtilis*. SpoVT_{NT} closely resembles the transition state regulator AbrB in structure and sequence (see 3.4.6.1, Fig. 33) while SpoVT_{CT} is similar to the CodY regulator, which is a sentinel of the nutrient state, in structure (see 3.4.6.2, Fig. 35) but only distantly in sequence.

The considerable similarity between SpoVT_{NT} and AbrB_{NT} strongly supports the hypothesis that the two regulators have similar DNA-binding properties (Dong et al., 2004; Xu and

Strauch, 2001). Exposed arginine residues along one face of the swapped-hairpin β -barrel most likely play an essential role (Bobay et al., 2005; Vaughn et al., 2000). The conserved arginines in the anti-parallel $\beta 2/\beta 2'$ -sheet (see 3.4.6.1, Fig. 33a and Fig. 41) are suitably oriented for docking into the major groove of B-DNA, as verified for AbrB and those located in the capping α -helices support the DNA-binding interactions, as proposed for AbrB (Bobay et al., 2005; Strauch et al., 2005). Similar features are observed in another swapped-hairpin transcription factor, MazE (see 3.4.6.1 and Fig. 41), which acts as the antidote of a toxin/antitoxin system (Kamada et al., 2003; Loris et al., 2003). MazE_{NT} shows DNA-binding activity by well-oriented arginines (Loris et al., 2003) (Fig. 41a). The binding to an “alternating palindrome” promoter sequence by docking into the major groove of DNA, is mediated by the β -hairpins of MazE_{NT} (Loris et al., 2003) which are comparable to the $\beta 1$ - $\beta 2/\beta 1'$ - $\beta 2'$ loops in SpoVT_{NT} (Fig. 41a).

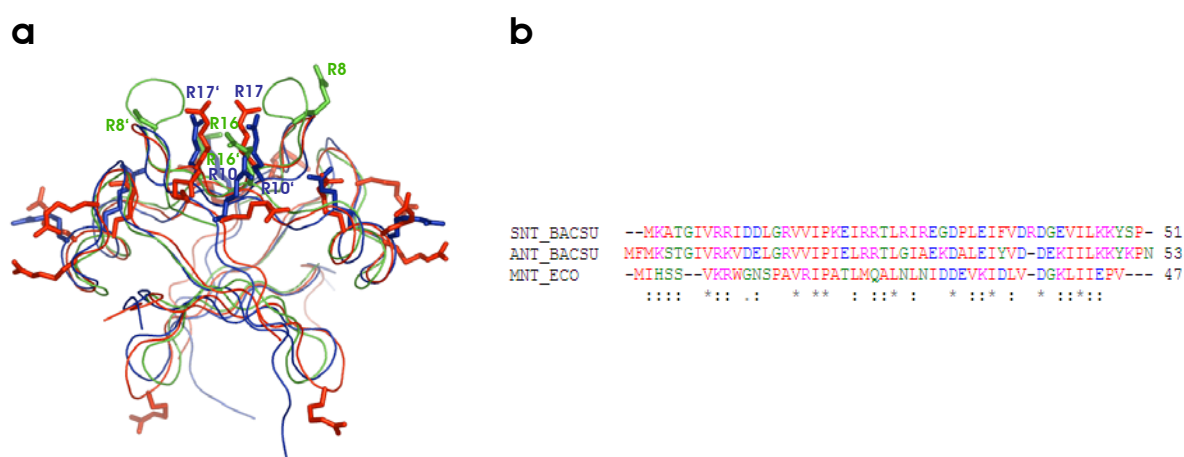


Figure 41. DBDs of SpoVT, AbrB, and MazE. (a) Ribbon representation of superposed dimeric SpoVT_{NT} (red), AbrB_{NT} (blue) (PDB entry 1YSF), and MazE_{NT} (green) (PDB entry 1MVF) with arginines shown as sticks. Arginines of AbrB_{NT} and MazE_{NT} involved in DNA-binding are labelled. Side chain of MazE_{NT} R8' presents C $_{\beta}$ and C $_{\gamma}$ atoms only. (b) Sequence alignment of *B. subtilis* SpoVT_{NT} (SNT_BACSU), *B. subtilis* AbrB_{NT} (ANT_BACSU), and *E. coli* MazE_{NT} (MNT_ECO). Colour-coding is based on ClustalW (Higgins et al., 1994); (*) invariant, (:) strongly conserved, and (.) semi-conserved amino acids.

The DNA-binding specificity of SpoVT_{FL} can be described as a “limited promiscuity” similar to that of AbrB (Bobay et al., 2006, Bobay et al., 2004); in both cases, the target promoters lack recognisable consensus binding motifs (Dong et al., 2004). Promoter sequences of the genes which are regulated by SpoVT_{FL} via recruiting the σ^G subunit of the RNAP show no consistent sequence pattern.

For the paralogs AbrB and Abh, which are very similar in sequence and structure, investigations on their different DNA binding properties were done (Bobay et al., 2006). Abh, the second structurally described AbrB-like transcription factor, is another transition state regulator in *B. subtilis* (Bobay et al., 2006). AbrB and Abh show in their N-terminal regions (residues 1-54, referred to as AbrB_{NT} and Abh_{NT}, respectively) 70% sequence identity with non homologous residues present near the N- and C-termini and in the linker region between the α -helix and the β 3-sheet. Structural variations between the two swapped-hairpin β -barrels are described for the important arginines Arg8, Arg15, Arg23, and Arg24 (Fig. 42). In particular, a significant reorientation of the α / β 3-linker was detected. Together with denotative differences in their surface charge potentials (Fig. 42), a correlation to their different DNA-binding specificities is drawn (Bobay et al., 2006).

SpoVT_{NT} and AbrB_{NT} vary in the amino acid composition of the linker which connects the α 1-helix to the β 3-strand as well. In SpoVT_{NT}, this linker interacts with the α 1-helix for stabilisation and possibly plays an important role in the flexibility of the helix relative to the β -barrel. Compared to AbrB_{NT}, the α -helices of SpoVT_{NT} provide a significant enhancement in negative charges which is based on the two additional arginines Arg27 and Arg29 (Fig. 42). The DNA-binding specificity of swapped-hairpin β -barrels might be dependent on the mobility and the charge property of their helices which leads to varying interactions with the DNA. For AbrB, an important role of the arginines Arg25 and Arg26 in DNA-binding was confirmed already (Vaughn et al., 2000). The positively charged helices of swapped-hairpin β -barrels probably support the adjustment of the anti-parallel β -sheet (β 2 and β 2') which exposes the arginines well-positioned to dock into the major groove of B-DNA.

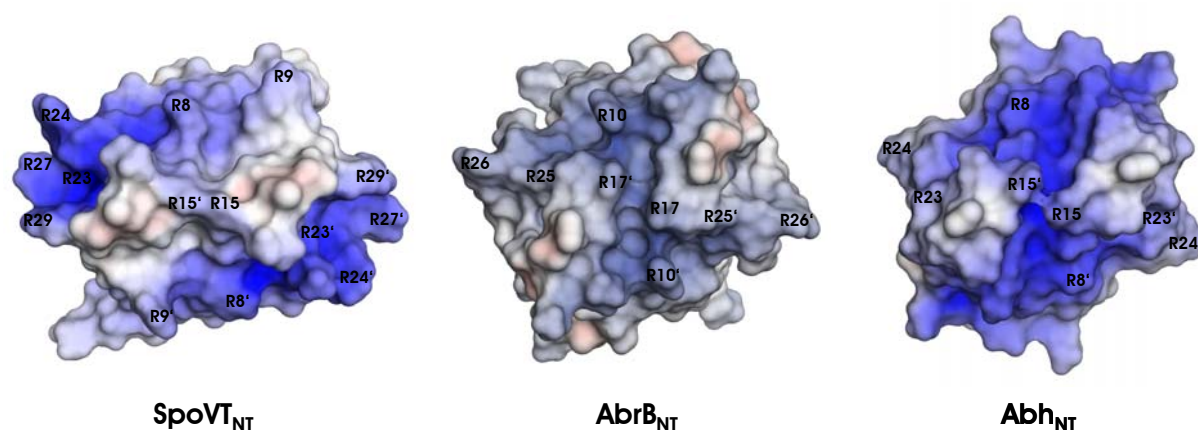


Figure 42. Surface Charge Potentials of DBDs of SpoVT, AbrB, and Abh. Surface representations of SpoVT_{NT} (left), AbrB_{NT} (PDB entry 1YSF) (middle), and Abh_{NT} (PDB entry 2FY9) (right) illustrating their surface charge potentials with view onto the anti-parallel $\beta 2/\beta 2'$ -sheets. Arginines are marked and surface charge potentials are coloured in blue and red for basicity and acidity, respectively (values coloured from -10 (red) to 10 (blue) kT/e).

Generally, β -sheets which represent the structural DNA-binding motif are rather rare in bacteria. The swapped-hairpin β -barrel describes a new β -sheet based DNA-binding motif and thus, determination of a complex structure with DNA would be of great interest.

4.3 Signal Sensing Domain (SSD) of *B. subtilis* SpoVT

SpoVT is the first structurally described protein which couples a swapped-hairpin β -barrel with a GAF domain.

GAF domains are SMBDs, "...whose principal biochemical role is to exert a regulatory effect and/or transmit signal by binding a small molecule" (Anantharaman, 2001). Within the SMBDs, GAF domains represent one of the largest and most widespread groups of SSDs and are especially prominent among bacteria (Anantharaman, 2001). The similarity between different GAF domains is structure based while sequence similarities are not frequent (Ho et al., 2000). The basic fold of GAF domains is a central anti-parallel β -sheet which is surrounded by α -helices.

The SSD of SpoVT_{CT}, SpoVT_{CT}, shows structural similarities to the GAF domain CodY_{NT} and the profilin-like IclR_{CT}, demonstrated by their superpositions depicted in Figure 43a. In respect of their sequences, they appear rather divergent (Fig. 43b).

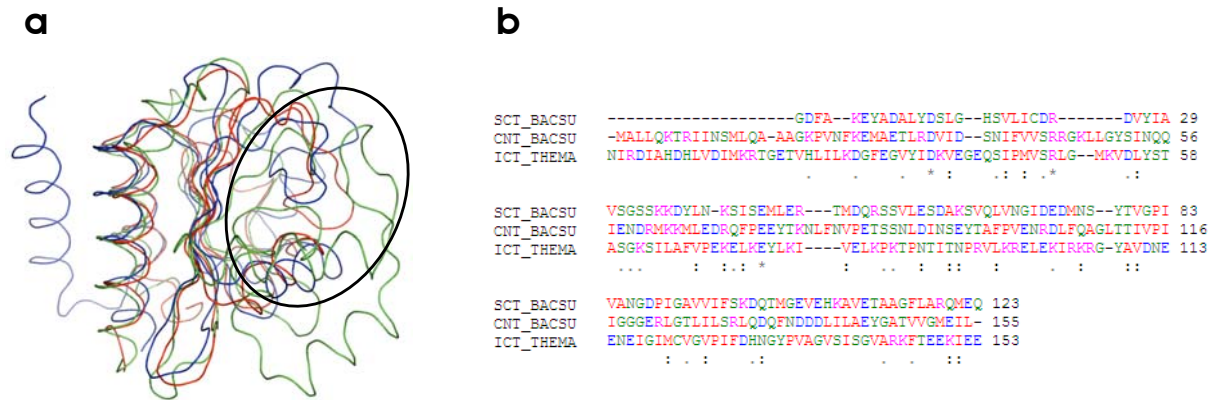


Figure 43. SSDs of SpoVT, CodY, and IclR. (a) Ribbon representation of superposed SpoVT_{CT} (red), CodY_{NT} (PDB entry 2B18) (blue), and IclR_{CT} (PDB entry 1MKM) (green) with ligand binding pocket marked by an ellipse. (b) Sequence alignment of SpoVT_{CT} (residues 56(1)-178(123); SCT_BACSU) and CodY_{NT} (residues 1-155, CNT_BACSU) of *B. subtilis* and IclR_{CT} of *T. maritima* (residues 76(1)-228(153), ICT_THEMA). Colour-coding is based on ClustalW (Higgins et al., 1994); (*) invariant, (:) strongly conserved, and (.) semi-conserved amino acids.

The structural similarity between SpoVT_{CT}, CodY_{NT} and IclR_{CT} is restricted to the central anti-parallel β -sheet and the helix bundles which are placed to one side of the β -sheets (r.m.s.d. of 1.5 Å, see 3.4.6.2). The potential ligand binding pockets, shaped at the other side of the β -sheet, differ clearly among each other (Fig. 43a). Especially IclR_{CT} distinguishes from SpoVT_{CT} and CodY_{NT}, regarding secondary structure elements defining the binding pocket.

GAF domains in their holo-form show the small molecule usually deeply embedded in the binding pocket (Vannini et al., 2002) and enclosed by loops and helices via a “clamp mechanism” (Zhang et al., 2002). IclR_{CT} (PDB entry 1MKM) binds a Zn atom in its binding pocket (Zhang et al., 2002), the TraR GAF domain locks the autoinducer *N*-(3-oxo-octanoyl)-L-homoserine lactone (Vannini et al., 2002), and the GAF-A/B domains from the product of the *Anabaena* adenylyl cyclase *cyaB2* gene bind negatively charged cyclic nucleotides. The ligand binding pocket of the *cyaB2* GAF domains is a partially charged cavity (Martinez et al., 2005) shaped by small residues mainly (Fig. 44). SpoVT_{CT} and the related CodY_{NT} (see 3.4.6.2) show a hydrophobic binding pocket partly

defined by bulky residues (i.e. Leu75, Ile98, Val120, and Phe151 in SpoVT_{CT} and Phe40, Val42, Leu79, and Ile113 in CodY_{NT}) (Fig. 44).

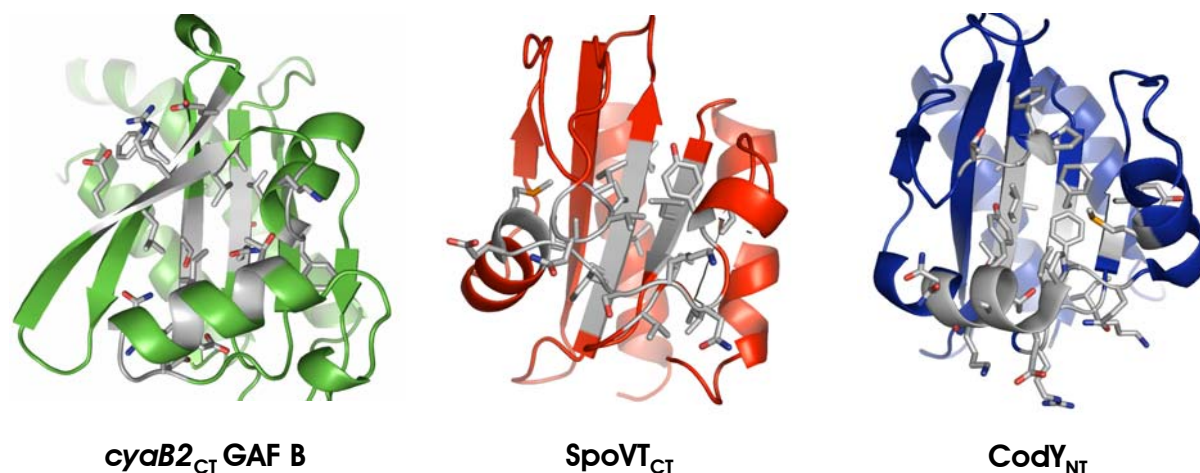


Figure 44. Ligand Binding Pockets of GAF Domains. Cartoon illustration of the GAF B domain of the product of the *Anabaena* adenylyl cyclase *cyaB2* gene (PDB entry 1YKD) (*cyaB2*_{CT} GAF B, left, green), SpoVT_{CT} (middle, red), and CodY_{NT} (PDB entry 2B18) (blue, right). Relevant residues of the ligand binding pocket are shown as sticks in element colour code.

CodY is known to sense intracellular GTP and BCAA levels (Ratnayake-Lecamwasam et al., 2001). An additive effect of both ligands on CodY was proven recently and hence, different binding sites for both ligands were assumed (Handke et al., 2008). Lately, the structure of the holo-form of CodY_{NT} was solved (Levdikov et al., 2006) which revealed the binding mode of the BCAAs valine and isoleucine to the ligand binding pocket. Both hydrophobic amino acids seemed to be attached to the binding pocket rather than enclosed (for isoleucine see Fig. 45). Thereby, the extensive β 3- β 4 loop of the CodY_{NT} binding pocket (residues Ile91-Pro99, (Levdikov et al., 2006), see 3.4.6.2, Fig. 35b) was bended inwardly (PDB entry 2B18 with isoleucine and 2HGV with valine) (Fig. 45). The superposition of SpoVT_{CT} and holo-CodY_{NT} in Figure 45 clearly demonstrates the differences in the conformation of the structural elements which define the particular ligand binding pocket. In SpoVT_{CT}, the β 7- β 8 loop is stretched out and the “clamp” (α 4-helix and β 7- β 8 loop) is closed compared to the open arrangement of the β 3- β 4 loop and the α 4-helix in CodY_{NT} (Levdikov et al., 2006).

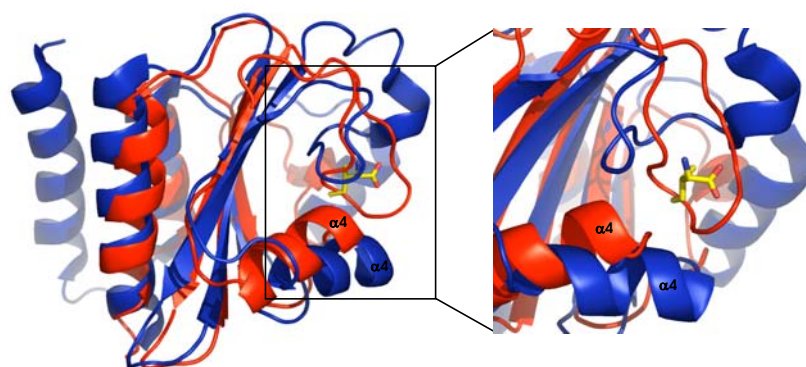


Figure 45. GAF Domains of SpoV_{CT} and CodY_{NT}. Superposition of SpoV_{CT} (red) and CodY_{NT} (blue) with isoleucine bound to CodY_{NT} (PDB entry 2B18) (left); zoom-in into the binding pocket with CodY_{NT} bound isoleucine (right). Isoleucine is represented in gold coloured sticks. α -helix involved in "clamp mechanism" (α 4) is labelled for each domain.

It is assumed that this "closed" state of SpoV_{CT} presents its apo-form and that a yet unknown molecule will bind in a regulatory capacity. The regulatory effect is thought to be caused by conformational changes throughout the SpoV_{CT} domain. For the homologous CodY_{NT}, conformational changes induced upon binding of BCAAs are known (Levdikov et al., 2006). In SpoV_{FL}, those rearrangements within SpoV_{CT} supposedly are translocated all over the protein and consequently, all over the tetrameric complex which then induce the DNA-binding activity of SpoV.

4.4 Dimerisation Mode of GAF Domains in *B. subtilis* SpoV

In addition to signal sensing, SSDs of transcription factors can be involved in the formation of oligomeric structures (see 4.1.2). In particular, GAF domains can act as multimerisation domains presenting a broad variety in the adopted multimerisation modes (Ho et al., 2000; Levdikov et al., 2006; Martinez, Wu et al., 2002; Vannini et al., 2002; Zhang et al., 2004).

Ho et al. published in the year 2000 the crystal structure of the YKG9 protein of *Saccharomyces cerevisiae* as the first structurally characterised GAF domain. The

protein with an unknown function was discovered to form an anti-parallel dimer with an interface formed by α -helices, β -sheets and loops (Ho et al., 2000). In 2002 and 2005, structures of GAF domains of the mouse PDE-2A and of the product of the adenylyl cyclase gene *cyaB2* of the cyanobacterium *Anabaena*, respectively were published by Martinez et al. Both proteins are dimers of tandem GAF-A/B domains. The PDE dimer is arranged in a parallel manner, while the adenylyl cyclase forms an anti-parallel dimer. The interaction of the monomers in both proteins occurs mainly through helical interactions and is entirely different to the YKG9 protein (Martinez et al., 2005; Martinez, Wu et al., 2002).

A helical interaction between GAF domains forming a four-helical coiled coil interface was recently published by Levnikov et al. (Levdikov et al., 2006) which is most similar to the dimer interface of SpoVT_{CT} (see 3.4.7, Fig. 36). In both proteins, the GAF domains are in an anti-parallel orientation but the interface of CodY_{NT} describes a parallel four-helical coiled coil in contrast to an anti-parallel four-helical coiled coil of the SpoVT_{CT} dimer. Both dimers form a right-handed supercoil due to the helical interactions but they show tremendous differences in their helix crossing angles (described in detail in 3.4.7). While in CodY_{NT} the monomers interact by a fairly straight arrangement, monomers of the SpoVT_{CT} dimer are significantly twisted against each other (Fig. 46).

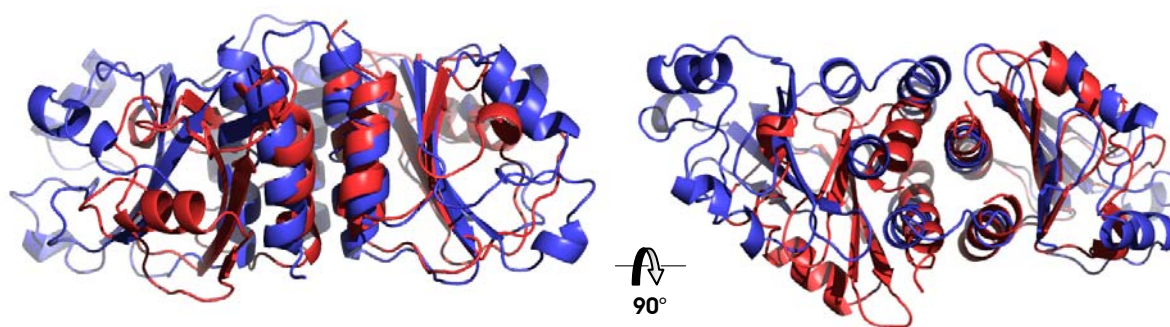


Figure 46. SpoVT_{CT} and CodY_{NT} Dimers. Superposition of dimers of SpoVT_{CT} (red) and CodY_{NT} (PDB entry 2B18) (blue) with sight at the dimer interface (left) and onto the interface mediating helix bundles (right).

The core geometries of the SpoVT_{CT} dimer interface include two layers with *complementary x-da packing* (see 3.4.7, Fig. 36), a helical conformation found in merely a few coiled coil structures (Hulko et al., 2006). The CodY_{NT} coiled coil adopts the

energetically advantageous canonical *knobs-into-holes* conformation in an unusual parallel helix arrangement (Gruber and Lupas, 2003).

Because of the different geometry of the dimer interface which was discovered for SpoVT_{CT}, it is stated that the dimerisation mode presented here is new in interacting GAF domains. For SpoVT_{FL}, this extraordinary arrangement is probably somehow decisive for the regulatory function.

4.5 Model for SpoVT Mediated Regulation

The findings about the σ^G -dependent forespore-specific transcriptional regulator SpoVT presented in this work, together with already known data of the protein, confirm the assumption that SpoVT is a GAF domain regulated transcription factor.

The described asymmetric SpoVT_{FL} tetramer, which is denoted as the inactive state of SpoVT (see 4.1.2), supports the observations that SpoVT_{FL} does not bind to DNA *in vitro*. It is suggested, that the distortion of the two swapped-hairpin DBDs in the SpoVT_{FL} tetramer hampers docking into two consecutive major grooves of specific DNA recognition sites. The asymmetric spiral-form of the complex is adhered by several intra- and intermolecular contacts, which are supposed to be responsible for the prevented adaption to the DNA segment.

Investigations on the SpoVT_{CT} domain discovered a new dimerisation mode for GAF domains with an uncommon interaction geometry. This feature is addressed to be somehow decisive for the switch between the inactive and active form of SpoVT_{FL}.

The idea that SpoVT is a GAF domain regulated transcription factor is confirmed by the structure of SpoVT_{CT} revealing a GAF fold. Despite the failure of identification of the small molecule which specifically binds to the SpoVT_{CT} GAF domain for regulatory effects, it is strongly believed that this is the key step in activation of SpoVT.

Based on those data, a model for the SpoVT mediated transcriptional regulation has been developed (Fig. 47).

The asymmetric conformation of tetrameric SpoVT_{FL} is adversarial to bind to specific DNA targets. In this inactive state, SpoVT_{FL} is unable to exert its regulatory function (Fig. 47, left). At a definite status during the sporulation progress, a certain signal molecule is present at a high concentration in the forespore chamber (Fig. 47, middle). The molecule binds specifically to the ligand binding pocket of the SpoVT_{CT} GAF domains in the SpoVT_{FL} tetramer. The ligand binding process induces conformational changes within the SpoVT_{CT} GAF domains which are transferred to the SpoVT_{NT} DBDs via the domain connecting linkers. Upon this, specified interactions within the tetrameric complex are impaired which enables SpoVT_{NT} DBDs to rearrange in a concerted action. A symmetric SpoVT_{FL} complex with a parallel alignment of the SpoVT_{NT} DBDs is formed (Fig. 47, right). This conformation of the SpoVT_{FL} tetramer features a high affinity towards specific DNA segments which represents the active form of SpoVT_{FL}. The accurately arranged swapped-hairpin DBDs dock into two consecutive major grooves of a DNA section presenting a compatible sequence pattern (Fig. 47, right). The transcription of genes, whose products are necessarily used in the forespore development, is initiated.

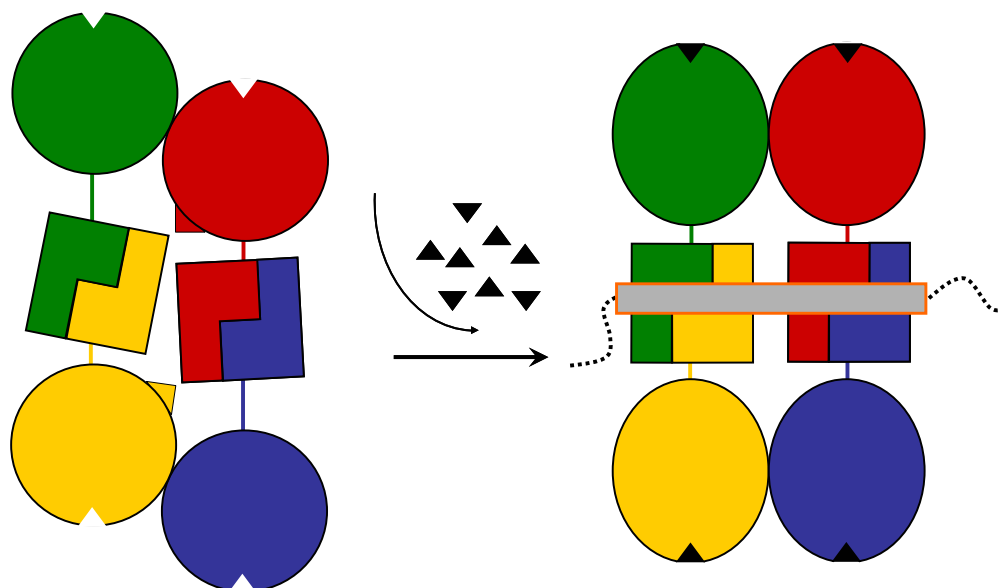


Figure 47. Model of Proposed Mechanism for SpoVT_{FL} Mediated Transcriptional Regulation. Scheme of proposed functionality of tetrameric SpoVT_{FL}. Inactive SpoVT_{FL} (left) is activated upon ligand binding and DNA-binding is induced (right). SpoVT_{FL} tetramer is coloured by subunits (according to Figure 24) with SpoVT_{CT} SSDs as filled circles (left) or ellipses (right) and SpoVT_{NT} DBDs as I-shaped bricks. Stabilisation of the asymmetric tetramer is represented by filled yellow and red triangles (left). The putative SpoVT specific ligand is depicted as filled black triangles and DNA is indicated as a dotted line with a grey bar framed in orange illustrating the DNA recognition site.

5. MATERIALS

5.1 Chemicals and Reagents

<i>Substance</i>	<i>Provider</i>	<i>Substance</i>	<i>Provider</i>
β -mercaptoethanol	Merck	K_2HPO_4	Merck
Acrylamide (Protogel)	Roth	KCl	Merck
Ammoniumpersulfate	Merck	KH_2PO_4	Merck
Bromophenol blue	Merck	Malachite green	Sigma
$CaCl_2$	Merck	Methanol	Merck
cGMP	Sigma	$MgCl_2$	Merck
Coomassie Brilliant Blue R-250	Serva	$MgSO_4$	Merck
$CuSO_4$	Sigma	$MnCl_2$	Sigma
Dipicolinic acid	Sigma	MOPS	Biomol
DTT	Merck	Na_2HPO_4	Merck
EDTA	Merck	NaCl	Merck
Eosine	Sigma	NaH_2PO_4	Merck
Ethanol	Riedel-de Haën	NaOH	Merck
$FeSO_4$	Sigma	PEG 200	Fluka
Glacial acid	Fluka	PEG 600	Fluka
Glutaraldehyde, 25% aqueous solution	Merck	SDS	Serva
Glycerol	Riedel-de Haën	Sulfosalicylic acid	J. T. Baker
Glycine	Merck	TCA	Riedel-de Haën
GTP	Sigma	TEMED	Serva
HCl	Merck	Tris, Trizma	Merck, Sigma
Imidazole	Merck	Triton X-100	Sigma
Isoleucine	Fluka	Tween 20	Sigma
		Valine	Fluka

5.2 Kits and Materials

Kits:

Kit

ABI Prism Big Dye Terminator version 3.1
 Champion pET100 Directional TOPO Expression Kit
 Crystallisation Kits

 LMW Gel Filtration Calibration Kit
 NativePAGE
 NuPAGE Bis-Tris Gel System
 PCR Master Mix and H₂O
 QIAprep Spin Miniprep Kit
 QIAquick PCR Purification Kit

Provider

Perkin Elmer Applied Biosystems
 Invitrogen
 Hampton Research, Sigma, Jena
 Biosciences, Emerald BioSystems
 Amersham Biosciences
 Invitrogen
 Invitrogen
 Roche
 Qiagen
 Qiagen

Materials:

Material

Affi-Gel beads
 BSA
 Cellulose membrane dialysis tubing
 Complete protease inhibitor cocktail
 Concentrators
 Crystallisation material and tools
 DNase
 Freundsches Adjuvant incomplete
 Horseradish peroxidase, goat anti rabbit
 Kanamycin
 Lysozyme
 Molecular weight marker
 Ni-NTA superflow beads
 PVDF membrane
 Slide-A-Lyzer dialysis cassettes
 Titermax Gold

Provider

Bio-Rad
 Serva
 Sigma
 Roche
 Amicon Millipore
 Hampton Research
 Roche
 Sigma
 Sigma
 Sigma
 Merck
 Fermentas
 Qiagen
 Millipore
 Pierce
 Sigma

Trypsin	Roche
Whatman paper 3MM	VWR
α -chymotrypsin	Sigma

5.3 Media, Buffers, and Solutions

5.3.1 Growth Media

Prepared growth media were autoclaved at 394 K and 2 bar for 20 min. Liquid growth media were routinely sterilised in Schikane flasks. Antibiotics for selection were added to cooled medium shortly before inoculation if necessary. In the case of media for agar plates, antibiotics were added at a temperature of ~ 323 K prior to pouring.

5.3.1.1 LB Medium

Luria Bertani (LB) medium for *E. coli* and *B. subtilis*:

1% (w/v)	bacto tryptone (Becton, Dickinson and Company)
0.5% (w/v)	bacto yeast extract (Becton, Dickinson and Company)
1% (w/v)	NaCl (171 mM)

pH 7.0, adjusted with NaOH

5.3.1.2 TB Medium

Terrific broth (TB) medium for *E. coli*:

1.2% (w/v)	bacto tryptone (Becton, Dickinson and Company)
2.4% (w/v)	bacto yeast extract (Becton, Dickinson and Company)
0.4% (w/v)	glycerol

pH 7.5, adjusted with 100 mM $\text{KH}_2\text{PO}_4/\text{K}_2\text{HPO}_4$ buffer

5.3.1.3 DSM Medium

Difco sporulation medium (DSM) for *B. subtilis*:

0.8% (w/v)	nutrient broth (Fluka)
0.1% (w/v)	KCl (13.4 mM)
0.025% (w/v)	MgSO ₄ (2.1 mM)

Supplements:

1 μ M	MnCl ₂
0.1 mM	CaCl ₂
0.1 μ M	FeSO ₄

Respective amounts of the filter-sterilised supplement stock solutions (see 5.3.3) were added after autoclaving.

5.3.1.4 LB Agar Plates

1% (w/v)	bacto tryptone (Becton, Dickinson and Company)
0.5% (w/v)	bacto yeast extract (Becton, Dickinson and Company)
1.5 g (w/v)	bacto agar (Becton, Dickinson and Company)
1% (w/v)	NaCl (171 mM)

pH 7.0, adjusted with NaOH

5.3.2 Buffers

<i>Method</i>	<i>Abbreviation</i>	<i>Composition</i>
<u>Ni-NTA buffers (NB)</u> pH 8.0, adjusted with NaOH	NB 1	50 mM NaH ₂ PO ₄ , 300 mM NaCl, 10 mM imidazole
	NB 2	50 mM NaH ₂ PO ₄ , 300 mM NaCl, 30 mM imidazole
	NB 3	50 mM NaH ₂ PO ₄ , 300 mM NaCl, 500 mM imidazole
	PBS	140 mM NaCl, 2.7 mM KCl, 10 mM Na ₂ HPO ₄ , 1.8 mM KH ₂ PO ₄
<u>10x PBS buffer</u>		
pH 7.3, adjusted with K ₂ HPO ₄		
<u>Antibody purification buffers (AB)</u>	AB 1	1 M Tris-HCl pH 7.5
	AB 2	10 mM Tris-HCl pH 7.5, 100 mM NaCl
	AB 3	10 mM Tris-HCl pH 7.5, 1 M NaCl
	AB 4	1 M Tris-HCl pH 8.0
<u>SDS-PAGE buffers (SPB)</u>	SPB 1	250 mM Tris-HCl pH 8.0, 7.5% (w/v) SDS, 12.5% β-mercaptoethanol, 25% glycerol, 0.025% bromo-phenol blue
	SPB 2	250 mM Tris-HCl pH 6.8, 0.5% (w/v) SDS, 0.96 M glycine
	SPB 3	1.5 M Tris-HCl pH 6.8, 0.5 mM EDTA, 0.4% (w/v) SDS
	SPB 4	1.5 M Tris-HCl pH 8.8, 0.5 mM EDTA, 0.4% (w/v) SDS
<u>Electro blotting buffers (EB)</u>	EB 1	300 mM Tris-HCl pH 10.4
	EB 2	25 mM Tris-HCl pH 10.4
	EB 3	25 mM Tris-HCl pH 9.4, 40 mM ε-aminocaproic acid
<u>Western blotting buffers (WB)</u>	WB 1	10 mM Tris-HCl pH 7.5, 150 mM NaCl
	WB 2	10 mM Tris-HCl pH 7.5, 150 mM NaCl, 3% (w/v) BSA
	WB 3	20 mM Tris-HCl pH 7.5, 500 mM NaCl, 0.2% (v/v) Triton X-100, 0.05% (v/v) Tween 20
<u>MOPS buffer</u>	MOPS	20 mM MOPS, 120 mM NaCl
pH 7.25, adjusted with NaOH		
<u>Limited proteolysis buffers (LPB)</u>	LPB 1	20 mM Tris-HCl pH 8.0, 1 mM MgCl ₂ , 1 mM DTT, 0.5 mM EDTA
	LPB 2	20 mM Tris-HCl pH 8.0, 1 mM MgCl ₂ , 1 mM DTT, 2 mM CaCl ₂
<u>Spore buffers (SB)</u>	SB 1	10 mM NaH ₂ PO ₄ /Na ₂ HPO ₄ pH 7.2
	SB 2	10 mM NaH ₂ PO ₄ /Na ₂ HPO ₄ pH 7.2, 1% (w/v) lysozyme, complete protease inhibitor cocktail
	SB 3	10 mM NaH ₂ PO ₄ /Na ₂ HPO ₄ pH 7.2, 500 mM NaCl
	SB 4	6 M urea, 50 mM DTT, 1% (w/v) SDS, pH 10.0
<u>Microseeding buffer</u>	MSB	100 mM HEPES, 25% (w/v) PEG 3350, 200 mM NaCl
pH 7.5, adjusted with NaOH		

Table 5. Buffers.

5.3.3 Solutions

- 0.025% Glutaraldehyde
- 0.1% Coomassie Brilliant Blue R250 in water:methanol:glacial acid = 45:45:10
- 100 mM Glycine pH 2.8
- 2% (w/v) Ponceau S in TCA : sulfosalicyl acid : ddH₂O = 30 : 30 : 40
- 2.5% (w/v) Eosine
- 3% (w/v), 10% (w/v), or 200 mg*ml⁻¹ BSA in 10 mM Tris-HCl pH 7.5, 150 mM NaCl
- 4% (w/v) CuSO₄
- 5% (w/v) Malachite green
- Coomassie destain: water : methanol : glacial acid = 45 : 45 : 10
- Pre-cast BCA (Sigma)
- SuperSignal West Pico Chemiluminescent Substrate (Pierce)

Stock solutions:

- 0.1 M CaCl₂
- 0.1 mM FeSO₄
- 1 M IPTG
- 1 mg*ml⁻¹ α-chymotrypsin
- 1 mg*ml⁻¹ Trypsin
- 1 mM MnCl₂
- 10 mg*ml⁻¹ Kanamycin
- 100 mM cGMP
- 100 mM DPA in 2.5 N NaOH or MeOH
- 100 mM GTP
- 100 mM Isoleucine
- 100 mM Valine
- 10xPBS buffer (see 5.3.2); for 1x PBS buffer, stock solution was diluted 1:10 with ddH₂O.
- 5% Lysozyme

Substances were dissolved in water, filter-sterilised, distributed to aliquots, and stored at 277 K or 253 K.

5.4 Strains, Plasmids, and Oligonucleotides

5.4.1 Strains

B. subtilis 168

Colonies of *Bacillus subtilis* subsp. *subtilis* strain 168 on an agar plate were a thankworthy donation by Dr. Janine Kirstein (Freie Universität Berlin).

E. coli chemically competent DH5 α cells

Library efficiency DH5 α competent cells (Invitrogen)

F⁻ ϕ 80/*lacZ* Δ M15 Δ (*lacZYA-argF*)U169 *recA1 endA1 hsdR17*(r_k⁻, m_k⁺) *phoA supE44 thi-1 gyrA96 relA1 λ* ⁻

E. coli chemically competent BL21 Star (DE3) cells

BL21 Star (DE3) one shot chemically competent *E. coli* (Champion pET100 Directional TOPO Expression Kit, Invitrogen)

F⁻ *ompT hsdS_B* (r_B⁻m_B⁻) *gal dcm rne131* (DE3)

5.4.2 Vector

To create constructs for the overexpression of the His₆-SpoVT_{FL} and the His₆-SpoVT_{CT} protein, the vector pET30b(+) (Novagen) (Fig. 48) was used. The *spoVT* open reading frame was amplified from *Bacillus subtilis* strain PY79 (prototroph, derived from strain 168, (Youngman et al., 1984)). The genes *his₆-spoVT_{FL}* and *his₆-spoVT_{CT}* were cloned into the vectors digested with *Nde*I and *Xho*I. Cloning procedures were carried out by Dr. Sergej Djuranovic, MPI for Developmental Biology, Tübingen* (Djuranovic, 2007).

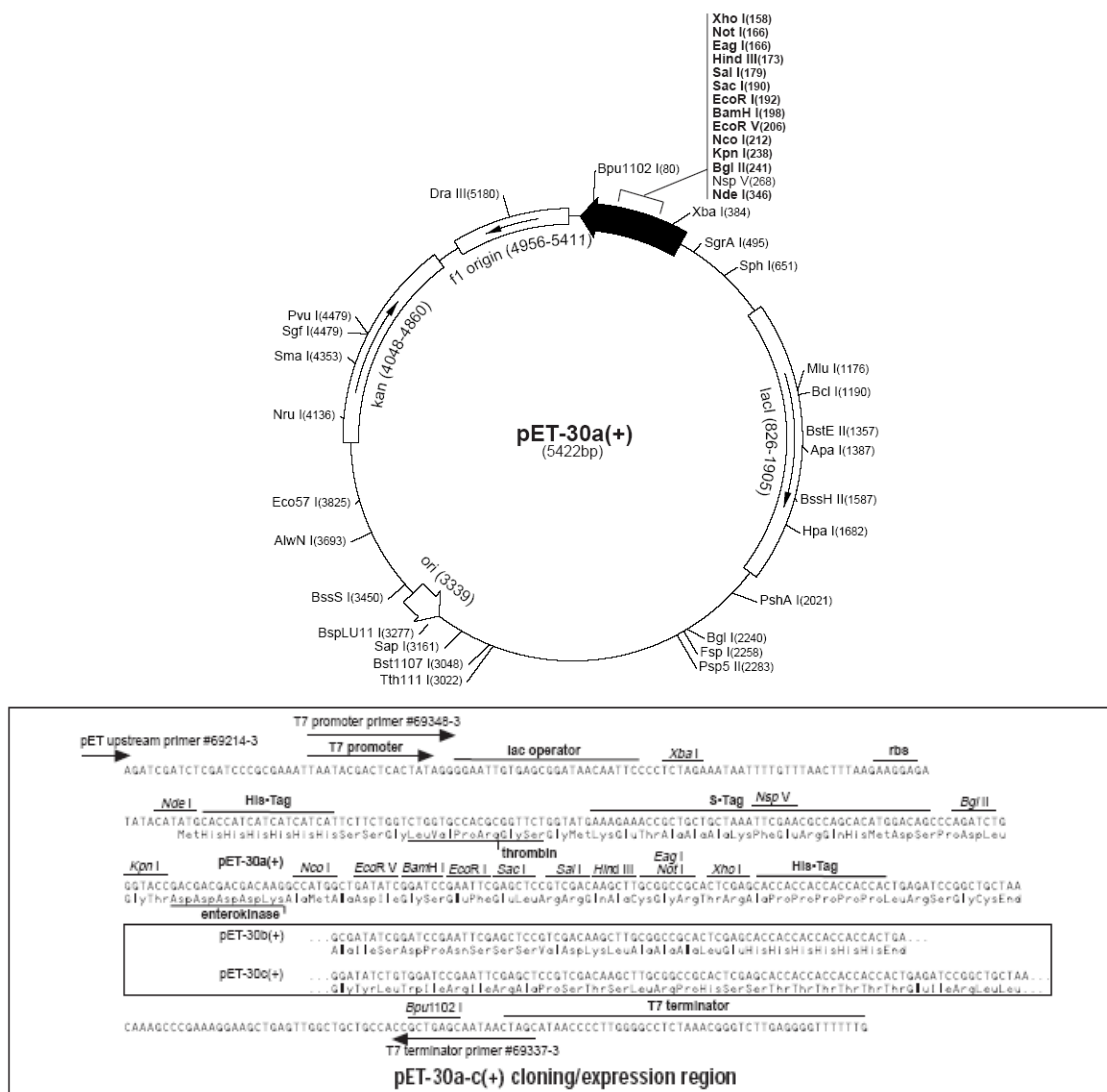


Figure 48. pET-30a-c(+) Vector Map. Vector map of the pET-30a-c(+) vector (Novagen) with kanamycin resistance gene (Kan^r) for overexpression of fusion proteins with an N-terminal His₆-tag in *E. coli*. Taken from <http://www.merckbiosciences.co.uk/docs/docs/PROT/TB095.pdf>.

5.4.3 Oligonucleotides

All oligonucleotides were purchased from Metabion. The desalted solutions provided oligonucleotide concentrations of 100 pmol·μl⁻¹.

T7 primer: promoter and terminator sequences for DNA sequencing

T7 pro (promoter sequence): 5'-TAATACGACTCACTATAGGG-3'

T7 term (terminator sequence): 5'-GCTAGTATTGCTCAGCGG-3'

The oligonucleotides were synthesised in a 0.02 μ mol scale.

Primer for DNA-binding tests

forSpVOp5' (SpoVT operon sequence forward):

5'-CGTAAATTTGTTACTCTCTGGTGTATATTACATTTGATGTGACGGATACTAATTTCAAGCGAG-GCGGAAGGTACATAAAGTAACTGCTTAGGTCTTT-3'

revSpVOp5' (SpoVT operon sequence reverse):

5'-AATACGACGTACGATACCGGTTGCTTTCATCTCTGGTGCCTCTCTTTCATTTGATGGTATAT-ACATGTGGGAAAGACCTAAAGCAGTTACTTTATGTAC-3'

The oligonucleotides were synthesised in a 0.04 μ mol scale.

5.5 Instruments and Devices

Centrifuges:

- Beckman Avanti J-20XP centrifuge, rotors JA 25.50 and JLA 8.1000
- Beckman Avanti J-25 centrifuge, rotor JA 25.50
- Beckman Optima LE-80K ultracentrifuge, rotors 45Ti and 60Ti
- Eppendorf centrifuge 5417R, rotor F 45-30-11
- Eppendorf centrifuge 5810 R, rotor A-4-62
- Hettich Rotixa/KS centrifuge, rotor 5094-684
- Sigma 4K15 swing-out rotor

SDS-PAGE devices:

- Gel Electrophoresis System Mighty Small II SE250/SE260 (Hoefer/Amersham Pharmacia Biotech AB)
- Multiple Gel Caster (in house)
- Power Supply EPS 300 (Pharmacia Biotech)
- XCell SureLock Electrophoresis Cell (Novex Mini-Cell) (Invitrogen)

Semi-Dry Blot Apparatus (in house)

DNA Thermal Cycler (Perkin Elmer)

Spectrometer:

- CD spectrometer (Spectropolarimeter Jasco J-715, Rev. 1.00, including Peltier element controller, JASCO Corporation)
- Spectrophotometer (ND-1000, NanoDrop Technologies Inc.)
- UV-Vis spectrometer, Ultrospec II (LKB Biochrom)

Isothermal Calorimetry Titrator (MicroCalorimeter VP-ITC, MicroCal)

X-ray Film Developer (X-OMAT 1000 Processor, Kodak)

Shaking Incubator Multitron AJ20 and GFL 3033 (Infors AG)

HPLC:

- ÄKTA Explorer and ÄKTA Basic High Pressure Liquid Chromatography (HPLC) system (Amersham Biosciences)
- Empty XK columns (Amersham Biosciences)
- HPLC/Mass Spectrometry (MS) system (Single Quatrupol API 165, Perkin Elmer Sciex; ReflexIII, Bruker, Daltronics, Bremen; Ultraflex II TOF/TOF, Bruker Daltronics, Bremen)
- SMART Chromatography System (Amersham Biosciences)
- Superdex 75 pre-packed gel filtration columns HiLoad 26/60 prepgrade and PC 3.2/30 (Amersham Biosciences)

Glass Eono-column column (Bio-Rad)

Microscopes:

- Light microscope Laborlux D (Leitz) with Hamamatsu Digital Camera C4742-95
- Light microscope Olympus Optical CO., LTD SZX12-ILLK200 with CCD camera Canon Power Shot A620

French Pressure Cell Press (Polytec GmbH, Aminco SLM Instruments)

Varioclav (H + P Labortechnik)

5.6 Computational Software

Sequence searches were performed with PSI-Blast server (Altschul et al., 1997) on the non-redundant protein sequence database at the National Center for Biotechnology Information[†] and with HHpred (Söding, 2005) on sequences from the Protein Data Bank, filtered at 70% sequence identity (PDB70). Sequence alignments were made with ClustalW (Higgins et al., 1994). Structure alignments were obtained from DALI (Holm and Sander, 1993) and were investigated further using the PISA database (Krissinel and Henrick, 2007) and the RMSD calculator (Claude et al., 2004).

X-ray data were processed using the software mentioned in corresponding chapters.

DNA sequences were checked with BioEdit.

Topology diagrams were generated using TopDraw (Bond, 2003) and figures were created with PyMOL[‡], CorelDraw and PowerPoint.

[†] www.ncbi.nlm.nih.gov

[‡] <http://pymol.sourceforge.net/>

6. METHODS

6.1 Molecular Biology and Microbiology

6.1.1 Molecular Biological Methods

6.1.1.1 Amplification of SpoVT Operon DNA Sequence by Polymerase Chain Reaction (PCR)

The DNA fragment including the SpoVT promoter sequence (see 2.4.2) was produced via a polymerase chain reaction (PCR) using overlapping primers (see 5.4.3). 1 μ l of each of the primer solutions (100 pmol* μ l⁻¹) were mixed with 12.5 μ l PCR Master Mix and filled up to 25 μ l with H₂O_{dest} (Roche).

The T_M was calculated according to the equation

$$T_M = 3 * \Sigma(C_i + G_i) + 2 * \Sigma(A_i + T_i).$$

The PCR was performed according to the the cycle scheme

Denaturation	368 K	30 sec	} 30 cycles
Annealing	358 K	5 sec	
Extension	345 K	5 sec	

Purification of the PCR reaction products was done using the Qiagen PCR Purification Kit following manufacturer's protocol (see 9.).

6.1.1.2 Isolation and Purification of Vector DNA from *E. coli*

5 ml of LB medium inclusive the relevant antibiotic for selection were inoculated with a single colony taken from an adequate LB agar plate. The cells grew overnight at 310 K and 200 rpm. Cells were harvested by centrifugation for 10 min at 3220*g and medium was decanted. Isolation of vector DNA was done by alkaline lysis of the cells following Qiagens QIAprep Spin Miniprep protocol using the commercial available Kit (see 9.).

6.1.1.3 Determination of DNA Concentration

DNA concentration was determined photometrically by measurement of the absorption of DNA solutions at 260 nm and 280 nm. Absorption of 1 at 260 nm corresponds to a solution containing 50 $\mu\text{g}\cdot\text{ml}^{-1}$ DNA. An $\text{OD}_{260}/\text{OD}_{280}$ ratio of 1.8 accounts for a solution yielding pure double stranded DNA.

6.1.1.4 DNA Sequencing

For DNA sequencing, 3 μl (~ 300 ng) of the isolated plasmid DNA obtained from *E. coli* DH5 α cells (see 6.1.1.2), were mixed with 1 μl of the 100 pmol* μl^{-1} primer solutions of the T7 promoter and the T7 terminator. To apply the chain-termination method, fluorescence labelled 2',3'-dideoxy nucleotides were added by using 3 μl of the BigDye Kit "3.1". The reaction sample was filled up to 20 μl with ddH₂O and reaction was processed by following the cycle programme

Initial denaturation	369 K	1 min	} 30 cycles
Denaturation	369 K	30 sec	
Annealing	323 K	30 sec	
Elongation	333 K	4 min	

Amplified PCR products were purified and analysed by the in house Core Facility.

6.1.2 Microbiological Methods

6.1.2.1 Transformation of Chemically Competent *E. coli* Cells

The plasmids encoding N-terminally His₆-tagged SpoVT_{FL} and N-terminally His₆-tagged SpoVT_{CT} were provided from Dr. Sergej Djuranovic, MPI for Developmental Biology, Tübingen* (Djuranovic, 2007).

The transformation procedure of chemically competent *E. coli* DH5 α cells (Library Efficiency, Invitrogen) for amplification of vector DNA was done according to manufacturer's protocol (see 9.).

The transformation procedure of chemically competent *E. coli* BL21 Star (DE3) cells (Champion pET100 Directional TOPO Expression Kit, Invitrogen) for protein overexpression was done corresponding manufacturer's protocol "Champion pET Directional TOPO Expression" (see 9.).

For selection of transformants, different volumes of the cell suspensions (10, 50, and 100 μ l) were plated onto selective LB agar plates (see 5.3.1.4). Overnight incubation was done at 310 K.

LB agar plates were used for short-term storage support of bacterial cells.

6.1.2.2 Long-term Stock Cultures

Long-term storage cultures were prepared using liquid cultures. Therefore, DMSO or pre-sterilised glycerol was added to overnight cultures to a final content of 7% or 30%, respectively. After vigorously vortexing, stock cultures were aliquoted and immediately frozen in liquid nitrogen and kept at 193 K.

6.1.2.3 Cultivation of *E. coli* and *B. subtilis*

High density liquid cell cultures of *E. coli* and *B. subtilis* were obtained in TB or LB medium. A starter culture of 35 ml LB medium containing an adequate antibiotic for selection if required, was inoculated with a small amount of cells of thawed stock cultures (see 6.1.2.2) or a single colony which was picked from an LB agar plate (see 6.1.2.1). After incubation overnight at 310 K and 200 rpm, the pre-culture was transferred into a larger volume of either TB or LB medium including antibiotic if required. For protein overexpression, routinely TB medium was used. 1 l cultures were inoculated with one pre-culture and 3 l cultures were inoculated with three pre-cultures, referring to an initial OD₆₀₀ of 0.1 - 0.2. The cultures were incubated at 310 K and 200 rpm. Overnight cultures usually obtained an OD₆₀₀ of approximately 2.5 which corresponds to ~ 5 g·l⁻¹ cell pellet wet weight.

6.1.2.4 Synchronisation of *B. subtilis* Cells

B. subtilis cells were routinely grown in LB medium. The cells were harvested at OD₆₀₀ of 0.7 - 0.8 by centrifugation for 15 min at 6000*g and room temperature. The cell pellet was resuspended in twice of the original volume in DSM medium (see 5.3.1.3). Growth of synchronised cells was performed at 310 K and 200 rpm.

6.1.2.5 Induction of Endospore Formation in *B. subtilis*

Sporulation of *B. subtilis* was induced by cultivation in nutrient-poor DSM medium (see 5.3.1.3). Synchronised cells (see 6.1.2.4) were cultivated at 310 K and 200 rpm till designated cell state. The sporulation process usually starts ~ 3 h after onset of the stationary phase. Endospore formation usually accomplishes within ~ 8 h and endospores are visible by observation under a light microscope appearing as light diffracting cell compartments.

6.1.2.6 Determination of Cell Density

Cell densities of *E. coli* and *B. subtilis* cultures in liquid medium were determined photometrically by measurement of the optical density (OD) at 600 nm wavelength using a UV-VIS spectrophotometer. High OD₆₀₀ readings were calculated by diluting the sample in culture medium to enable measurement in the linear range of 0.1 - 0.5 OD₆₀₀.

6.1.2.7 Growth Curve of Bacteria in Liquid Cultures

For growth phase determination of bacteria in liquid cultures, samples were taken from incubating cultures in periodic intervals and treated as described in 6.1.2.6. Collected data were illustrated as a growth curve in logarithmic scale.

6.1.2.8 Staining of Endospores

Staining of *B. subtilis* endospores was performed accordingly to Raketle (Winkle, 1979). In this procedure, a drop of *B. subtilis* liquid culture in DSM was transferred to a microscope slide, dried on air, and heat-fixed. The slide was covered with malachite green solution (see 5.3.3) and heated near to boiling. The solution was kept hot for about 10 min without drying up. Malachite green solution was added if necessary. The slide was thoroughly washed-up with ddH₂O and counterstained with eosine (see 5.3.3) for 5 min. The stain was washed away with ddH₂O and the slide air-dried. Analysis was done in a bright field microscope with 40x objective and oil immersion. Endospores are stained in green while remaining cells appear red because of eosine incorporation. As a negative control, *B. subtilis* cells were cultivated in a non-sporulation medium (LB medium), treated as described, and analysed.

6.2 Protein Chemistry

6.2.1 Heterologous Overexpression of Proteins in *E. coli*

E. coli BL21 Star (DE3) cells for protein overexpression (see 6.1.2.1) were cultivated at 310 K and 200 rpm in TB medium containing $50 \mu\text{g} \cdot \text{ml}^{-1}$ kanamycin. Induction of protein overexpression was performed at $\text{OD}_{600} \sim 0.7$ with 1 mM IPTG (isopropyl-1-thio- β -D-galactopyranoside). The overexpression of recombinant proteins was accomplished in 4 h. The cells were harvested by centrifugation at $15900 \times g$ for 20 min at 277 K. Cell pellets which were not further processed subsequently, were stored at 193 K.

6.2.2 Purification of His-tagged Proteins from *E. coli* under Native Conditions

The purification procedure was done following the protocol of Dr. Sergej Djuranovic, MPI of Developmental Biology, Tübingen* (Djuranovic, 2007) which was, with minor modifications, based on the Qiagen manufacturer's protocol (see 9.).

The cell pellet was resuspended in NB 1 (see 5.3.2) and lysis enforced performing the *French press* method twice. DNase was added to digest DNA and to decrease the viscosity of the suspension. After removal of the insoluble cell particles by centrifugation ($48400 \times g$, 1 h, 277 K), the lysate was incubated with Ni-NTA material (Ni-NTA Superflow, Qiagen) pre-equilibrated with NB 1. Coupling of the His₆-tagged protein to the Ni-NTA matrix was achieved via batch-incubation at room temperature for 30 min by gently end-over-end rotation. The suspension was transferred into an empty XK chromatography column and at this stage connected to the ÄKTA system (Amersham Biosciences). Unspecifically bound contaminants were removed by extensive washing with NB 2 (see 5.3.2) (~ 10 column volumes). The immobilised His₆-tagged protein was eluted with NB 3 (see 5.3.2) in 3 ml fractions by applying a gradient within a range of 30 column volumes. $10 \mu\text{l}$ of each of the eluted fractions were tested with respect to protein content and quality by SDS-PAGE (see 6.2.6). Fractions containing the desired protein were pooled. Buffer exchange, if required, was done by dialysis (see 6.2.10) against suitable buffers.

6.2.3 Generation of Polyclonal Rabbit Antibodies

Prior to immunisation of the rabbit, a stable emulsion between the aqueous antigen solution (SpoVT_{FL}) and the adjuvant was prepared. 0.5 ml of the two-step purified His₆-tagged SpoVT_{FL} protein with a concentration of 2.31 mg*ml⁻¹ in 1x PBS buffer (see 5.3.2) were mixed with 0.5 ml of "Titermax Gold" adjuvant (Sigma). Thereby, the protein solution was added to the Titermax solution so that the aqueous phase entered the oil phase. This was done in two stages using each half of the amount of the protein solution for mixing with the adjuvant. 1 min of extensive mixing caused a sudden increase of the viscosity of the white coloured emulsion. For vigorously mixing, the double hub needle method was applied. The stability of the water-in-oil emulsion was tested by placing a drop of emulsion on water. A blood sample of ~ 1 ml was taken from the rabbit (pre-serum) and the emulsion was injected to induce the first immunisation reaction (day 1).

To gain the serum from the blood, the blood was stirred with a glass rod for ~ 1 min and left at room temperature for 1 h. The blood was stirred again, cooled at 277 K overnight, stirred once more, and centrifuged for 30 min at 5000*g. The supernatant was collected, aliquoted, and the serum was stored at 253 K.

A blood sample of the rabbit was taken at day 44 and prepared as described above. Immediately, the second immunisation was done with an emulsion prepared as described above using "Freundsches adjuvant incomplete" (Sigma) instead of "Titermax Gold". At day 54, another blood sample was taken from the rabbit and treated as described. The third immunisation was carried out, comparably to the second immunisation procedure, at day 77 and again a blood sample was taken before injection. The serum for testing the titer was derived from the blood sample taken at day 89 which was prepared as described. To test the titer, immuno blots were carried out with several amounts of antigen and serial dilutions of the serum (1:100 – 1:5000). Due to a good titer, the terminal blood of the rabbit was obtained at day 99. A volume of ~ 35 ml rabbit blood was treated as described to gain the serum. The serum was aliquoted and stored at 253 K.

6.2.4 Purification of Polyclonal Antibodies

Antibody isolation of the rabbit blood serum was performed via the Affi-Gel method (Bio-Rad). The activation procedure of the gel support was performed, with minor alterations, according to manufacturer's protocol (see 9.). The antigen (SpoVT_{FL} protein) was coupled to the N-hydroxysuccinimide ester of a derivatised crosslinked agarose (Affi-Gel). In this method, best binding properties are achieved at a pH near or below the isoelectric point of the protein. Here, Affi-Gel 15 was used which facilitates binding of acidic proteins (isoelectric point below 6.5, pI of SpoVT_{FL}: 5.46). Coupling of the protein was carried out in 1x PBS buffer.

4 ml of the thawed blood serum were buffered with AB 1 (see 5.3.2) to a final molarity of 10 mM. After centrifugation (10 min, 3220*g), the supernatant was incubated with the activated Affi-Gel. Antigen-antibody interaction occurred in 1 h at 277 K by end-over-end rotation. The slurry was poured into an empty chromatography column (Glass Eono-column column, Bio-Rad) to perform gravity flow chromatography. The flow through (serum) was added once more, followed by three washing steps with AB 2 (see 5.3.2), three washing steps with AB 3 (see 5.3.2), and three washing steps with 1x PBS buffer (see 5.3.2). Fractional elution of the antigen-antibody complex was induced via a pH-shift by application of 5 column volumes 100 mM glycine solution pH 2.8. Subsequently, the eluates were buffered with AB 4 (see 5.3.2) to a final molarity of 10 mM. The fractions were checked for antibody content by SDS-PAGE analysis (see 6.2.6). Protein positive fractions were pooled and dialysed against 1x PBS at 277 K overnight (see 6.2.10). The buffer was exchanged and dialysis was continued for 1 h. The antibody solution was aliquoted and stored at 253 K.

6.2.5 Fast Cell Lysis for Determination of Protein Content

To determine the protein inventory of *E. coli* and *B. subtilis* cells, 100 µl samples were taken from liquid cultures at a definite point in time. The cells were pelleted by centrifugation at 10000*g for 10 min and lysed by adding 10 µl of 5x SPB 1 (see 5.3.2). The samples were boiled for 7 min, centrifuged for 2 min, and analysed by SDS-PAGE (see 6.2.6).

6.2.6 SDS-Polyacrylamide Gel Electrophoresis

Protein analysis regarding molecular mass, quality, purity, and even quantity is provided by an SDS-PAGE (sodium dodecylsulfate polyacrylamide gel electrophoresis) experiment. A discontinuous buffer system was used and SDS-PAGE performed under denaturing conditions referred to Laemmli (Hames, 1990). Gels were prepared with a content of 13% or 17% acrylamide for the separating gels and 7.5% for the stacking gels.

A batch of 10 gels was prepared as follows:

- Stacking gel 7.5%: 13.1 ml 30% Protogel, 13.1 ml SPB 3 (see 5.3.2), 250 μ l ammonium-persulfate, 50 μ l TEMED, 26.25 ml ddH₂O
- Separating gel 13%: 32.5 ml 30% Protogel, 18.75 ml SPB 2 (see 5.3.2), 250 μ l ammonium-persulfate, 50 μ l TEMED, 23.75 ml ddH₂O
- Separating gel 17%: 42.5 ml 30% Protogel, 18.75 ml SPB 2 (see 5.3.2), 250 μ l ammonium-persulfate, 50 μ l TEMED, 13.75 ml ddH₂O.

Polymerised gels were clamped into Mighty Small II units (Amersham Biosciences) and covered with 1x SPB 4 (see 5.3.2). 1x or 5x SPB 1 (see 5.3.2) was added to the protein samples and after boiling for max. 10 min, the samples and a protein molecular weight marker (Fermentas) were filled into the wells of the stacking gel. Electrophoresis was carried out under constant cooling at 200 V and 40 - 80 mA using an electrophoresis power supply (Pharmacia Biotech). After the electrophoresis run, the proteins were fixed and the gels stained in a Coomassie suspension (see 5.3.3) for ~ 45 min. Destaining (see 5.3.3) of the gels was performed till distinct protein bands became visible.

Commercially available Bis-Tris polyacrylamid gradient gels (NuPAGE, Invitrogen) were also in use. Electrophoresis was performed according to manufacturer's protocol (see 9.).

6.2.7 Native Polyacrylamide Gel Electrophoresis

Native polyacrylamide gel electrophoresis (NativePAGE, Invitrogen) using pre-cast gels was done corresponding to manufacturer's protocol (see 9.).

6.2.8 Electro Blotting

Electro blotting is a method for an electrochemical transfer of denatured proteins from a polyacrylamide gel onto a solid support. Here, the semi-dry blotting technique was applied. The solid support was provided by a PVDF membrane (Immobilon-P, Millipore). The membrane was activated by incubation in methanol for 15 sec. The protein samples of interest were separated in a polyacrylamide gel by running a SDS-PAGE (see 6.2.6). Afterwards, the gel and the membrane were overlaid and packed in a batch of buffer-moist Whatman paper sheets. The proteins in the electric field move from the cathode to the anode. The pack was arranged as:

Cathode -

4 pieces of Whatman sheets in EB 3

Gel in EB 3

Membrane in EB 2

2 pieces of Whatman sheets in EB 2

4 pieces of Whatman sheets in EB 1

Anode +

The block was clamped between two electrode plates of a home-made device. The transfer was enforced in ~ 2.5 h at room temperature and 30 mA provided by a power supply (Pharmacia Biotech).

6.2.9 Immuno (Western) Blotting

Western Blot analysis is a very specific and sensitive immunological method of protein identification. For this, proteins of interest were transferred from a polyacrylamide gel onto a solid support via electro blotting as described in 6.2.8. To check the efficiency of the protein transfer, the membrane was stained with a Ponceau S solution (see 5.3.3) for 30 sec and transferred protein bands became visible. The stain was thoroughly washed away with ddH₂O. The membrane was treated with WB 1 (see 5.3.2) two times for 10 min each. For blocking, the membrane was incubated in WB 2 at room temperature for 3 h by end-over-end rotation. Unbound BSA was washed away with WB 3 (10 min) and WB 1 (2 times, 10 min each). The primary antibody (polyclonal rabbit IgG, see 6.2.4) was applied in a 1:10000 dilution in WB 2 by overnight end-over-end rotation at 277 K. Accurately washing in WB 1 (several times) was performed prior to adding the secondary antibody (goat anti-rabbit IgG, horseradish, Sigma, 1:50000 dilution in WB 2). Incubation was done for 1 h at 277 K by end-over-end rotation. The membrane was washed several times in WB 1, covered with a 1:1 mixed luminol/H₂O₂ reaction solution (Pierce) and incubated for 3 min (see 9.). Protein bands which were specifically recognised by the polyclonal rabbit antibody became visible by subsequently exposing the membrane to X-ray films. Exposure was done several times for different time periods and the films were developed by standard film developing methods.

6.2.10 Dialysis

The removal of low molecular components of protein solutions and/or exchange of the medium was done by dialysis. Dialysis tubes (Sigma) or cassettes (Pierce) made up of a semi-permeable cellulose membrane with a specific cut-off were filled with a protein solution and transferred into the desired medium. Substances of smaller size than the cut-off passed the membrane and by-and-by, conditions within the dialysis tube or cassette adapted to the surrounding solution. In normal case, dialysis was carried out at 277 K overnight. Tubes and cassettes were treated as described by manufacturer's protocol (see 9).

6.2.11 Ultrafiltration

Enhancement of protein concentration was performed by the ultrafiltration method. Specific cut-off membranes in pre-cast devices (Amicon, Millipore) hinder proteins of equivalent and larger sizes to pass the membrane. Smaller proteins and molecules can cross the membrane by an applied centrifugal force. The procedure was done according to manufacturer`s protocol (Millipore, see 9.).

6.2.12 Determination of Protein Concentration

6.2.12.1 UV Absorption

The concentration of protein solutions was determined by spectroscopic methods at a wavelength of 280 nm using an UV-Vis spectrometer or a spectrophotometer (NanoDrop). Light absorption of proteins is mainly caused by the presence of the aromatic amino acids tyrosine (Tyr) and tryptophane (Trp). Based on the extinction coefficient of the protein which was computed using the equation

$$\varepsilon(\text{protein}) = n(\text{Tyr}) * \varepsilon(\text{Tyr}) + n(\text{Trp}) * \varepsilon(\text{Trp}),$$

($\varepsilon(\text{Tyr}) = 1490$, $\varepsilon(\text{Trp}) = 5500$ at 280 nm in aqueous solution)[§],

the protein concentration was calculated with respect to Lambert Beer´s law

$$E = \varepsilon * d * c$$

(ε = extinction coefficient, n = number of amino acids, E = extinction, d = path length, c = concentration of protein).

[§] <http://www.expasy.ch/tools/protparam-doc.html>

6.2.12.2 BCA Protein Essay

Alternatively, protein concentration determination was done by the BCA (bicinchoninic acid) assay. Based on the biuret reaction, in which proteins reduce Cu^{2+} ions under alkaline conditions, a purple coloured complex between emerging Cu^+ ions and BCA (Pierce) is formed. Distinct protein dilutions were measured colourimetrically at 562 nm using an UV-Vis spectrometer after completion of the reaction. Protein concentrations were calculated by a standard curve. The experimental setup was done following manufacturer's protocol (Pierce, see 9.).

6.2.13 Chemical Crosslinking

The bifunctional agent glutaraldehyde is commonly used for conjugation of proteins. Glutaraldehyde induces intra- and intermolecular interactions via formation of Schiff's bases using the primary amino groups especially of lysines. Such covalently linked protein complexes can be analysed by SDS-PAGE.

Crosslinking of SpoVT_{FL} and SpoVT_{CT} was done each with $\sim 60 \mu\text{g}$ of protein and 0.025% glutaraldehyde in $20 \mu\text{l}$ reaction batches. Samples were incubated for 10 min at 303 K and subsequently, $20 \mu\text{l}$ of SPB 1 were added. $10 \mu\text{l}$ were applied to SDS-PAGE analysis (see 6.2.6).

6.3 Biochemistry

6.3.1 Chromatography

6.3.1.1 Affinity Chromatography

The initial protein purification step was performed by affinity chromatography with a Ni-chelating material (Ni-NTA superflow, Qiagen) (see 6.2.2) or Affi-Gel (see 6.2.4). In metal affinity chromatography, sepharose beads with exposed functional NTA (nitrilotriacetic acid) groups and complexed Ni-atoms, which are able to specifically immobilise His-tagged proteins, were used (IMAC). For specifications of the Affi-Gel see 6.2.4. Protein purification procedures were carried out, with minor alterations, based on manufacturer's protocol (Bio-Rad, see 9.).

Batch-incubation of cell lysate with pre-equilibrated Ni-NTA material for purification of His₆-tagged proteins was followed by an application to an HPLC system for an automated protein purification process. Batch-incubation and the gravity flow method were used for purifying polyclonal antibodies. Elution of His-tagged proteins was induced by adding high amounts of imidazole or EDTA, or applying a pH-shift. The latter was used for elution of polyclonal antibodies.

6.3.1.2 Gel Filtration Chromatography

Preparative gel filtration chromatography was performed as a second protein purification step to achieve a higher degree of purity. A HiLoad 26/60 Superdex 75 prepgrade column (Amersham Biosciences) with a separation range for proteins of a molecular weight between 3 kDa and 70 kDa was used. Binding studies (analytical gel filtration chromatography) were done using the SMART chromatography system (Amersham Biosciences) and a gel filtration column Superdex 75 PC 3.2/30 (Amersham Biosciences). At a flow rate of 40 $\mu\text{l} \cdot \text{min}^{-1}$, ~ 45 μl of a protein solution with a concentration of 1.5 $\text{mg} \cdot \text{ml}^{-1}$ for SpoVT_{FL} and 3 $\text{mg} \cdot \text{ml}^{-1}$ for SpoVT_{CT}, incubated with

10 mM of potential binding partners, were analysed. For calibration, proteins of a definite mass were applied (LMW calibration kit, Amersham Biosciences, see 9.). Gel filtration chromatography experiments were done in MOPS buffer (see 5.3.2) following manufacturer's protocols (Amersham Biosciences, see 9.).

6.3.2 High Performance Liquid Chromatography/Mass Spectrometry (HPLC/MS)

High performance liquid chromatography/mass spectrometry (HPLC/MS) was done for exact mass analysis of proteins. Protein solutions were separated on a reversed phase column (Waters Symmetry C₄ column, particle size 3.5 μ m - stationary phase) in an aqueous solution (mobile phase).

After ionisation of the sample, emerging free ions were analysed concerning their mass/charge ratio (m/z) and converted into a mass spectrum.

6.3.3 Matrix Assisted Laser Desorption Ionisation/Time of Flight/Mass Spectrometry (MALDI/TOF/MS)

Identification of proteins was done by matrix assisted laser desorption ionisation/time of flight/mass spectrometry (MALDI/TOF/MS). In this method, purified proteins are checked regarding their amino acid sequence by laser beam based ionisation out of a condensed phase.

Slices of Coomassie stained protein bands in a polyacrylamide gel (see 6.2.6) were excised and digested with trypsin. Generated peptides were mixed with a specific matrix material for protection against direct exposure to the laser beam. After evaporation of the sample, the crystalline mixture was applied to the MS system.

6.3.4 N-terminal Amino Acid Sequencing

Alternatively, identity of proteins was checked by the N-terminal sequencing method. Proteins were transferred onto a solid support (PVDF membrane) by electro blotting (see 6.2.8). The membrane was incubated in a Coomassie solution (see 5.3.3) until distinct protein bands became visible. Slices of the protein bands were excised and the Edman degradation technique was applied for successive determination of the primary structure of the proteins.

6.3.5 Limited Proteolysis

Limited proteolysis was done with trypsin and α -chymotrypsin. Reaction batches contained 84 μg of the protein (either SpoVT_{FL} or SpoVT_{CT}), 10 mM of the potential ligand, 10 mM CaCl₂ in the case of DPA as ligand candidate, and either 0.26 μg trypsin or 0.52 μg α -chymotrypsin. 120 μl of LPB 1 (see 5.3.2) were added to trypsin containing samples and 120 μl of LPB 2 (see 5.3.2) were added to samples including α -chymotrypsin, resulting in final batch volumes of $\sim 150 \mu\text{l}$ each. For DNA-binding tests, 4 μg DNA (promoter region of SpoVT operon, see 6.1.1.1) were included into the batch mixture. As a control, BSA was used in every variation of the experiment in the same amount compared to the analytical protein. The samples were incubated at 298 K with slightly shaking. At different points in time (0, 5, 10, 20, 30, 60, and 120 min), 20 μl of the reaction solutions were mixed with 20 μl of 1x SPB 1 (see 5.3.2), boiled, and analysed by SDS-PAGE (see 6.2.6).

6.3.6 Preparation of *B. subtilis* Spores

B. subtilis cells were removed from liquid sporulation culture at definite time points. The cells were pelleted at 3220*g for 10 min, medium was removed by decanting, and the pellet was washed once with SB 1 (see 5.3.2). The pellet was suspended in SB 2 (see 5.3.2) and incubated at room temperature for 10 min. After a centrifugation step, the pellet was washed repeatedly with SB 3 (see 5.3.2) at room temperature. For following

SDS-PAGE analysis (see 6.2.6), the extant pellet was solubilised in 0.1 ml SPB 1 (see 5.3.2) and boiled at 372 K for 10 min.

Alternatively, purified spores were resuspended in ddH₂O and pelleted by centrifugation for 6 min. The spores were suspended in SB 4 (see 5.3.2) and incubated at 310 K for 20 min. The sample was centrifuged for 6 min and using the pellet, the extraction procedure was repeated. Both supernatants were pooled, mixed with SPB 1, (see 5.3.2) boiled, and analysed by an SDS-PAGE (see 6.2.6).

6.4 Molecular Biophysics

6.4.1 X-ray Crystallography

6.4.1.1 Protein Crystallisation, Soaking, Co-crystallisation, and Seeding

The equipment for performing 3D-crystallisation was purchased from Hampton Research.

For 3D-crystallisation trials, the protein concentration was adjusted to a certain final concentration via ultrafiltration (see 6.2.11).

Proteins were crystallised by vapour diffusion in hanging drops of 5 μ l volume against 500 μ l reservoir solution at 291 K. Drops contained a 1:1 volume ratio of 10 mg*ml⁻¹ or 20 mg*ml⁻¹ protein in MOPS and crystallisation buffer. Crystallisation conditions were screened with commercially available reagents (Hampton Research, Sigma, Jena Biosciences, Emerald BioSystems). Optimisation of the initial crystallisation conditions, if necessary, was performed by providing additives (Hampton Research, Additive screen). 2.5 μ l of the protein solution were mixed with 2 μ l of the crystallisation condition buffer and 0.5 μ l of additive solution.

Drops with existing crystals were used for testing the ligand binding property of SpoVT via soaking. Therefore, 0.1 μ l of solutions containing potential binding partners (cGMP,

isoleucine, and DPA) were added to the drop to a final content of 10 mM. Diffusion of the small molecules enables its association to the protein and probably specific binding to the protein binding site occurs. Several days of incubation under known conditions followed.

Another way of performing binding studies is provided by co-crystallisation. The protein and the putative binding partner are incubated prior to preparation of the crystallisation trials. Protein solutions of SpoVT_{CT} were mixed with solutions of cGMP, GTP, or isoleucine to a final content of 10 mM of potential ligand. To SpoVT_{FL} protein solutions, a DNA fragment defining the promotor sequence of SpoVT was added (see 6.1.1.1) in each case. Crystallisation trials of the protein solutions were carried out by hanging drop vapour diffusion (see above).

A method for crystal multiplication is described by seeding. In performing the micorseeding technique, existing crystals are carefully touched by a whisker which picks up seeds from the crystal. The whisker is streaked in a pre-equilibrated drop (SpoVT_{CT} protein solution together with crystallisation solution MSB, see 5.3.2) and at most, the crystals grow along the streak line.

6.4.1.2 Crystal Mounting and Data Collection

For data collection, single crystals were mounted using cryo-crystallography tools from Hampton Research. Synthetic pre-mounted cryoloops of suitable size (0.025 - 0.4 mm) were used for removing crystals from the drops. Mounted SpoVT_{FL} crystals were frozen directly in liquid nitrogen. Crystals of SpoVT_{CT} and its Se-Met derivate were treated with mother solution containing 5% (v/v) PEG 200 for cryo-protection prior to freezing. The mounted crystals were stored in liquid nitrogen.

Diffraction data were collected at the Swiss Light Source (SLS) beamline PXII X10SA at the Paul Scherrer Institut (PSI) in Villigen, Switzerland. The data were recorded on a standard mar225 CCD detector featuring an active area of 225 x 225 mm². Image data were collected at 100 K at wavelengths of 0.978 Å for SpoVT_{FL} and 0.979 Å for the SpoVT_{CT} crystals. Data sets of 280° with an oscillation range of 1° were collected. For the SpoVT_{CT} Se-Met derivate, a single anomalous dispersion (SAD) experiment was performed and

data were collected at the selenium absorption edge (0.979 Å). Prior to data collection, a fluorescence scan was obtained to detect the absorption maximum of the selenium.

6.4.1.3 Data Processing and Phasing

Direct structure determination of crystals is based on an anomalous dispersion of X-ray scattering factors. For phase determination, isomorphous (MIR, multiple isomorphous replacement) and anomalous (MAD, multiwavelength anomalous dispersion) methods are used. The endogenous anomalous scatterer selenium was incorporated into SpoVT_{CT} to replace methionine with seleno-methionine for phase determination by selenium-based MAD phasing (SAD) (Hendrickson et al., 1990).

The SAD data of the Se-Met SpoVT_{CT} crystal were integrated, merged and scaled using the programme XDS/XSCALE (Kabsch, 1993). Intensity data were converted into amplitudes using TRUNCATE (French and Wilson, 1978). Six Se sites were located and experimental phases were calculated at 2.1 Å resolution using SOLVE/RESOLVE (Terwilliger, 2000; Terwilliger and Berendzen, 1999).

Data of native SpoVT_{FL} and SpoVT_{CT} protein crystals were processed as described above. The SpoVT_{FL} structure was determined by molecular replacement in MOLREP (Vagin and Teplyakov, 1997) using the SpoVT_{CT} model as search model (1.5 Å, R/R_{free} 19.7% and 22.6%, respectively).

6.4.1.4 Model Building and Refinement

For SpoVT_{CT}, a partial model was built automatically with RESOLVE (Terwilliger, 2003) and the remainder of the protein was built manually. The initial model was further refined by several cycles of model rebuilding with COOT (Emsley and Cowtan, 2004) and automatic refinement using REFMAC (Murshudov et al., 1997). Solvent waters were added using the automated ARP/wARP programme (Perrakis et al., 2001).

The refined model of SpoVT_{CT} was used as search model for solving the structure of SpoVT_{FL} by molecular replacement (see 6.4.1.3). To improve the density of the N-terminal domain, which could not be placed by molecular replacement using one

chain of the NMR-structure of the N-terminal domain of AbrB (PDB entry 1YFB), the prime-and-switch routine of the RESOLVE programme was applied. The structure of SpoVT_{FL} was completed by density fitting the N-terminal part of AbrB into the solvent flattened map. Residues different between the N-termini of AbrB and SpoVT were exchanged and the model refined with non-crystallographic symmetry (NCS) restraints using iterative cycles of model building and refinement with COOT and REFMAC as mentioned above. The geometry was finally evaluated with PROCHECK (Laskowski et al., 1993).

6.4.2 Circular Dichroism (CD) Spectroscopy

Circular dichroism (CD) spectroscopy is a light absorption based method for analysis of the secondary structure of proteins. Thereby, the differences in the absorbance of right- and left-circularly polarized light by a substance are determined. Measurements were done on a J-715 spectropolarimeter (JASCO Corporation) with protein concentrations of 145 $\mu\text{g}\cdot\text{ml}^{-1}$ for SpoVT_{FL} and 165 $\mu\text{g}\cdot\text{ml}^{-1}$ for SpoVT_{CT}. Analyses were done in MOPS buffer. Determination of CD spectra was performed with 300 μl of the protein solutions in 8 scans in the far-UV spectral region within the wavelength range of 195 nm to 260 nm. Heat denaturing experiments were determined in the range of 277 K up to 363 K and in the wavelength range of 280 nm to 215 nm. The temperature was checked by an incorporated Peltier element controller (JASCO Corporation).

6.4.3 Isothermal Titration Calorimetry (ITC)

Isothermal titration calorimetry (ITC) is a method to study the binding of small molecules (ligands) to macromolecules (proteins) by determination of the thermodynamic parameters of the interaction. ITC experiments were performed to identify the ligand binding specificity of SpoVT. SpoVT_{FL} and SpoVT_{CT} in MOPS buffer were each tested regarding their binding specificity towards GTP, cGMP, isoleucine, and valine. 2 ml of a 50 μM protein solution were titrated with 400 μl of a 1 mM solution containing the potential ligand. In the experimental progress, 50 titration steps, each of 360 sec duration, were passed at 293 K.

7. ABBREVIATIONS

μg	microgram	DSM	Difco sporulation medium
μl	microlitre	DMSO	dimethylsulfoxide
μm	micrometre	DTT	dithiothreitol
μmol	micromole	E	SpoVT _{FL} monomer with elongated linker
3D	three-dimensional	<i>E. coli</i>	<i>Escherichia coli</i>
A	albumine	EB	electro blotting buffer
Å	Angstrom	EDTA	ethylenedinitrilotetraacetic acid
AB	antibody purification buffer		<i>Escherichia coli</i> FhIA
Abh	antibiotic resistance protein B homolog	e.g.	for example
Abh _{NT}	N-terminal domain of antibiotic resistance protein B homolog	ESI	electro spray ionisation
AbrB	antibiotic resistance protein B	FhIA	formate hydrogen lyase A
AbrB _{NT}	N-terminal domain of antibiotic resistance protein B	FT	flow through
ADP	adenosine diphosphate	GA	glutaraldehyde
AMP	adenosine monophosphate	GAF	cGMP-specific and -stimulated phosphodiesterases, <i>Anabaena</i>
ATP	adenosine triphosphate		adenylate cyclases, and germination protein E
<i>B. globigii</i>	<i>Bacillus globigii</i>	GerE	growth protein EL
<i>B. subtilis</i>	<i>Bacillus subtilis</i>	GroEL	guanosine triphosphate
BCA	bicinchoninic acid	GTP	hour
BCAA	branched-chain amino acid	h	4-(2-hydroxyethyl)-1-piperazineethanesulfonic acid
BglI	<i>Bacillus globigii</i> type II restriction endonuclease I	HEPES	helix-loop-helix
b. i.	before induction	HLH	Hidden Markov model
bp	base pair	HMM	haemoglobin-like protein gene
BSA	bovine serum albumine	<i>hmp</i>	high pressure liquid chromatography
C	Celsius, C-terminus	HPLC	helix-turn-helix
CL	cell lysate	HTH	isocitrate lyase regulator
cAMP	cyclic adenosine monophosphate	IclR	C-terminal domain of isocitrate lyase regulator
CCD	charge-coupled device	IclR _{CT}	that is
CD	circular dichroism	i.e.	immunoglobulin G
cGMP	cyclic guanosine monophosphate	IgG	immobilised metal affinity chromatography
cm	centimetre	IMAC	isopropyl-1-thio-β-D-galactopyranoside
CodY	cytosine deaminase Y	IPTG	isothermal titration calorimetry
CodY _{NT}	N-terminal domain of cytosine deaminase Y	ITC	Kelvin
coxA	cortex protein A gene	K	kanamycin
csgA	controlled by sigma G protein A gene	Kan	kilocalorie
CT A	chymotrypsinogen A	kcal	kilodalton
<i>cyaB2</i>	adenylate cyclase GAF-B2 gene	kDa	kiloelectron volt
<i>cyaB2</i> _{CT}	C-terminal part of adenylate cyclase GAF-B2 gene product	keV	25.6 mV, 0.593 kcal/mole at 25 °C
DBD	DNA-binding domain	kt/e	litre
ddH ₂ O	double distilled water	I	load
dmol	dezimole	L	Luria Bertani
DMSO	dimethylsulfoxide	LB	liquid chromatography
DNA	desoxyribonucleic acid	LC	light microscope
DPA	dipicolinic acid	LM	

Abbreviations

LMW	low molecular weight	SAD	single anomalous dispersion
LPB	limited proteolysis buffer	SASP	small acid-soluble spore protein
M	molar; molecular weight marker	SB	spore buffer
m/z	mass per charge ratio	SDS	sodium dodecylsulfate
mA	milliampere	Se	selenium
MAD	multiwavelength anomalous dispersion	sec	second
MALDI	matrix assisted laser desorption ionisation	Se-Met	seleno-methionine
MazE	ma-ze ("what is it?")	SFT	SpoVT _{FL} flow through
MazE _{NT}	N-terminal domain of ma-ze	<i>sleB</i>	spore cortex-lytic enzyme B gene
mdeg	millidegree	SLS	Swiss Light Source
mg	milligram	SMBD	small-molecule-binding domain
min	minute	SPB	SDS-PAGE buffer
MIR	multiple isomorphous replacement	SpoOA	stage 0 sporulation protein A
ml	millilitre	SpoIID	stage III sporulation protein D
mm	millimetre	SpoVT	stage V sporulation protein T
mM	millimole	SpoVT _{CT}	C-terminal domain of stage V sporulation protein T
MOPS	3-(N-morpholino) propanesulfonic acid	SpoVT _{FL}	full-length stage V sporulation protein T
MPI	Max Planck Institute	SpoVT _{NT}	N-terminal domain of stage V sporulation protein T
MraZ	murein region A protein Z	SSD	signal sensing domain
MS	mass spectrometry	SW	SpoVT _{FL} wash
MSB	microseeding buffer	T	temperature
mV	millivolt	T _{2.5}	time of highest SpoVT expression level
N	N-terminus	TAD	trans-activation domain
NB	Ni-NTA buffer	TB	terrific broth
NCS	non-crystallographic symmetry	TCA	trichloroacetic acid
ng	nanogram	TEMED	N,N,N',N'-tetramethyl ethylenediamine
nm	nanometre	TLS	twin lattice symmetry
NMR	nuclear magnetic resonance	TM	<i>Thermotoga maritima</i>
No.	number	T _m , T _M	melting temperature
NTA	nitrilotriacetic acid	TOF	time of flight
OA	ovalbumine	TraR	transcriptional activator protein R
OD	optical density	Tris	tris (hydroxymethyl) aminomethane
PAGE	polyacrylamide gel electrophoresis	UV	ultraviolet
PBS	phosphate buffer solution	UV-Vis	ultraviolet and visible
PCR	polymerase chain reaction	V	Volt
PDB	protein data bank	v/v	volume per volume
PDE	phosphodiesterase	W	wash
PEG	polyethyleneglycol	WB	western blotting buffer
PFAM	protein family	w/v	weight per volume
pI	isoelectric point	ZnF	Zinc-finger
pmol	picomole	σ	sigma factor
PSI	Paul Scherrer Institute	λ	wavelength
r.m.s.d.	root mean square deviation	θ	molar ellipticity
RNA	ribonucleic acid		
RNAP	ribonucleic acid polymerase		
rpm	rounds per minute		
RsfA	sigma F regulator A		
S	SpoVT _{FL} monomer with structured linker		

8. REFERENCES

- Altschul, S., Madden, T., Schaffer, A., Zhang, J., Zhang, Z., Miller, W. and Lipman, D. (1997) Gapped BLAST and PSI-BLAST: a new generation of protein database search programs. *Nucleic Acids Research*, **25**, 3389-3402.
- Anantharaman, V. (2001) Regulatory potential, phyletic distribution, and evolution of ancient, intracellular small-molecule-binding domains. *Journal of Molecular Biology*, **307**, 1271-1292.
- Aravind, L. and Ponting, P. (1997) The GAF domain: an evolutionary link between diverse phototransducing proteins. *Trends in Biochemical Sciences*, **22**, 458-459.
- Bagyan, I., Hobbot, J. and Cutting, S. (1996) A compartmentalized regulator of developmental gene expression in *Bacillus subtilis*. *Journal of Bacteriology*, **178**, 4500-4507.
- Baleja, J. D., Anderson, F. and Sykes, B. D. (1991) Different Interactions of *cro* repressor dimer with the left and right halves of OR3 operator DNA. *Journal of Biological Chemistry*, **266**, 22115-22124.
- Bender, G. R. and Marquis, R. E. (1985) Spore heat resistance and specific mineralization. *Applied & Environmental Microbiology*, **50**, 1414-1421.
- Benson, L. M., Vaughn, J. L., Strauch, M. A., Bobay, B. G., Thompson, R., Naylor, S. and Cavanagh, J. (2002) Macromolecular assembly of the transition state regulator AbrB in its unbound and complexed states probed by microelectrospray ionization mass spectrometry. *Analytical Biochemistry*, **306**, 222-227.
- Bobay, B. G., Andreeva, A., Mueller, G. A., Cavanagh, J. and Murzin, A. G. (2005) Revised structure of the AbrB N-terminal domain unifies a diverse superfamily of putative DNA-binding proteins. *FEBS Letters*, **579**, 5669-5674.
- Bobay, B. G., Bensons, L. M., Naylor, S., Feeney, B., Clark, A. C., Goshe, M. B., Strauch, M. A., Thompson, R., Cavanagh, J. (2004) Evaluation of the DNA-binding tendencies of the transition state regulator AbrB. *Biochemistry*, **43**, 16106-16118.
- Bobay, B. G., Mueller, G. A., Thompson, R. J., Murzin, A. G., Venters, R. A., Strauch, M. A. and Cavanagh, J. (2006) NMR structure of AbhN and comparison with AbrBN: FIRST insights into the DNA binding promiscuity and specificity of AbrB-like transition state regulator proteins. *Journal of Biological Chemistry*, **281**, 21399-21409.
- Bond, C. S. (2003) TopDraw: a sketchpad for protein structure topology cartoons. *Bioinformatics*, **19**, 311-312.
- Britton, R. A., Eichenberger, P., Gonzalez-Pastor, J. E., Fawcett, P., Monson, R., Losick, R. and Grossman, A. D. (2002) Genome-wide analysis of the stationary-phase sigma factor (sigma-H) regulon of *Bacillus subtilis*. *Journal of Bacteriology*, **184**, 4881-4890.
- Brock, T. D., Madigan, M. T., Martinko, J. M. and Parker J. (1994) *Biology of Microorganisms*, 7. Edition, Prentice Hall International Editions.
- Cavalier-Smith, T. (1987) The origin of eukaryote and achaeobacterial cells. *Annals of the New York Academy of Science*, **503**, 17-54.
- Chen, S., Jancrick, J., Yokota, H., Kim, R. and Kim, S. H. (2004) Crystal structure of a protein associated with cell division from *Mycoplasma pneumoniae* (GI: 13508053): a novel fold with a conserved sequence motif. *Proteins*, **55**, 785-791.
- Chen, S., Vojtechovsky, J., Parkinson, G. N., Ebright, R. H. and Berman, H. (2001) Indirect readout of DNA sequence at the primary-kink site in the CAP-DNA complex: DNA

- binding specificity based on energetics of DNA kinking. *Journal of Molecular Biology*, **314**, 63-74.
- Claude, J. B., Suhre, K., Notredame, C., Claverie, J. M. and Abergel, C. (2004) CaspR: a web server for automated molecular replacement using homology modelling. *Nucleic Acids Research*, **32**, 606-609.
- Coles, M., Djuranovic, S., Söding, J., Frickey, T., Koretke, K., Truffault, V., Martin, J. and Lupas, A. N. (2005) AbrB-like transcription factors assume a swapped hairpin fold that is evolutionarily related to double-psi beta barrels. *Structure*, **13**, 919-928.
- Djuranovic, S. (2007) Evolution of substrate recognition domains of the AAA proteins. *Max-Planck-Institute of Developmental Biology, Proteinevolution*. Tübingen, Germany, Eberhard Karls University Tübingen.
- Dong, T. C., Cutting, S. M. and Lewis, R. J. (2004) DNA-binding studies on the *Bacillus subtilis* transcriptional regulator and AbrB homologue, SpoVT. *FEMS Microbiology Letters*, **233**, 247-256.
- Ducros, V. M.-A., Lewis, R. J., Verma, C. S., Dodson, E. J., Leonard, G., Turkenburg, J. P., Murshudov, G. N., Wilkinson, A. J. and Brannigan, J. A. (2001) Crystal structure of GerE, the ultimate transcriptional regulator of spore formation in *Bacillus subtilis*. *Journal of Molecular Biology*, **306**, 759-771.
- Dworkin, M. and Kaiser, D. (1993) *Myxobacteria II*, American Society for Microbiology.
- Emsley, P. and Cowtan, K. (2004) Coot: model-building tools for molecular graphics. *Acta Crystallographica Section D - Biological Crystallography*, **60**, 2126-2132.
- Errington, J. (2003) Regulation of endospore formation in *Bacillus subtilis*. *Nature Reviews. Microbiology*, **1**, 117-126.
- French, G. S. and Wilson, K. S. (1978) *Acta Crystallographica Section A - Foundations of Crystallography*, **34**, 517.
- Fuchs, G. and Schlegel, H. G. (2006) *Allgemeine Mikrobiologie*. 8. Edition, Stuttgart, Thieme Verlag.
- Gruber, M. and Lupas, A. N. (2003) Historical Review: Another 50th anniversary - new periodicities in coiled coils. *Trends in Biochemical Sciences*, **28**, 679-685.
- Hames, B. D. (1990) *Gel Electrophoresis of Proteins: A Practical Approach*. Oxford, Oxford University Press.
- Handke, L. D., Shivers, R. P. and Sonenshein, A. L. (2008) Interaction of *Bacillus subtilis* CodY with GTP. *Journal of Bacteriology*, **190**, 798-806.
- Hendrickson, W. A., Horton, J. R. and LeMaster, D. M. (1990) Selenomethionyl proteins produced for analysis by multi-wavelength anomalous diffraction (MAD) – a vehicle for direct determination of 3-dimensional structure. *EMBO Journal*, **9**, 1665-1672.
- Higgins, D., Thompson, J., Gibson, T., Thompson, J. D., Higgins, D. G. and J., G. T. (1994) CLUSTAL W: improving the sensitivity of progressive multiple sequence alignment through sequence weighting, position-specific gap penalties and weight matrix choice. *Nucleic Acids Research*, **22**, 4673-4680.
- Ho, Y. S., Burden, L. M. and Hurley, J. H. (2000) Structure of the GAF domain, a ubiquitous signaling motif and a new class of cyclic GMP receptor. *EMBO Journal*, **19**, 5288-5299.
- Hoch, J. A. (1993) Regulation of the phosphorelay and the initiation of sporulation in *Bacillus subtilis*. *Annual Review of Microbiology*, **47**, 441-465.
- Holm, L. and Sander, C. (1993) Protein structure comparison by alignment of distance matrices. *Journal of Molecular Biology*, **233**, 123-138.

- Hulko, M., Berndt, F., Gruber, M., Linder, J. U., Truffault, V., Schultz, A., Martin, J., Schultz, J. E., Lupas, A. N. and Coles, M. (2006) The HAMP domain structure implies helix rotation in transmembrane signaling. *Cell*, **126**, 929-940.
- Igarashi, T. and Setlow, P. (2006) Transcription of the *Bacillus subtilis* gerK operon, which encodes a spore germinant receptor, and comparison with that of operons encoding other germinant receptors. *Journal of Bacteriology*, **188**, 4131-4136.
- Jordan, S. R. and Pabo, C. O. (1988) Structure of the lambda complex at 2.5 Å resolution: Details of the repressor-operator interaction. *Science*, **242**, 893-899.
- Kabsch, W. (1993) *Journal of Applied Crystallography*, **26**, 795-800.
- Kamada, K., Hanaoka, F. and Burley, S. K. (2003) Crystal structure of the MazE/MazF complex: molecular bases of antidote-toxin recognition. *Molecular Cell*, **11**, 875-884.
- Krissinel, E. and Henrick, K. (2007) Inference of macromolecular assemblies from crystalline state. *Journal of Molecular Biology*, **372**, 774-797.
- Kunst, F., Ogasawara, N., Moszer, I., Albertini, A. M., Alloni, G., Azevedo, V., Bertero, M. G., Bessi eres, P., Bolotin, A., Borchert, S., Borriss, R., Boursier, L., Brans, A., Braun, M., Brignell, S. C., Bron, S., Brouillet, S., Bruschi, C. V., Caldwell, B., V., C., Carter, N. M., Choi, S. K., Codani, J. J., Connerton, I. F. and Danchin, A. (1997) The complete genome sequence of the gram-positive bacterium *Bacillus subtilis*. *Nature*, **390**, 249-256.
- Laskowski, R. A., MacArthur, M. W., Moss, D. S. and Thornton, J. M. (1993) PROCHECK: a program to check the stereochemical quality of protein structures. *Journal of Applied Crystallography*, **26**, 283-291.
- Le Breton, Y., Mohapatra, N. P. and Haldenwang, W. G. (2006) In vivo random mutagenesis of *Bacillus subtilis* by use of TnYLB-1, a mariner-based transposon. *Applied & Environmental Microbiology*, **72**, 327-333.
- Levdikov, V. M., Blagova, E., Joseph, P., Sonenshein, A. L. and Wilkinson, A. J. (2006) The structure of CodY, a GTP- and isoleucine-responsive regulator of stationary phase and virulence in gram-positive bacteria. *Journal of Biological Chemistry*, **281**, 11366-11373.
- Loris, R., Marianovsky, I., Lah, J., Laeremans, T., Engelberg-Kulka, H., Glaser, G., Muyldermans, S. and Wyns, L. (2003) Crystal structure of the intrinsically flexible addiction antidote MazE. *Journal of Biological Chemistry*, **278**, 28252-28257.
- Martinez, S. E., Beavo, J. A. and Hol, W. G. J. (2002) GAF Domains: Two-Billion-Year-Old Molecular Switches that Bind Cyclic Nucleotides. *Molecular Interventions*, **2**, 317-322.
- Martinez, S. E., Bruder, S., Schultz, A., Zheng, N., Schultz, J. E., Beavo, J. A. and Linder, J. U. (2005) Crystal structure of the tandem GAF domains from a cyanobacterial adenylyl cyclase: modes of ligand binding and dimerization. *Proceedings of the National Academy of Sciences of the United States of America*, **102**, 3082-3087.
- Martinez, S. E., Wu, Y. A., Glavas, N. A., Tang, X. B., Turley, S., Hol, W. G. J. and Beavo, J. A. (2002) The two GAF domains in phosphodiesterase 2A have distinct roles in dimerization and in cGMP binding. *PNAS*, **99**, 13260-13265.
- Matthews, B. W. (1968) Solvent content of protein crystals. *Journal of Molecular Biology*, **33**, 491-497.
- Moreno-Campuzano, S., Janga, S. C. and Perez-Rueda, E. (2006) Identification and analysis of DNA-binding transcription factors in *Bacillus subtilis* and other Firmicutes--a genomic approach. *BMC Genomics*, **7**, 147.

- Murshudov, G. N., Vagin, A. A. and Dodson, E. J. (1997) Refinement of Macromolecular Structures by the Maximum-Likelihood Method. *Acta Crystallographica Section D - Biological Crystallography*, **53**, 240-255.
- Newman, M., Lunnen, K., Wilson, G., Greci, J., Schildkraut, I. and Phillips, S. E. V. (1998) Crystal structure of restriction endonuclease BglI bound to its interrupted DNA recognition sequence. *EMBO Journal*, **17**, 5466-5476.
- Pabo, C. O. and Sauer, R. T. (1992) Transcription factors - structural families and principles of DNA recognition. *Annual Review of Biochemistry*, **61**, 1053-1095.
- Patterson, A. L. (1934) A Fourier series method for the determination of the components of interatomic distances in crystals. *Physical Review*, **46**, 372 - 376.
- Pérez-Rueda, E. and Collado-Vides, J. (2000) The repertoire of DNA-binding transcriptional regulators in Escherichia coli K-12. *Nucleic Acids Research*, **28**, 1838-1847.
- Pérez-Rueda, E., Collado-Vides, J. and Segovia, L. (2004) Phylogenetic distribution of DNA-binding transcription factors in bacteria and archaea. *Computational Biology and Chemistry*, **28**, 341-350.
- Perrakis, A., Harkiolaki, M., Wilson, K. S. and Lamzin, V. S. (2001) ARP/wARP and molecular replacement. *Acta Crystallographica Section D - Biological Crystallography*, **57**, 1445-1450.
- Piggot, P. J. and Hilbert, D. W. (2004) Sporulation of Bacillus subtilis. *Current Opinion in Microbiology*, **7**, 579-586.
- Ratnayake-Lecamwasam, M., Serror, P., Wong, K. W. and Sonenshein, A. L. (2001) Bacillus subtilis CodY represses early-stationary-phase genes by sensing GTP levels. *Genes of Development*, **15**, 1093-1103.
- Slepecky, R. A. and Leadbetter, E. R. (1994) Ecology and relationships of endospore-forming bacteria: changing perspectives. *American Society for Microbiology*, 195-206.
- Söding, J. (2005) Protein homology detection by HMM-HMM comparison. *Bioinformatics*, **21**, 951-960.
- Söding, J., Biegert, A. and Lupas, A. N. (2005) The HHpred interactive server for protein homology detection and structure prediction. *Nucleic Acids Research*, **33**, 244-248.
- Sonenshein, A. L., Hoch, J. A. and Losick, R. (1993) Bacillus subtilis and other gram-positive bacteria: biochemistry, physiology, and molecular genetics. *American Society for Microbiology*.
- Steil, L., Serrano, M., Henriques, A. O. and Volker, U. (2005) Genome-wide analysis of temporally regulated and compartment-specific gene expression in sporulating cells of Bacillus subtilis. *Microbiology*, **151**, 399-420.
- Steitz, T. A. (1990) Structural studies of protein-nucleic acid interaction: the sources of sequence-specific binding. *Quarterly Reviews of Biophysics*, **23**, 205-280.
- Stragier, P. and Losick, R. (1996) Molecular genetics of sporulation in Bacillus subtilis. *Annual Review of Genetics*, **30**, 297-341.
- Strauch, M. A., Ballar, P., Rowshan, A. J. and Zoller, K. L. (2005) The DNA-binding specificity of the Bacillus anthracis AbrB protein. *Microbiology*, **151**, 1751-1759.
- Terwilliger, T. C. (2000) Maximum likelihood density modification. *Acta Crystallographica Section D - Biological Crystallography*, **56**, 965-972.
- Terwilliger, T. C. (2003) Automated main-chain model building by template matching and iterative fragment extension. *Acta Crystallographica Section D - Biological Crystallography*, **59**, 38-44.

- Terwilliger, T. C. (2003) SOLVE and RESOLVE: automated structure solution and density modification. *Methods in Enzymology*, **374**, 22-37.
- Terwilliger, T. C. and Berendzen, J. (1999) Automated MAD and MIR structure solution. *Acta Crystallographica Section D - Biological Crystallography*, **55**, 849-861.
- Vagin, A. and Teplyakov, A. (1997) MOLREP: an automated program for molecular replacement. *Journal for Applied Crystallography*, **30**, 1022-1025.
- Vannini, A., Volpari, C., Gargioli, C., Muraglia, E., Cortese, R., De Francesco, R., Neddermann, P. and Marco, S. D. (2002) The crystal structure of the quorum sensing protein TraR bound to its autoinducer and target DNA. *EMBO Journal*, **21**, 4393-4401.
- Vaughn, J. L., Feher, V., Naylor, S., Strauch, M. A. and Cavanagh, J. (2000) Novel DNA binding domain and genetic regulation model of *Bacillus subtilis* transition state regulator abrB. *Nature Structure Biology*, **7**, 1139-1146.
- Wang, S. T., Setlow, B., Conlon, E. M., Lyon, J. L., Imamura, D., Sato, T., Setlow, P., Losick, R. and Eichenberger, P. (2006) The forespore line of gene expression in *Bacillus subtilis*. *Journal of Molecular Biology*, **358**, 16-37.
- Whittenbury, R., Davies, S. L., Davey, J. F. and Schink, B. (1970) Exospores and cysts formed by methane utilizing bacteria. *Journal of General Microbiology*, **61**, 219-226.
- Winkle, S. (1979) *Mikrobiologische und serologische Diagnostik: mit Berücksichtigung der Pathogenese und Epidemiologie*. Stuttgart, Urban & Fischer.
- Wyss, O., Neumann, M. G. and Socolofsky, M. D. (1961) Development and germination of the *Azotobacter* cyst. *Journal of Biophysical and Biochemical Cytology*, **10**, 555-565.
- Xu, K. and Strauch, M. A. (2001) DNA-binding activity of amino-terminal domains of the *Bacillus subtilis* AbrB protein. *Journal of Bacteriology*, **183**, 4094-4098.
- Yao, F. and Strauch, M. A. (2005) Independent and interchangeable multimerization domains of the AbrB, Abh, and SpoVT global regulatory proteins. [erratum appears in J Bacteriol. 2005 Nov;187(21):7546]. *Journal of Bacteriology*, **187**, 6354-6362.
- Youngman, P., Perkins, J. B. and Losick, R. (1984) Construction of a cloning site near one end of Tn917 into which foreign DNA may be inserted without affecting transposition in *Bacillus subtilis* or expression of the transposon-borne erm gene. *Plasmids*, **12**, 1-9.
- Zhang, K. Y., Card, G. L., Suzuki, Y., Artis, D. R., Fong, D., Gillette, S., Hsieh, D., Neiman, J., West, B. L., Zhang, C., Milburn, M. V., Kim, S. H., Schlessinger, J. and Bollag, G. (2004) A glutamine switch mechanism for nucleotide selectivity by phosphodiesterases. *Molecular Cell*, **15**, 279-286.
- Zhang, R. G., Kim, Y., Skarina, T., Beasley, S., Laskowski, R., Arrowsmith, C., Edwards, A., Joachimiak, A. and Savchenko, A. (2002) Crystal structure of *Thermotoga maritima* 0065, a member of the IclR transcriptional factor family. *Journal of Biological Chemistry*, **277**, 19183-19190.
- Zhao, H., Msadek, T., Zapf, J., Madhusudan, Hoch, J. A. and Varughese, K. I. (2002) DNA complexed structure of the key transcription factor initiating development in sporulating bacteria. *Structure*, **10**, 1041-1050.
- Zoraghi, R., Corbin, J. D. and Francis, S. H. (2004) Properties and functions of GAF domains in cyclic nucleotide phosphodiesterases and other proteins. *Molecular Pharmacology*, **65**, 267-278.

9. APPENDIX

Amersham Biosciences:

- Gel Filtration Column HiLoad 26/60 Superdex 75 prepgrade
([http://www6.gelifesciences.com/aptrix/upp00919.nsf/Content/A729A28AA52A894CC1256EB400417EDB/\\$file/71502020AF.pdf](http://www6.gelifesciences.com/aptrix/upp00919.nsf/Content/A729A28AA52A894CC1256EB400417EDB/$file/71502020AF.pdf))
- Gel Filtration Column Superdex 75 PC 3.2/30
([http://www6.gelifesciences.com/aptrix/upp00919.nsf/Content/BB42DD3E4A6C0D15C1256EB40044A98B/\\$file/71606300AH.pdf](http://www6.gelifesciences.com/aptrix/upp00919.nsf/Content/BB42DD3E4A6C0D15C1256EB40044A98B/$file/71606300AH.pdf))
- Gel Filtration Calibration Kit
([http://www6.gelifesciences.com/aptrix/upp00919.nsf/Content/94339EC8D376AF11C12571BC00811DDA/\\$file/28-4038-41PL_Rev_B_2007_WEB.pdf](http://www6.gelifesciences.com/aptrix/upp00919.nsf/Content/94339EC8D376AF11C12571BC00811DDA/$file/28-4038-41PL_Rev_B_2007_WEB.pdf))

Bio-Rad:

- Activated Immunoaffinity Support (Affi-Gel)
(http://www.bio-rad.com/webmaster/pdfs/9115_Activated_Affinity.pdf)

Invitrogen:

- Library Efficiency DH5 α Competent Cells
(<http://tools.invitrogen.com/content/sfs/manuals/18263012.pdf>)
- Champion pET Directional TOPO Expression Kit
(http://tools.invitrogen.com/content/sfs/manuals/pettopo_man.pdf)
- NativePAGE Novex Bis-Tris Gel System
(http://tools.invitrogen.com/content/sfs/manuals/nativepage_man.pdf)
- NuPAGE Technical Guide
(http://tools.invitrogen.com/content/sfs/manuals/nupage_tech_man.pdf)

Millipore:

- Amicon Ultra-4/15 Centrifugal Filter Devices
([http://www.millipore.com/userguides.nsf/a73664f9f981af8c852569b9005b4eee/b4dcbc6be6274e94852572c200701f88/\\$FILE/ATTY6HU4/PR02496A_web.pdf](http://www.millipore.com/userguides.nsf/a73664f9f981af8c852569b9005b4eee/b4dcbc6be6274e94852572c200701f88/$FILE/ATTY6HU4/PR02496A_web.pdf),
[http://www.millipore.com/userguides.nsf/a73664f9f981af8c852569b9005b4eee/a50b8057dc203885852572c2006ec963/\\$FILE/ATTWDFLK/PR02497A_web.pdf](http://www.millipore.com/userguides.nsf/a73664f9f981af8c852569b9005b4eee/a50b8057dc203885852572c2006ec963/$FILE/ATTWDFLK/PR02497A_web.pdf))

Pierce:

- BCA Protein Assay Kit
(<http://www.piercenet.com/files/1296as4.pdf>)
- ECL Western Blotting Substrate
(<http://www.piercenet.com/files/1743as4.pdf>)
- Slide-A-Lyzer Dialysis Cassettes
(<http://www.piercenet.com/files/0729dh5.pdf>)

Qiagen:

- The QIAexpressionist
(http://www1.qiagen.com/HB/QIAexpressionist_EN)
- QIAprep Miniprep Handbook
(http://www1.qiagen.com/HB/QIAprepMiniprepKit_EN)
- QIAquick Spin Handbook
(http://www1.qiagen.com/HB/QIAquickSpinKit_EN_1)

10. ACKNOWLEDGEMENT - DANKSAGUNG

Prof. D. Oesterhelt, meinem Doktorvater, möchte ich ganz herzlich danken für die Betreuung und die Möglichkeit in seiner Abteilung arbeiten zu dürfen. Die Experimentierbedingungen in der Abteilung und im Institut waren hervorragend. Besonders dankbar bin ich, dass Prof. Oesterhelt in schwierigen Zeiten eine sichere Anlaufstelle für mich war.

Ganz großer Dank gebührt meinem Betreuer Dr. Kornelius Zeth. Durch ihn wurde mein Traum von der Biochemie ein Stück mehr Wirklichkeit. Das Eintauchen in die Strukturbiochemie war spannend und lehrreich. Ich danke für seine Unterstützung und ich schätze sehr, dass ich an zahlreichen Konferenzen teilnehmen konnte, um Kontakte zu knüpfen und Kooperationen zu entwickeln.

An Dr. Martin Grninger ein außerordentliches Dankeschön für das Korrekturlesen dieser Arbeit.

Für die Erstellung des Zweit-Gutachtens danke ich Prof. K.-P. Hopfner (LMU, Genzentrum).

Prof. A. Lupas und Dr. Sergej Djuranovic (MPI für Entwicklungsbiologie, Abt. Proteinevolution, Tübingen) möchte ich danken für die konstruktive Zusammenarbeit und wissenschaftliche Unterstützung im Rahmen dieser Arbeit.

Dr. Patrik Johansson half bei kristallographischen Problemen, vielen Dank dafür.

Ein Dank geht an Dr. Janine Kirstein und Prof. K. Turgay (FU Berlin, Abt. Mikrobiologie) für das Zusenden von *Bacillus subtilis*-Zellen und für so manchen Ratschlag.

Bei Guckus (Dr. R. Guckenberger, Abt. Baumeister) möchte ich mich herzlich bedanken für die Einführung in die Welt der Rasterkraftmikroskopie - eine beeindruckende Technik. Dabei seien auch Dr. Jens Schiener und Mirjam Classen dankend erwähnt.

Für die Kooperation in anderen Projekten möchte ich meinen Dank aussprechen bei Prof. M. Rief, Christof Gebhard (TU Garching, Abt. Physik), Dr. D. Dougan (La Trobe Universität, Abt. Biochemie, Melbourne, Australien) und Ronny Schmidt (ZMBH, Abt. Bukau), bei Dr. P. Zwickl (Abt. Baumeister), bei Dr. F. Führer (Abt. Biologie der Mikroorganismen, RU Bochum) und Prof. T. Ogura (Kumamoto Universität, Abt. Molekulare Zellbiologie, Japan) und bei Dr. Rainer Nikolay (Roche, Wien).

Nicht unerwähnt sollte die wahrlich angenehme und unkomplizierte Laborzeit mit Dr. Reinhard Albrecht, Stephanie (Steffi) Bleicken, Dr. Martin Grninger, Ursula (Ursel) Heider, Thomas Meins, Christl (Kiki) Weyrauch und Dr. Petra Wollmann bleiben. Auf gegenseitige Hilfe und Diskussionsbereitschaft war immer Verlass (besonderer Dank an Steffi für den Notfalleinsatz während eines 24 Std-Experiments und an Petra für die notwendige Kommunikation!).

Bei Kiki möchte ich mich für die Sequenzierungsarbeiten bedanken, bei Ursel für die Einführung in die Labor-Politik und die Abwicklung sämtlicher Bestellungen.

Vielen Dank an Fr. Haack für ihre Hilfe in allen organisatorischen, bürokratischen und auch unbürokratischen Angelegenheiten.

Dr. J. Tittor danke ich herzlich für die Unterstützung bei der Einrichtung eines ergonomischen Schreibplatzes.

Meinen PraktikantInnen Verena Loleit, Antonia Asen, Michael Horn, Gabor Meser, Martin Schmitt und Johannes Schilling, sowie Diplomandin Ines Subota bin ich dankbar für ihr engagiertes Mitwirken an den jeweiligen Projekten.

Guckus, Mirjam, Manuela und Harry möchte ich danken für die Durchsicht von Teilen dieser Arbeit.

Für zahllose diverse „in house“ Analysen, die für diese Arbeit, oder für andere Projekte wichtig waren, danke ich Lizzy Weyher-Stingl, Wolfgang Straßhofer, Dr. S. Suppmann, Judith Scholz und Ralf Zenke (Core Facility), Reini Mentele und Isabella Mathes (Abt. Lottspeich), Sigi Bauer, Bea Scheffer und Dr. F. Siedler (Abt. Oesterhelt) und Brigitte Kühlmorgen (Abt. Baumeister). Ich danke Elena Nigg (Abt. Nigg) für Tipps in Sachen „Polyklonale Antikörper“ und dem Tierhaus, insbesondere Claudia Theiler für das Versorgen des Kaninchens, welches so brav, aber leider umsonst, meine anti-SpoVT-Antikörper produzierte.

Dr. C. Struppler (Waldburg-Zeil-Kliniken, Oberammergau) möchte ich gesondert erwähnen. Sie hat eine entscheidende Rolle gespielt während diese Arbeit entstand und mit ihrem Einsatz und ihrer Entschlossenheit zum Erfolg mit beigetragen (großen Dank auch an Abbott, hoch lebe die Forschung!).

Kosta Konstantinidis und Christoph Schwarz danke ich für die lustigen Tennisstunden.

Meinen langjährigen Freunden in der Heimat, sowie in Plattling und Vilshofen, in Straubing, Regensburg und München an dieser Stelle ein herzliches „Vergelt´s Gott“ für all die Erlebnisse, für den Spaß, für die geistreichen und albernsten Gespräche, für die entpannenden und wohltuenden Freizeit-, Sport- und Saunaaktionen und für vieles mehr, v. a. aber für das Gefühl Freunde zu haben.

Ein großes DANKE an Harry, meinen „Tranquilizer“, dafür, dass er immer liebevoll und geduldig war und für den Einblick in die Facetten des Lebens.

Meine Eltern und Geschwister verdienen den größten Dank. Ohne deren Rückhalt und Vertrauen wäre vieles in meinem Leben nicht möglich gewesen. Dafür, dass sie Loyalität und Solidarität tatsächlich leben und mit Wagemut und Durchhaltevermögen ihr Dasein bestreiten verdienen sie großen Respekt und Bewunderung.

11. CURRICULUM VITAE

Curriculum Vitae	
	Iris Asen * 21.12.1975 in Vilshofen Single
Education	
1982-1986	Basic School in Außernzell
1986-1995	Grammar Boarding School at the Ursulinen convent in Straubing
<i>Qualification</i>	General qualification for university entrance
Academic Studies	
11/1995-07/1996	Diploma Chemistry at the University of Regensburg
11/1996-01/2003	Grammar School teacher in Biology and Chemistry at the University of Regensburg
<i>Academic Thesis</i> 10/2000-10/2001	Biochemical characterisation of a bacterial hyaluronidase in the department of Prof. A. Buschauer (Pharmaceutical Chemistry II) supervised by Prof. G. Bernhardt at the University of Regensburg
<i>Graduate Degree</i>	First State Examination Grammar School teacher in Biology and Chemistry in Bavaria at the University of Regensburg
Industrial Experience	
07/2000-09/2000	Internship at Siemens in the department ZT MF 3 "Kunst- und Funktionswerkstoffe" in Erlangen
09/2003-11/2003	Internship at the biotechnological concern "Crelux" (formerly "Sireen") at the IZB in Martinsried near Munich
Ph.D. since 01/2004	 "The Structure of SpoVT - A Regulator of Sporulation in <i>Bacillus subtilis</i> " in the department of Prof. D. Oesterhelt (Membrane Biochemistry) supervised by Dr. K. Zeth at the Max Planck Institute for Biochemistry in Martinsried near Munich
Martinsried, at	14.05.2008

Curriculum Vitae	
	<p>Iris Asen * 21.12.1975 in Vilshofen Ledig</p>
Schulbildung	
1982-1986	Grundschule in Außernzell
1986-1995	Gymnasium und Internat im Kloster der Ursulinen in Straubing
<i>Schulabschluß</i>	Allgemeine Hochschulreife
Studium	
11/1995-07/1996	Diplom Chemie an der Universität Regensburg
11/1996-01/2003	Lehramt Biologie und Chemie an Gymnasien an der Universität Regensburg
<i>Zulassungsarbeit</i> 10/2000-10/2001	Biochemische Charakterisierung einer bakteriellen Hyaluronidase am Lehrstuhl von Prof. A. Buschauer (Pharmazeutische Chemie II) unter der Leitung von Prof. G. Bernhardt an der Universität Regensburg
<i>Studienabschluß</i>	Erstes Staatsexamen für Lehramt Biologie und Chemie an Gymnasien in Bayern an der Universität Regensburg
Industrieerfahrung	
07/2000-09/2000	Betriebspraktikum bei Siemens im Fachzentrum ZT MF 3 „Kunst- und Funktionswerkstoffe“ in Erlangen
09/2003-11/2003	Biotechnologisches Praktikum bei „Crelux“ (ehemals „Sireen“) im IZB in Martinsried bei München
Promotion	
seit 01/2004	„The Structure of SpoVT - A Regulator of Sporulation in <i>Bacillus subtilis</i> “ in der Abteilung von Prof. D. Oesterhelt (Membranbiochemie) unter der Leitung von Dr. K. Zeth am Max-Planck-Institut für Biochemie in Martinsried bei München
Martinsried, am	14.05.2008